UNIVERSITY OF CATANIA

DEPARTMENT OF BIOLOGICAL, GEOLOGICAL AND ENVIRONMENTAL SCIENCES

Ph.D. PROGRAM COURSE IN GEOLOGICAL, BIOLOGICAL AND ENVIRONMENTAL SCIENCES

XXIX CYCLE

LOREDANA LEGGIO

Functional analysis of two alternative transcripts from *porin1* gene of *Drosophila melanogaster* and involvement of corresponding 5'UTR sequences in the translation control

Analisi funzionale dei due trascritti alternativi del gene *porin1* di *Drosophila melanogaster* e coinvolgimento delle rispettive sequenze 5'UTR nella regolazione della traduzione

TUTOR: Chiar.ma Prof.ssa Angela Messina

RIASSUNTO

Il VDAC (Voltage Dependent Anion-selective Channel) è un canale anionico dipendente dal voltaggio presente nella membrana mitocondriale esterna (OMM) di tutti gli organismi eucarioti. Tale canale permette il passaggio di nucleotidi, ioni e piccoli metaboliti da e verso il citosol grazie ad una struttura a barilotto β, con l'estremità N-terminale strutturata a formare un'α-elica rivolta verso lo spazio intermembrana e coinvolta nel processo di apertura e chiusura del poro. Esso assume la conformazione di massima apertura a voltaggi applicati di poco diversi da 0 mV; mentre a voltaggi superiori a 20 mV, sia in positivo che in negativo, il VDAC passa alla conformazione "chiusa". L'importanza di tale poro è dettata dalla sua localizzazione cellulare, che gli permette di interagire con moltissimi enzimi e proteine direttamente o indirettamente partecipanti a numerosi pathways cellulari e, di conseguenza, ne giustifica il coinvolgimento in diverse patologie umane. Molte informazioni disponibili sul VDAC derivano da studi condotti sul ceppo *Δpor1* del lievito *Saccharomyces cerevisiae,* un ceppo deleto del gene *vdac* (*por1*) endogeno. L'assenza del VDAC provoca nel lievito l'impossibilità di utilizzare i mitocondri per effettuare la respirazione cellulare. Questo difetto rende il ceppo *Δpor1* incapace di crescere su fonti di carbonio non fermentabili, come il glicerolo, sia in condizioni normali e soprattutto alla temperatura restrittiva di 37°C. Tale difetto viene complementato in seguito a trasfezione con la sequenza codificante il VDAC umano che, una volta espresso, si inserisce in OMM permettendo così al lievito di recuperare il fenotipo indotto dalla delezione del VDAC endogeno. La complementazione del difetto di crescita del ceppo *Δpor1* si ottiene anche con la sequenza codificante il VDAC (*Porin1*) di *Drosophila melanogaster*, sotto il controllo del promotore per il gene omologo di lievito. In *D. melanogaster* sono espresse due isoforme di VDAC, VDAC1 e VDAC2. *Dm* VDAC1 è dal punto di vista strutturale e funzionale equivalente all'isoforma 1 dei VDAC dei mammiferi o a POR1 del lievito. In seguito al completamento del progetto genoma della *Drosophila* è stata definita l'organizzazione genomica (numero di esoni, di introni, regioni UTR e siti di poliadenilazione) della famiglia dei geni VDAC: 4 geni (*porin1, porin2, cg17139 e gc17140*) disposti a breve distanza l'uno dopo l'altro a formare un *cluster* sul cromosoma 2L. Il gene *porin1* codifica per la principale isoforma VDAC, sempre espressa in tutti i tessuti e stadi di sviluppo della mosca. Il gene *porin1* è formato da 5 esoni, di cui gli esoni 1A e 1B, totalmente costituiti da sequenza 5'UTR, sono tra loro

alternativi. Infatti, in seguito a splicing alternativo vengono prodotti due trascritti contenti all'estremità 5' l'esone 1A o l'esone 1B seguiti dalla medesima sequenza codificante per VDAC. I trascritti alternativi 1A-VDAC e 1B-VDAC vengono prodotti in tutti gli stadi di sviluppo dalla mosca e in tutti i tessuti ma in proporzioni diverse, con 1A-VDAC dieci volte più abbondante di 1B-VDAC. Sorprendentemente, dati di letteratura suggeriscono che il trascritto 1B-VDAC sia improduttivo, ovvero non sia tradotto, facendo così ipotizzare che possa svolgere una diversa funzione cellulare.

In base alle informazioni conosciute, i principali obiettivi di questa tesi sono stati: 1) comprendere i meccanismi molecolari responsabili della mancata traduzione dell'mRNA 1B-VDAC; 2) indagare sul significato in *Drosophila melanogaster* della produzione del trascritto alternativo 1B-VDAC improduttivo. A tal fine, in una fase iniziale del lavoro è stato studiato, nel lievito *S. cerevisiae*, il comportamento delle due varianti di splicing di *porin1* di *D. melanogaster*. Si è così determinato che, in seguito a trasfezione con 1B-VDAC, il lievito *Δpor1* non recupera il fenotipo difettivo, mentre la trasfezione con 1A-VDAC permette al lievito mutante di complementare il difetto di crescita su fonti di carbonio non fermentabili. Questo risultato dimostrava che il trascritto 1B-VDAC nel lievito come nella mosca non è tradotto, suggerendo l'esistenza di un meccanismo di controllo comune in entrambi gli organismi. Considerando che l'unica differenza fra i trascritti alternativi per VDAC riguarda la differente sequenza delle 1A- e 1B-5'UTR, abbiamo concentrato la nostra attenzione su di esse. In particolare, abbiamo innanzitutto verificato che le 5'UTR-1A e 1B svolgessero la stessa funzione anche in associazione a geni reporter come la Green Fluorescent Protein (GFP) e la Luciferase (Luc). Tali studi, condotti sia in lievito che in cellule HeLa, hanno evidenziato che con entrambi i reporter, e in entrambi i tipi cellulari, la sequenza 1A-5'UTR promuoveva la traduzione della coding a cui essa era stata fusa mentre la sequenza 1B-5'UTR inibiva la traduzione delle medesime ORF, in entrambi i tipi cellulari. Questi risultati ci hanno indotto a focalizzare la nostra attenzione sulle differenze esistenti fra le due sequenza 5'UTR alternative allo scopo di individuare soprattutto caratteristiche distintive proprie della 1B-5'UTR in grado di poter influire negativamente sul processo di traduzione. Pertanto, mediante esperimenti di mutagenesi, abbiamo individuato una regione interna alla 1B-5'UTR in grado di influire negativamente sulla traduzione della sequenza codificante la proteina VDAC o la proteina reporter. In seguito poi ad una analisi proteomica effettuata esclusivamente sulle proteine in grado di legare la sequenza interna "regolatoria" della 1B-5'UTR sono

state individuate alcune putative RNA-binding protein (RBP) in grado di svolgere il supposto controllo regolatorio.

Infine si è voluto verificare che i risultati ottenuti in lievito e in cellule di mammifero fossero riproducibili in cellule di *D. melanogaster.* Gli esperimenti di trascrizione e traduzione *in vitro* del gene *luciferase* fuso alle due 5'UTR alternative in esame hanno dimostrato che 1A-Luc è molto più espresso rispetto a 1B-Luc in presenza di estratti cellulari di *Dm*. Tali risultati sono stati poi confermati dagli esperimenti condotti direttamente nelle cellule embrionali S2L di *D. melanogaster*.

Complessivamente, i dati ottenuti consentono di formulare le seguenti ipotesi:

- l'azione inibitoria sulla traduzione operata nel lievito dalla sequenza 1B-5'UTR è probabilmente associata all'azione di specifiche RBP in grado di legare la sequenza interna 16-31. Nel lievito tale meccanismo è di per sé sufficiente a garantire la repressione della traduzione della coding di un gene reporter come dell'mRNA full-length per VDAC, dimostrando così che la 1B-5'UTR contiene tutte le informazioni necessarie a produrre l'effetto inibitorio sulla sintesi proteica nel lievito;
- in *Drosophila* la sequenza 3'UTR del trascritto 1B-porin è indispensabile ai fini della messa in atto del meccanismo di repressione della traduzione dello stesso trascritto. Nella mosca infatti la sequenza 1B esplica il suo effetto inibitorio su coding diverse da quella del gene *porin1* (es. per un gene reporter) e prive della 5'UTR originale. Viceversa, la sequenza 1B non spegne la traduzione della sequenza codificante *porin1* mancante della 5'UTR originaria.
- la 1A-5'UTR rappresenta in generale una sequenza in grado di amplificare la traduzione della sequenza codificante a cui viene fusa. Infatti fondendo la 1A-5'UTR alla coding di geni reporter si ottiene, sia in *Drosophila* come in cellule HeLa, un notevole incremento dell'espressione della relativa proteina. Invece, trasfettando le cellule di mosca con il trascritto eterologo 1A-porin non si ottiene un aumento dei livelli di porina. Ciò induce a pensare che nella mosca le potenzialità della sequenza 1A-5'UTR sono in qualche modo tenute sotto controllo.
- In *Drosophila* la sequenza 3'UTR del trascritto 1A-porin svolge probabilmente un ruolo ai fini del controllo dei livelli di porina endogena. Infatti transfettando le cellule di mosca con il costrutto 1A-VDAC-HA, quindi privo della sequenza 3'UTR, la corrispondente porina è tradotta a livelli di molto inferiori a quelli ottenuti con il costrutto 1B-VDAC-HA.

ABSTRACT

VDAC (Voltage Dependent Anion-selective channel) is a voltage-dependent anion selective channel, a pore forming protein located in the outer mitochondrial membrane (OMM) of all eukaryotic organisms. This protein allows the passage of nucleotides, ions and small metabolites between cytosol and mitochondria. VDAC has a β-barrel structure with its N-terminal forming an α-helix inserted into the pore and involved in the gating process. VDAC takes a maximum open state at voltage around 0mV; while at voltages greater than 20mV, for positive and negative values, VDAC switches to a "closed" state. The crucial role of this channel is dictated by its strategic position, able to interact with many enzymes, proteins or metabolites directly or indirectly involved in several cellular pathways, explaining thus its involvement in many diseases. Most of the available information about VDAC derive from studies conducted on the *Δpor1* strain of *Saccharomyces cerevisiae*, which is devoid of the endogenous VDAC gene (*por1*). Consequently, *Δpor1* yeast strain is unable to use mitochondria to perform cellular respiration. This defect results in the inability for *Δpor1* strain to grow on unfermentable carbon sources, such as glycerol, under usual grow conditions or at restrictive temperature of 37°C. This phenotype is complemented by transfection with sequences coding for mammalian VDACs, showing that heterologous VDACs work as well as yeast VDAC. Interestingly, the growth defect of *Δpor1* yeast strain is recovered also by transfection with the sequence coding for *porin1*, the principal isoform of VDAC in *Drosophila melanogaster (Dm)*. In *Dm* two isoforms of VDAC are expressed, VDAC1 and VDAC2. *Dm* VDAC1 corresponds, considering its structure and function, to isoform 1 of mammalian VDAC, VDAC1, or to POR1 of yeast. The *Drosophila melanogaster* genome sequencing project was completed in March 2000. Thanks to it has been possible to define in fly the genomic organization (number of exons, introns, UTR regions and polyadenilation sites) of VDAC gene family. Exactly, in *Dm* there are four VDAC genes (*porin1, porin2, cg17139* and *cg17140*), tightly closed and forming a cluster on the chromosome 2L. *porin1* gene encodes for the principal VDAC isoform, always expressed in any tissue and in all fly developmental stages. *porin1* gene is made up by five exons, of which exon 1A and exon 1B, being 5'UTR sequences, are alternative between them. In fact, by means an alternative splicing process two transcripts are produced containing at the 5'-end or the exon 1A or the exon 1B, followed by the same coding sequence. The alternative transcripts 1A-VDAC and 1B-

VDAC are produced in all developmental stage of fly and in any tissue. Thanks to a previous work from our team we know that 1B-VDAC transcript is unproductive because it is not translated. This result allowed us to speculate about a different cellular function for this 1B-VDAC transcript, respect the canonical 1A-VDAC mRNA.

Considering all data known, the main objectives of my thesis work were: 1) understanding the molecular mechanisms responsible of the failing of 1B-VDAC mRNA translation; 2) investigate about the meaning in *D. melanogaster* of the alternative unproductive 1B-VDAC mRNA. For this purposes, in the first part of the work, the behaviour of the two alternative splicing variants of *D. melanogaster porin1* has been studied in *S. cerevisiae*. In particular, we determined that 1B-VDAC sequence is not able to recover the defective phenotype of *Δpor1* yeast strain, while the transfection of *Δpor1* strain with 1A-VDAC sequence complemented on glycerol the growth defect of mutant yeast. This result demonstrated that 1B-VDAC transcript is untranslated in yeast, like in fly, suggesting that in either organisms must be a common mechanism acting on the mRNA translation control.

In consideration that the only difference between the two *porin1* alternative transcripts regards the sequence of 1A- or 1B-5'UTR regions, first of all we focused our work on the analysis of them. In particular we wanted to verify if 1A- or 1B-5'UTRs work in the same way of original *porin1* mRNAs also when fused to reporter genes, as *Green Fluorescent Protein* (GFP) or *Firefly Luciferase* (Luc). Therefore, we firstly studied in *S. cerevisiae* and in mammalian cells the effect of 1A and 1B sequences fused to reporter genes: the obtained results showed that, in yeast as in HeLa cells, 1A-5'UTR always promotes the translation of any coding sequence fused to it, while 1B-5'UTR sequence inhibits the translation of the same tested ORFs. These results have thus induced us to focus our attention on the sequence differences present in the two alternative 5'UTRs, in order to identify the distinct features owned in each one 5'UTR. A proteomic analysis was performed exclusively on the proteins able to bind the regulatory sequence inside the 1B-5'UTR; thus we identified some RNA-binding proteins able to play the hypothesized regulative control.

Finally, we wanted to verify that results obtained in yeast and in mammalian cells were even reproducible in *Drosophila melanogaster* cells. Experiments of *in vitro* transcription and translation of luciferase gene fused to the 1A- and 1B-5'UTR revealed that 1A-Luc is much more expressed than 1B-Luc, in the presence of *Dm* cell extracts. Interestingly, by *in vivo* experiments performed by transfection of intact *Dm* SL2 cells

we highlighted that the 1B-5'UTR sequence was able to inhibit the translation only when fused to ORF from reporter gene while was ineffective when fused to *porin1* coding sequence. Our results also demonstrated that 1A-5'UTR sequence is able to produce, in any cell system tested, a remarkable expression increase of each gene reporter fused to it; while, the expression of VDAC protein was significantly reduced after transfection in SL2 cells of heterologous 1A-VDAC-HA mRNA.

Taken together, these data allow to formulate the following hypothesis:

- The inhibitor role played by the 5'UTR 1B sequence on translation in yeast is probably associated to the action of specific RBPs able to bind the inner sequence 16-31. In yeast this mechanism is itself sufficient to guarantee the translational repression of the coding sequence of a gene reporter as well as the full-length mRNA of *porin1* gene, demonstrating in this way that the 5'UTR 1B contains all necessary information for inducing inhibition of protein synthesis in yeast;
- In *Drosophila* the 3'UTR sequence of 1B-VDAC transcript is indispensable for carry out the translational repression mechanism of the same transcript. In fly indeed, the 1B-Luc construct is never expressed while the same 5'UTR-1B fused to the *porin1* coding sequence does not influence translation of the same porin;
- The 5'UTR 1A represents in general a sequence able to amplify translation of any coding sequence fused to it. Indeed, fusing the 5'UTR 1A with coding sequences of gene reporters we obtained always a noticeable increase in the expression of the relative protein. This effect is not detectable in fly cells where, after transfection with the heterologous transcript 1A-porin, an increase of the endogenous amount of VDAC protein is not obtained.
- In *Drosophila* the 3'UTR sequence of 1A-VDAC transcript plays probably a role in controlling endogenous levels of VDAC. Indeed, by transfecting fly cells with the 1A-VDAC transcript which does not contain the 3'UTR sequence, the VDAC protein is only weakly translated.

INDEX

1 INTRODUCTION

1.1 Bacterial and mitochondrial porins

1.1.1 The ancestors of VDAC

Porin represents a specific class of proteins characterized by the ability of inserting in a lipid membrane and forming pores that allow the communication between both side of the membrane. Porins were discovered by Nikado and Varaa in 1985 in the outer membrane of Gram-negative bacteria. In order to protect themselves from a hostile environment, bacteria developed a protective complex cell envelope that allows selective passage of nutrients from the outside, and waste products from the inside. In bacteria three principal layers can be distinguished: the outer membrane (OM), the peptidoglycan cell wall, and the inner membrane (IM). The two membranes delimit two aqueous compartments, the cytoplasm and the periplasm, and are characterized by the presence of different types of proteins. The OM is a specific feature of Gram-negative bacteria because it lacks in Gram-positive bacteria (Galdiero et al.,2012). Proteins intercalated in the OM can be divided into two classes: lipoproteins and proteins that traverse the membrane. Lipoproteins have lipid moieties that fit them in the inner part of the OM and are thus not supposed to be trans-membrane proteins. Proteins that cross the OM can be also divided into three more specific classes: (I) non-specific or general porins, (II) specific channels, (III) high affinity, energy-dependent transport systems.

(I) General porins are water-filled channels whose permeation is based on the concentration of solutes at the two sides of the membrane, and no specific binding-sites are visible in the inner side of the porins (Galdiero et al., 2007; Pages et al., 2008).

(II) Specific channels produce water-filled channels, but, differently from the general porins, they have specific binding-sites that allow the passage of a unique class of solutes and the diffusion rate increases when the amount of solute is low, while it decreases when its concentration is high, following the same kinetic of the Michaelis - Menten enzyme kinetics. This behaviour characterizes this type of

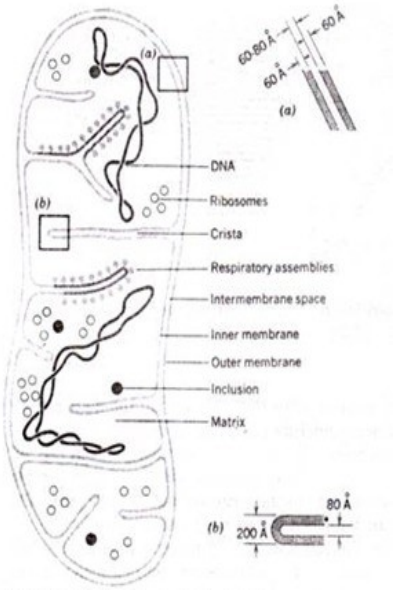

Figure 1: the generalized mitochondrion

porins that for this reason are called channels to distinguish them from the general porins. (III) High affinity, energy-dependent transport systems are protein complexes that work together to allow the passage of a specific solute that binds the site in the channel with higher affinity (Nikaido, 1992). The bacterial general porins, called OMPs (outer membrane proteins) (Schirmer et al.,1995. Forst et al., 1998) have been well characterized and many of them assume a β-barrel conformation serving as molecular filters for hydrophilic substances or mediating the transport of nutrients and ions across the membrane into the periplasm. In some cases some small β-barrels act as anchor and promote bacterial adhesion to mammalian cells. Porins are the most abundant type of proteins in the OM and are essentially trimeric β-barrels forming channels with various grades of selectivity. The first high-resolution X-Ray structure of bacterial porins was published in 1990/1991 and since then many additional porin structures have been determined with a high similarity in architecture. The trimeric structure of porin shows the archetypical fold of 16 β-strands connected by extraplasmic loops and periplasmic turns and these types of porins were classified as general or non-specific porins (e.g. Omp32, OMPrp and Phoe); while 18 strands porins were classified as substrate-specific porins (e.g. Scry and Lamb), both of which are trimeric. Porins are typically of oval shape and the monomer has a dimension of laterally 30-35Å and -50Å in height. The principal feature of this structure is to be a closed barrel, obtained by pairing the first and the last β-strand in an antiparallel way. All strands are connected by eight or nine loops, facing to the extracellular environment and seven or eight small turns to the periplasmic side. Bacterial porins present a constriction at the barrel centre that is formed by the insertion of the long loop L3 that influences the permeability of the pore. OMPs are synthesized in the cytosol with the presence of N-terminal cleavable signal peptides that address them to the periplasm and probably are transported into the periplasm thanks to their hydrophobicity; once arrived in the periplasm, they are refolded into their stable β-barrel conformations and are ready to insert in the outer membrane.

1.1.2 Porins of the outer mitochondrial membrane

Given the similarity between bacteria and mitochondria, it was hypothesized that porin structures could be conserved during the evolution. In fact, the endo-symbiotic hypothesis of the origin of mitochondria and chloroplasts states that they are descendent

from specialized bacteria that were able to survive to endocytosis by another prokaryote, possibly an archeabacterium, to become stably incorporated into the cytoplasm. The symbiont bacteria retained the capacity to conduct cellular respiration using glycolysis and fermentation thus conferring a considerable evolutionary advantage to the host. As it is known, the present mitochondria contain only the genes needed to code for mitochondria-specific proteins, but probably they lost much of their independence, since the protein-coding genes are not enough to organize a whole cell. The endosymbiotic theory proposes that former mitochondrial DNA constantly escaped from the organelle, becoming integrated into nuclear DNA. Nowadays the vast majority of mitochondrial proteins are encoded by nuclear genes, and many of these are endosymbiotic acquisitions from the mitochondrial ancestor. Mitochondria are organelles whose size, shape, structural organization and number per cell can significantly vary depending on the cell type, the specific tissue and, obviously, the organism; for example unicellular eukaryotes contain only one larger mitochondrion. In general, inside the cell, mitochondria usually are concentrated in metabolically active areas of the cell where significant ATP utilization is occurring, and their distribution can change with time. Most mitochondria are ovoid bodies with a diameter between 0.5 and 1.0 μm and a length up to 7 μm; they are enclosed by two distinct membranes, the outer membrane (OM) and the inner membrane. The inner membrane divides the organelle's volume into two places: the matrix, consisting of a gel-like fluid, and the inner membrane space. The matrix contains some enzymes of the Krebs cycle, and suspended in the matrix are various copies of circular DNA and ribosomes. There are also other inclusions like filaments and tubules, as well as granules. The inter membrane space contains some enzymes and generally is devoid of specific inclusions. The inner membrane appears to be thicker (6.0-8.0 nm) than the outer membrane (about 6.0 nm) and has a greater surface area because it has folds that extend into the matrix. These projections are called cristae and noticeable vary in number and shape. The cristae of mitochondria in higher animal cells may almost bridge the matrix. Usually the cristae extend parallel to one another across the long axis of the mitochondrion but in some cells they lie longitudinally or form a network.

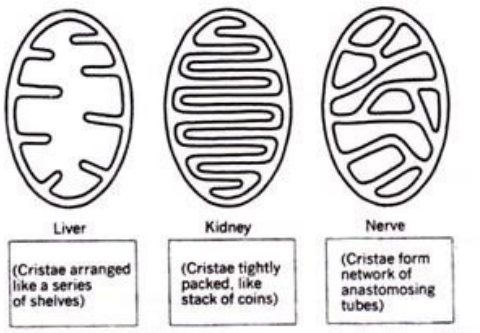

Figure 2: Various arrangements of cristae in the mitochondrion

Chemically, the IM and the OM are qualitatively and quantitatively distinct and also from other intracellular membranes. The IM is much richer in proteins than the OM and the proteins are more deeply anchored in the membrane. The OM contains much more phospholipids than the IM and contains most of the membrane cholesterol; the inner membrane indeed is rich in cardiolipin. Proteins of the IM are extrinsic and attached to the matrix side with spherical diameters of 8.0-9.0 nm which reflect the enzymatic function. In addition to their chemical and structural differences, the two membrane differ in permeability. The OM allows passage of substances of a molecular weight up to 4000 Da while, in contrast, the inner membrane has a reduced permeability and in particular it is only selectively permeable to substances with a molecular weight above 100-150 Da. This difference in permeability is necessary to have different environments where different processes can occur. The permeability of the outer mitochondrial membrane is due to the Voltage dependent anion selective channels, or VDAC, that represents the most abundant protein in this compartment.

1.1.2.1 VDAC, the principal porin of the outer mitochondrial membrane

VDAC is the acronym of Voltage-Dependent Anion Channel for its ability to change its conformation in relation to voltage variations. In particular, it is able to sense the inner membrane potential at level of the junction between the two membranes. The channel properties of VDAC have been studied thanks to reconstitution experiments of the purified protein into a planar lipid bilayer. When inserted in artificial membranes, it shows symmetrical bell-shaped voltage dependent conductance with the highest conductance of 4 nS in 1M KCl at low potentials between -20 and +20 mV (Colombini, 1989). At low potentials, VDAC is in the fully open state and selectively conducts small ions with higher preference for anions, such as phosphate, chloride, adenine nucleotides, glutamate and others. At higher positive or negative potentials, > 30-60 mV, the VDAC conductance is reduced and the selectivity shifts to small cations becoming impermeable to ATP and ADP (Benz, 1994; Shoshan-Barmatz

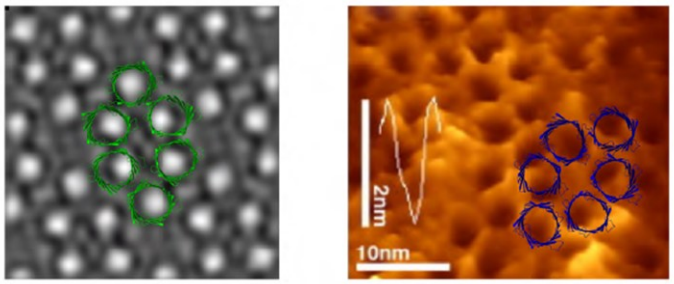

Figure 3: the 3D structure overlaid on EM (left panel) and AFM images (right panel)

et al., 2010). The voltage sensor that responds to changes in transmembrane voltage is believed to be localized in the N-terminal α-helical segment of the channel, but the gating mechanism has not yet been resolved. Its relationship between measured conductance and applied potential can be seen as a bell-shaped curve:

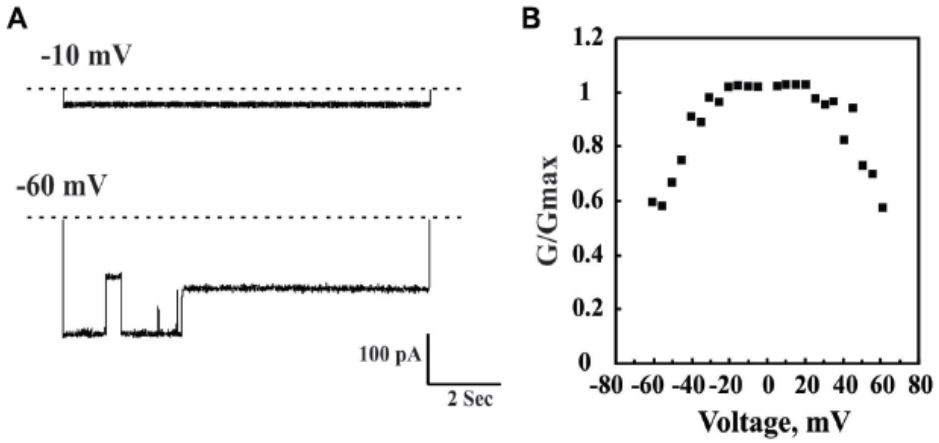

Figure 4: Channel properties of bilayer-reconstituted purified VDAC1. (A) a typical activity recording of VDAC incorporated into a PLB is presented as current traces obtained in response to voltage steps form 0 mV to either -10 or -60 mV. In symmetric solution (1M NaCl), when the voltage was changed from -0 to 10-V, the channel opens and remains stable in this conformation for up to 2h. However, when the voltage was changed from 0 to -60 mV, the current first increased, due to a greater driving force. However, within less than 1 s, channel conductance decreased and VDAC assumed multiple conductance states. The dashed line indicates the zero current level, while the sub-states of the channel are indicated by arrowheads. (B) Multi-channel recordings of the average steady-state conductance of VDAC are presented as a function of voltage. The conductance (G_0) at a given voltage was normalized to the conductance at -10 mV (G_{max}). this voltage-dependent behaviour is well known for VDAC.

1.2 VDAC structure and functions

VDAC is a polypeptide of 283 amino acids and since the mid-1970s various hypothesis have been formulated to understand its transmembrane organization using numerous techniques, including circular dichroism (CD), atomic force microscopy (AFM), electron microscopy, NMR, crystallography and others. The 3D structure of recombinant VDAC1 was finally resolved in 2008 using a combination of the X-Ray crystallography and NMR. Such studies showed a barrel composed of 19 antiparellel and amphipathic β-strands with β1 and β19 being in parallel conformation; (**Fig. 5**) the β-barrel structure forms a pore of 2 nm in diameter.

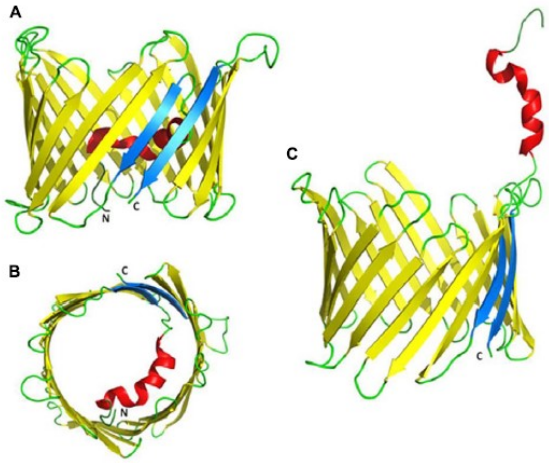

Figure 5: Proposed three-dimensional structure of VDAc1 by Bayrhuber et al.,2008; Hiller et al., 2008; Ujiwal et al., 2008. (A) Side-view of the X-ray crystal structure of mouse VDAC1(Ujiwal et al., 2008) in a ribbon representation. The β-barrel is formed by 19 β-strands and the N-terminal helix is folded into the pore interior. B-strands 1 and 9 are parallel and coloured blue. Loops and unstructured regions are coloured green. (B) Top-view of VDAC1 with the N-terminal inside the pore. (C) VDAC1 in a proposed conformation with the N-terminal outside the channel where it can interact with other

The N-terminal domain of VDAC1 consists of 25 amino acids and has a strong tendency to fold as an α-helix located inside the pore (Ujwal et al., 2008). Because of its localization in the outer mitochondrial membrane, VDAC interacts with various cytosolic proteins mediating metabolic and signaling cross-talk between mitochondria and cytosol (Shoshan-Barmatz et al., 2006). The most important interactions of VDAC1 are with Glycerol kinase (Adams et al., 1991), Creatine kinase (Schlattner et al., 2001), Hexokinase (Azoulay-Zohar et al., 2004; Pastorino et al., 2005; Abu-Hamad et al., 2008), C-Raf kinase (Le Mallay et al., 2002), Tubulin (Rostovtseva et al., 2008b), ANT (Vyssokikh et al., 2003), mtHSP70, as well as Bcl-2 family members (Adams et al., 2007; Llambi et al., 2011).

1.2.1 VDAC and neurodegenerative diseases

Since few years it has emerged that VDAC is involved in various neurodegenerative diseases like ALS (amyotrophic lateral sclerosis), Alzheimer's and Parkinson's diseases and others. For example, Alzheimer's disease, that involves multiple molecular and cellular events, is characterized by synaptic damage and mitochondrial dysfunction. These two events are related to an age-dependent accumulation of Aβ and phosphorylated tau in neurons. Several studies reported also mitochondrial abnormalities like changes in mitochondrial DNA, decreased mitochondrial enzyme activity, increased mitochondrial fragmentation and decreased mitochondrial fusion (Reddy, 2009). In particular Aβ and phosphorylated tau associated with mitochondrial membranes directly interact with VDAC1, resulting in the blockage of mitochondrial permeability transition pores and a disruption in the transport of proteins and metabolites (Manczak et al., 2012; Reddy, 2013).

1.2.2 Involvement of VDAC in Amyotrophic Lateral Sclerosis (ALS)

Amyotrophic lateral sclerosis is a neurodegenerative disease characterized by the progressive degeneration of motor neurons. About 20-25% of familial ALS cases are associated to the presence of mutations in the superoxide dismutase 1(SOD1) and the mutant SOD1 is able to produce aggregates which associate with the cytoplasmic side of mitochondria, causing the mitochondrial failure. One of the most known mutations of SOD1 is the G93A. It has been demonstrated that mutant SODG93A, but not the wild type SOD1, is able to interact with VDAC reducing the VDAC cannel activity and producing thus mitochondrial dysfunction and cell death. VDAC represents the physiological receptor of Hexokinases, which catalyze the glucose phosphorylation and, by binding to VDAC1, they can preferentially access to ATP. When HKs bind to VDAC1, VDAC loses its propensity to interact with pro-apoptotic protein Bax, resulting in the protection of cell from apoptosis. Since in spinal cord of ALS rat have been detected reduced levels of HKs, degeneration of motor neurons is correlated to high levels of mutant SOD1G93A which interact with VDAC1 (Magrì et al., 2016).

1.2.3 Human VDAC: three different isoforms

Three isoforms of VDAC protein, VDAC1, VDAC2 and VDAC3 have been identified in mammals (Blachly-Dyson et al., 2001). These VDAC isoforms share approximately 70% identity with functional and structural homology. The three proteins have similar molecular weight (30-35 kDa) and are expressed in all tissue types, with VDAC1 higher by one or two orders of magnitude than the other two isoforms (Messina et al., 2012), and play different roles inside the cell. Recombinant VDAC1 and VDAC2 showed channel activity upon reconstitution into an artificial planar lipid bilayer (PLB) and recently hVDAC3 was also reconstituted into PLB showing slight voltage-dependent conductance (Checchetto et al., 2014) . VDAC1 was firstly thought to be localized exclusively in the OMM, but afterwards it was found in cell compartments other than mitochondria, including the plasma membrane (De Pinto et al., 2010), the sarcoplasmatic reticulum of skeletal muscles (Shoshan-Barmatz et al., 1996), the endoplasmic reticulum (ER) and in caveolae and caveolae-like domains. This kind of channel is thought to contain an N-terminal signal peptide responsible for targeting to the cell membrane (Buettner et al., 2000), but this form of the protein remains a matter

of dispute. The three-dimensional structure of the principal isoform of VDAC, VDAC1, was determined at atomic resolution by three independent groups in 2008 (Bayrhuber et al., 2008; Hiller et al., 2008; Ujwal et al., 2008). Mouse VDAC1 differs from human VDAC1 by just four amino acid substitutions that are, threonine 55 to asparagine, methionine 129 to valine, alanine 160 to serine and isoleucine 227 to valine. In contrast to VDAC1, structural characterization of VDAC2 and 3 is rather limited. Recently, the structure of Zebrafish VDAC2 was resolved at 2.8 Å resolution, revealing to be dimeric (Schredelseker et al., 2014). VDAC3 differs from the other two isoforms for the presence of six cysteines exposed to the oxidizing environment of the mitochondrial intermembrane space, with the possibility to form different types of intramolecular disulfide bonds, modulating its size pore and current (Guardiani et al., 2016).

1.3 *Saccharomyces cerevisiae* life cycle

S. cerevisiae is one of the most widely used eukaryotic model organism to study aging, regulation of gene expression, signal transduction, cell cycle, metabolism, apoptosis, neurodegenerative disorders, and many others biological processes. At least 30% of genes implicated in human diseases may have orthologous genes in the yeast proteome. *S. cerevisiae* is an unicellular organism which have different phases in its life cycle. In the presence of sufficient nutrients, yeast cells duplicate every 100 minutes or so. The haploid cell has 17 chromosomes that are duplicated during the mitotic cell cycle and then distributed to each cell. The "mother" cell gives rise to an ellipsoidal daughter cell constituted of new cell surface material. Under particular environmental conditions yeast cells abandon the proliferation mode.

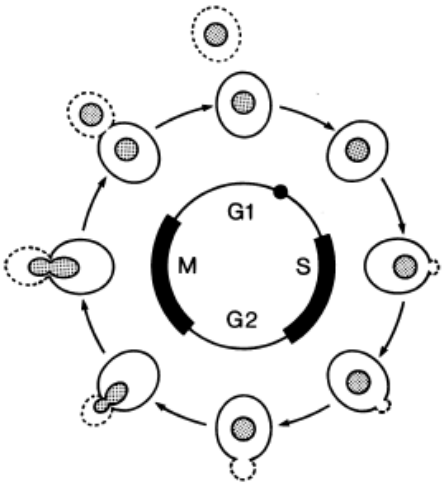

Figure 6: S. cerevisiae mitotic cell cycle. The phases of the cell cycle are in proportion of their length. The mother cell is drawn with a solid line; the daughter bud and cell are drawn with a dotted line. The shaded material represent the cell nucleus

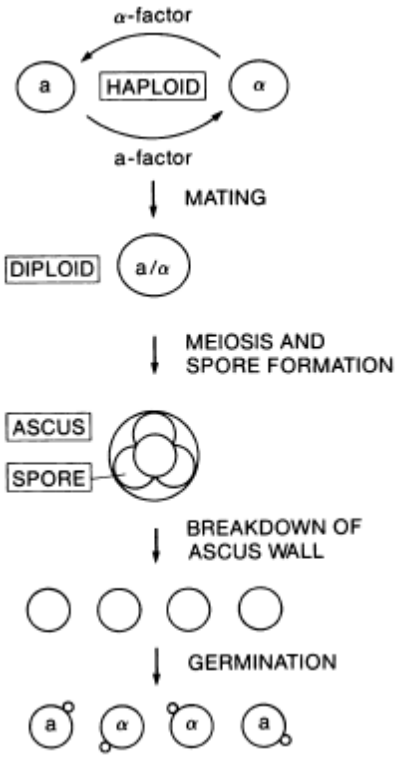

Figure 7: Transition of the life cycle of *S. cerevisiae*. All three cell types a, α and a/α, are capable of undergoing mitotic cell division. In this diagram is explained the transition that occur in the life cycle: mating of haploids yields a diploid and meiosis of a diploid yields haploid cells. a/α cells produce an ascus, which contains the four haploid spores that result from the meiosis of the diploid cell. The germinating spores have a specific mating type.

For example, when nutrients are not enough, they stop as unbudded cells in the G1 phase of the cell cycle, where they survive well, whether nutrients are available. Another environmental influence that arrests the proliferation mode is the proximity of another yeast cell with which it can mate. In fact, the partner cell, of different mating type, transiently arrests other's cell cycle in the G1 phase and then undergoes cell fusion. *S. cerevisiae* can exist in three specialized cell types, a, α and a/α, which play different roles in the life cycle. All cell types undergo mitotic cell divisions. The mating type a and α can mate efficiently each other, producing a diploid cell thanks to cell and nuclear fusion. The product of mating is the zygote that has a distinctive shape and gives rise to daughter diploid cells by budding. The a/α diploid cell is the third specialized cell type and it is unable to mate with either a or α cells. However it undergoes meiosis forming four haploid meiotic progeny, each of which is contained in a spore coat. All four products from a single meiosis are enclosed together in a sac, the ascus (Herskowitz, 1988).

1.3.1 Yeast VDACs: *por1* and *por2*

For its characteristics, *S. cerevisiae* is one of the most important model organisms used in molecular biology, pharmacology and medical research. Being an unicellular organism it is easy to study metabolic pathways that resulted to be largely conserved. Considering the importance of VDAC, it has been thought, for a long time, that in *S. cerevisiae* there is only a single VDAC gene. This gene, named *por1,* encodes a 283-aminoacids protein which forms pores well characterized in artificial phospholipid bilayer. The presence of another VDAC isoform emerged when a Δ*por1* yeast strain was produced. As VDAC is responsible for the primary pathway for the movement of metabolites across the OMM, it was expected that cells without VDAC

were not able to perform respiration. Surprisingly, Δ*por1* cells were able to grow on glycerol-based media at elevated temperature (37°C) (Blachly-Dyson et al., 1990). In this way a second yeast VDAC gene (*por2*) was identified. YVDAC2 has 49% amino acid sequence identity to the previously identified VDAC protein,YVDAC1. The ability of YVDAC2 of forming pores is actually under investigation.

1.4 *Drosophila melanogaster*: an important model organism for genetic and molecular studies

1.4.1 *Drosophila* life cycle

Drosophila is a holometabolous insect, with larval and pupal stage prior to the adult stage. The adult *Drosophila* live for more than 10 weeks and during this time, mating takes place. Fertilization is internal and, inside the female's body, the sperms are stored in a seminal receptacle. The higher egg production occurs between the fourth and seventh day after females emerge and eggs hatch in 22-24 hours at 25°C. The larva that emerges is called the *first instar larva*. After 25 hours, it molts into a larger wormlike form, the *second instar larva*, that molts again into the *third instar larva,* after another 24 hours. This is the largest form of larva and it starts to climb upward out of its food, in order to undergo pupation after 30 hours. The pupa is a stationary stage where larva is metamorphosing into the adult fly, also called the *imago*. During this period, pupa lyses most of the larval structures, except the Malpighian tubules, fat bodies and gonads that are kept as well. After 3-4 days of pupal stage, the adult, or imago, emerges from the pupal eclosion. Adult males are sexually active within hours of emerging, while females don't have ripe eggs until two days after eclosion.

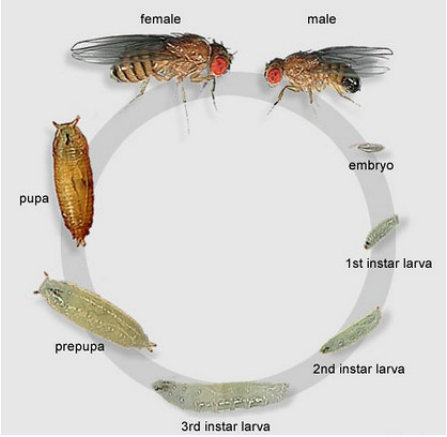

Figure 8: The life cycle of *Drosophila melanogaster*

1.4.2 A powerful model system for studying human diseases

Drosophila melanogaster is considered an important and powerful model system for understanding the basic biological etiology of human disease and development, thanks to the higher degree of conservation of fundamental biological processes coupled with the broad repertoire of genetic approaches (Bier, 2005; Pandey et al., 2011; Ugur et al., 2016). In fact, 75% of human disease-related genes have a functional homologous in *Drosophila* (Chien et al., 2002; Reiter et al., 2001), and homologous human and fly proteins share about 40% sequence identity and this increases to 80-90% or higher in conserved functional domains (Rubin et al., 2000). *Drosophila* has about 14,000 genes organized in four chromosomes and three of these represent 96% of the animal's genome (Adams et al., 2000). Compared to humans, the fly has 1/20 as much DNA, 1/8 as many chromosomes and 1/2 as many genes (Lander et al., 2001; Venter et al., 2001). The fly is an accessible model to work with thanks to the rapid generation time (8.5 days at 25°C); large family size (with hundreds of genetically identical progeny within days), and small size (Ashburner et al., 1987). At the organismal level, the fly has many structures equivalent to the human such as heart, lung, liver, kidney, gut, reproductive tract and brain (Behr, 2010; Jeibmann et al., 2009; Lesch et al., 2012; Roeder et al., 2012; Wolf et al., 2008; Ugur et al., 2016). In the fly brain there are more than 100,000 neurons, which govern insect locomotion, circadian rhythms, mating, aggression and feeding (Simpson, 2009). For example, thanks to the visual system of the adult fly, we have key information about vision as well as development (Baker et al., 2014; Borst et al., 2015; Paulk et al., 2013; Wernet et al., 2014). Two methods have proven successful in generating *Drosophila* models for human congenital disorders: the forward and reverse genetic approaches.

Forward genetic screen consists in a random genome-wide mutagenesis to generate progeny with an aberrant phenotype(s). Identification of individual mutated genes permits to discover genes involved in any given process. Identification of different genes with shared loss-of function phenotypes leads to the discovery of genetic pathways. Traditionally, X-ray, chemical and transposon mutagenesis were used for forward genetic screens in *Drosophila*, which have uncovered numerous genetic pathways involved in development and conserved in humans. Reverse genetic screen instead starts from the targeted mutagenesis of any given gene designed to understand the gene's biological function. Mutagenesis can be obtained via numerous mechanisms,

such as RNAi and CRISPR/cas9. With the RNA interference method cells are depleted of a specific target mRNA. A cytoplasmic double-stranded RNA is expressed in the cell and processed into a single-stranded RNA molecules that are used then as templates to target and degrade complementary mRNA in the cell. The CRISPR/Cas9 method induces double-stranded breaks in the genome. Cas9 binds the guide RNA that pairs with genomic DNA and induces the double breaks. Improper repair at these breakpoints in the germline cells lead to mutations that can be isolated in the next generation. The double-stranded breaks can induce also the incorporation of foreign DNA containing homology arms surrounding the break point.

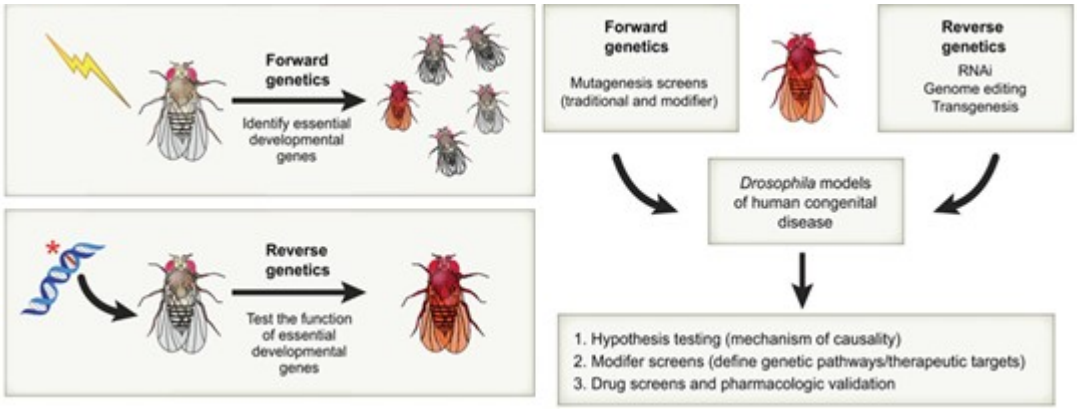

Figure 9 : Forward and reverse genetic approaches in Drosophila. Forward genetics uncovers the genetic basis of phenotype. Mutagenesis by any means is used to generate mutant flies with aberrant phenotypes (indicated by the red fly), which are used as a starting point for gene discovery. Reverse genetics refers to the discovery of gene function through the targeted disruption of genes (here indicated by an *) and the analysis is of the resulting phenotype(s).

1.4.3 Studies of VDAC in *Drosophila melanogaster*

One of the first analysis of *Drosophila melanogaster* VDAC was done by Messina and coworkers., 1996. They purified VDAC from adult flies and used it as antigen to raise antibodies in mice. The antibodies were highly reactive against *Drosophila* VDAC and thus were used for screening a λgt11 *D. melanogaster* cDNA library. A positive clone was subcloned into the pUC 19 vector and the whole inserted sequence was sequenced. The subclone was used as a probe to isolate larger cDNA clones and several messages were collected. The coding sequence contained 840 nucleotides, including the starting ATG. By Edman degradation of the N-terminal sequence of the purified polypeptide, was confirmed the identity of this protein as *D. melanogaster* mitochondrial porin VDAC. The open reading frame corresponded to a protein of 279 amino acids and its deduced molecular weight was 30189 Da.

Comparison with other knows Porins showed the 55,7 % identity with HVDAC2, the 52% with bovine VDAC, the 30,3% with N. crassa VDAC and others.

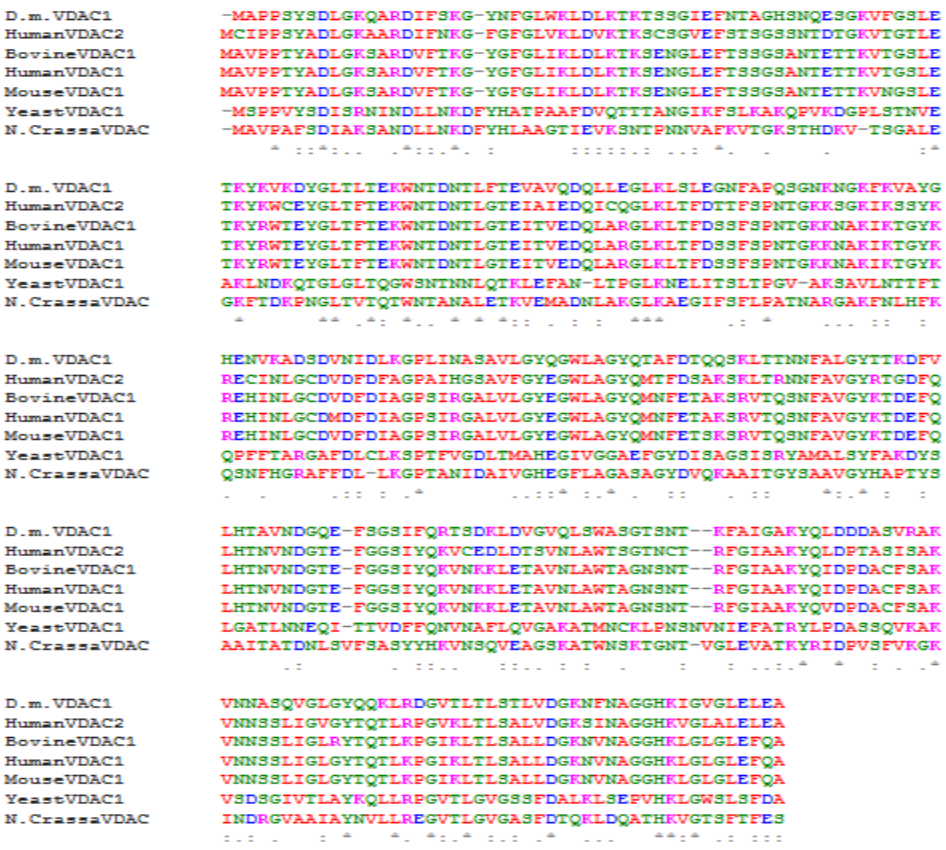

Figure 10: multiple alignment of VDACs from different species

1.4.4 Genomic organization of the *porin* gene: three *porin*-like genes are located near the *porin* gene locus.

In all studied organisms more than one VDAC isoforms are present in the genome. In *Drosophila melanogaster* the 31-kDa VDAC protein encoded by the *porin1* gene shares significant homology with the predicted proteins encoded by three genes that flank the *porin1* gene at the chromosomal position 32B3-4. The genomic organization was deduced in silico by alignment of the genomic sequences with the EST sequences in the BDGP collection. The four transcription units are all on the same strand, and the coding sequences are all interrupted by two introns of similar length, and in particular the first exon occurs at the same position in all four genes. On the other hand, the intron in the 5'UTR is only present in the *porin* gene. The distances separating the four *porin*-like genes are very short and this suggests that they may be transcribed as a polycistronic transcript. When VDAC protein was aligned with the predicted proteins derived from the three flanking genes, it was observed that VDAC and CG17137

differed from CG17139 and CG17140 sequences because the latter pair possessed an additional sequence preceding the standard N-terminus. The CG17137 is also characterized by the insertion of a 10-amino acid stretch at position 290, that encodes for an acid cluster that is only found in this protein; this *porin*-like gene was named *porin2*. The highest sequence conservation was observed between VDAC and CG17137 (42% identity and 65% similarity), and between CG17139 and CG17140 (47% identity and 67% similarity). A lower homology was observed between VDAC and CG17139/CG17140 (23% and 26% identity and 42% and 44% similarity, respectively) (Oliva et al., 2002).

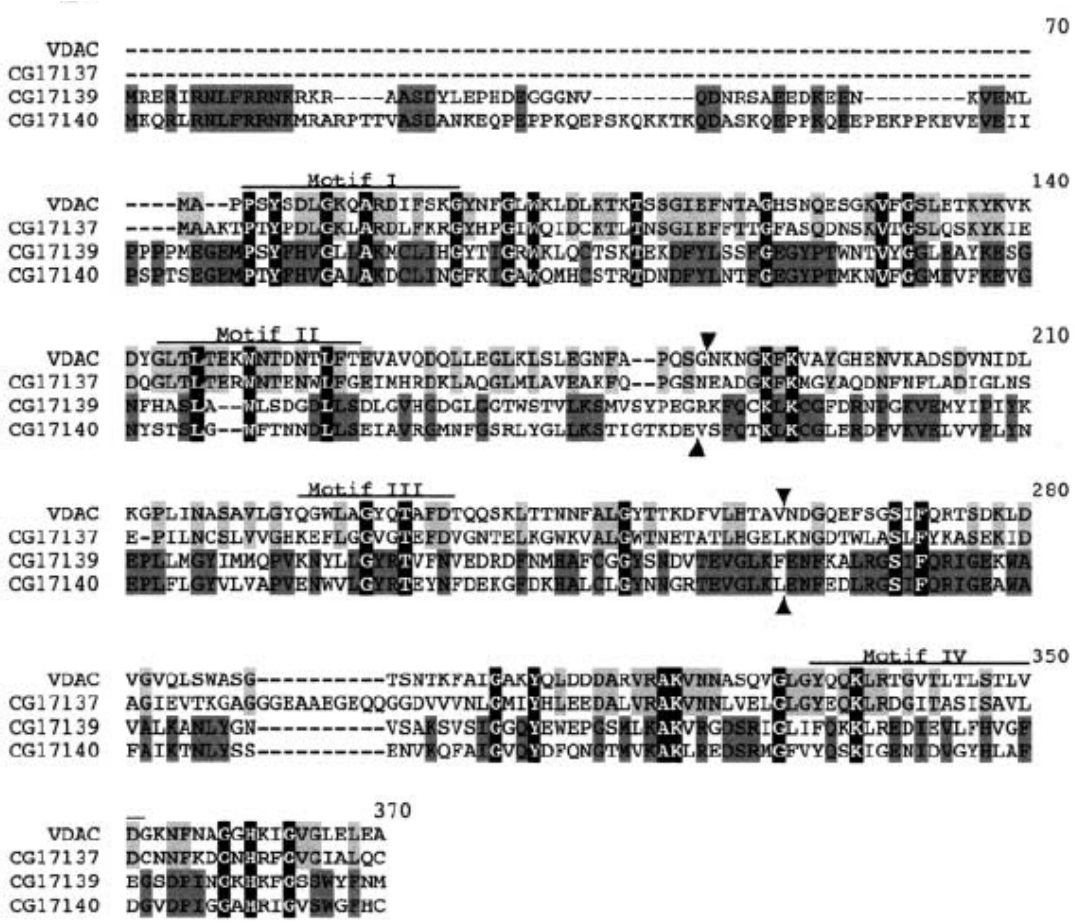

Figure 9: Comparison of VDAC with the predicted proteins from the three porin-like genes

1.4.5 Characterization of the second isoform of *porin* in *Drosophila melanogaster*

Given the elevated homology between *porin1* gene and CG17137, recombinant proteins were produced using pQE30 expression vector, expressed into BL21 bacterial cells. Since the electrophysiological properties of the purified and refolded *Dm*VDAC1

in black lipid bilayer membranes were identical to those measured with the native mitochondrial VDAC of *D. melanogaster*, the features of recombinant DmVDAC2 were studied. Recombinant DmVDAC2 was purified from inclusion bodies and refolded, showing a pore forming activity in lipid bilayer membranes with a long lifetime at low voltage. DmVDAC2 preferentially formed channels with a single channel conductivity of 4,5 nS in 1M KCl. The channel forming activity however was lower than that of DmVDAC1, since at least a 10 times highest concentration of DmVDAC2 was needed to obtain the same number of reconstituted channels as compared with DmVDAC1. The voltage dependence of DmVDAC2 was also investigated, and most surprising, DmVDAC2 did not display any voltage dependence. Furthermore, DmVDAC2 showed preferential movements of cations through the channel, indicating that the two VDAC isoforms exhibit different ion selectivity (Aiello et al., 2004).

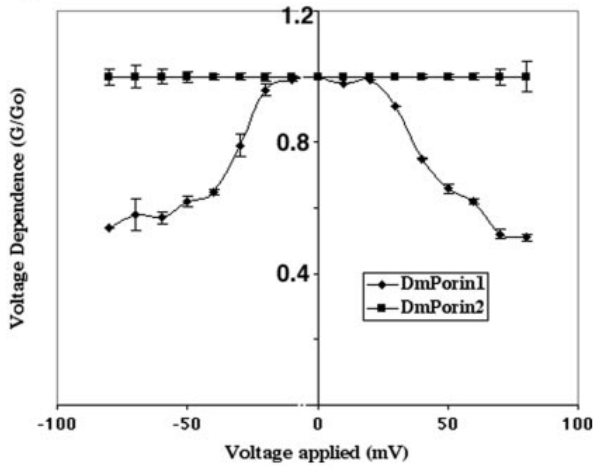

Figure 12: Voltage dependence G/G_0 comparison of DmVDAC1 and DmVDAC2. Voltage dependence *G*/*G*0 comparison of DmVDAC1 and DmVDAC2. Voltage dependence *G*/*G*0 was a function of the applied voltage. DmPorin2 is not voltage-dependent.

1.4.6 Identification of alternative 5'UTRs in *porin* transcripts

As reported in Oliva et al. 1998, to study the genomic organization of *porin1* gene in *Drosophila melanogaster*, a published cDNA clone containing the whole transcript sequence for VDAC (1370 bp), named 7T21 (acc. No. X92408) (Messina et al., 1996) was used as a probe to screen a genomic library in EMBL3 derived from Canton-S strain. The clone EM1T was chosen for further analysis of sequencing. The

exons of *porin* were identified by comparison of the genomic sequences with the cDNA. The consensus dinucleotides for splice sites, GT and AG, were respectively found next to the 5' end 3' boundaries of the introns, showing that the *D. melanogaster porin* gene contains four exons separated by three introns. The beginning of the first exon was deducted by 5'RACE-PCR experiments performed on *D. melanogaster* Oregon-R third instar larvae poly(a)+ RNA. After reverse transcription, nested primers were designed in the DNA protein-coding region and the amplified PCR products were sub-cloned into a T-vector plasmid and some positive clones were sequenced. Sequence analysis showed the expression of two different 5'-untranslated extensions fused to the coding sequence. The ratio between the two 5'UTRs was 10:1 for the 5'UTR corresponding to the cDNA 7T21 sequence. The second sequence instead corresponded to another genomic region enclosed between exons I and II. This sequence is followed by the –GT splice-site canonical sequence. The exon corresponding to the cDNA was indicated as exon 1A, while the new one, corresponding to an alternative mRNA was named exon 1B. Exon II (320 bp) and exon III (228 bp) exclusively contain coding sequences. The first three bases of the exon II correspond to the ATG starting codon, while the TAA stop codon is contained in the remaining 298 coding bp in the exon IV, together with the 3'UTR sequence. Two putative poly-adenylation sites were detected in the 3'UTR at the positions 3607 and 3904.

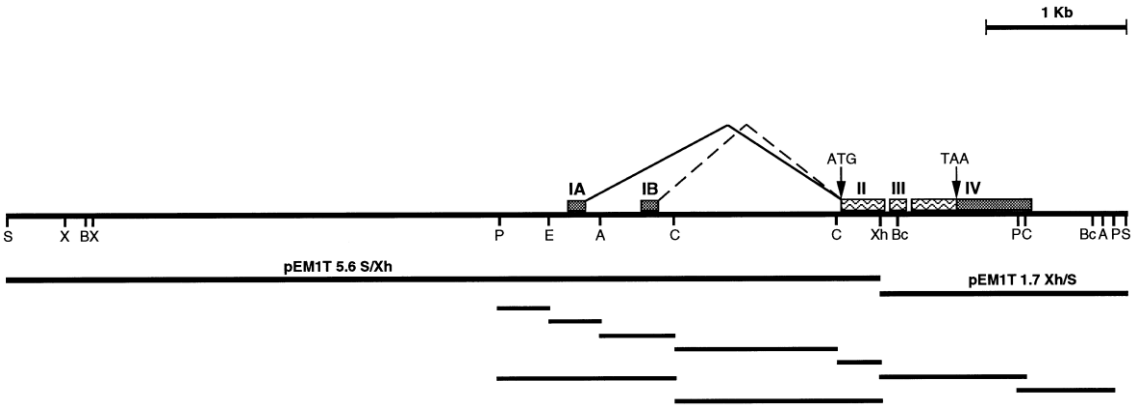

Figure 13: Structural organization of D. melanogaster *porin* gene (clone EM1T)
Exons are shown as boxes above the line and are numbered IA (486^600), IB (1014^1137), II (2485^2805), III (2881^3108), IV (3178 to the end). The positions of the ATG starting codon and of the TAA stop codon are evidenced. Exon II precisely starts with the ATG. Coding regions are clearer, while non-coding regions are shadowed. ER sites are indicated (A: AccI; B: BamHI; Bc: BclI; C: ClaI; E: EcoRI; P: PstI; S: SalI; X: XbaI; Xh: XhoI). IA and IB are two alternative leader exons. Under the gene structure the clones sequenced are reported. A SalI/SalI clone of about 7 kbp from an EMBL3 *D. melanogaster* genomic library was analyzed.

1.4.7 Analysis of developmental specificity of VDAC transcript containing the exon 1B

In *D. melanogaster* there is a low over-representation of specific sequences of *Drosophila* promoters. Concerning exon IA, a TATA sequence is placed at 441, but its position is -45 with respect to the transcription starting site. Also a CAAT sequence was found on the reverse strand at 405 (-80), and a CCAAT, also on the reverse strand, was found at 920 (-84) with respect to the transcription starting site of exon IB; two regions rich in GC, but without canonical sequences and no putative TATA-box were observed between this location and the IB transcription starting site. To verify the *in vivo* production of the VDAC transcript containing the exon IB, and to study its possible developmental specificity, RT-PCR experiments were performed on poly(A)+ RNAs from *D. melanogaster* embryos, larvae and adults of both sexes. The primers used were Por1R, a primer derived from the exon 1B, and two primers localized upstream the two putative poly-adenilation sites, por3F and Por2F.

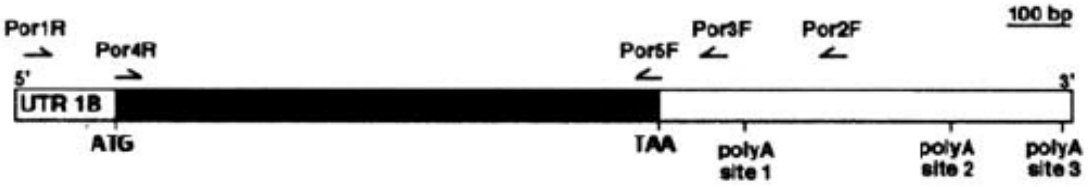

Figure 10: A VDAC mRNA with an alternative 5'UTR is constitutively expressed in *Drosophila melanogaster*. RT-PCR analysis was performed on poly(A)+ RNA from Oregon-R. Schematic representation of the transcript encompassing sequences complementary to exon 1B. possible polyadenylation sites are marked. The translated region is indicated by the filled box.

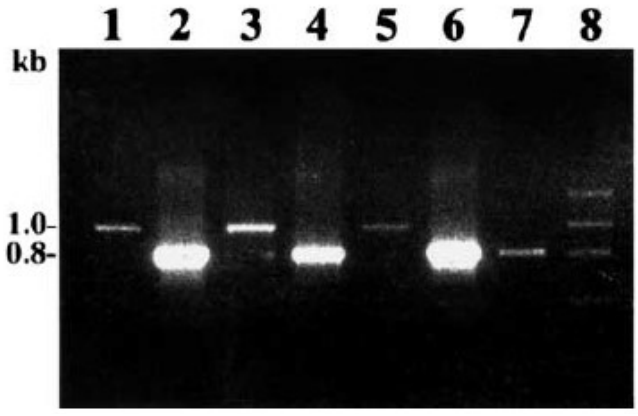

Figure 11: Agarose gel showing amplified RT-PCR products. In the lanes 1, 3 and 5 the Por1R primer which is specific for exon 1B, was used together with Por3F primer, derived from the 3'UTR. The resulting products were re-amplified using Por4R and Por5F primers, inside the coding sequence (lanes 2,4,6). Lane 1, poly(A)+ RNA template isolated from 0-3 h embryos; lane 3, poly(A)+RNa template isolated from third-instar larvae; lane 5, poly(A)+RNA template isolated from adult flies; lane 7, control obtained by amplification on the porin cDNA with internal primers.

A single amplification product of the expected length (1065 bp) was observed at all developmental stages with the Por3F primer, but no product was observed using the Por2F primer. A nested PCR experiment using two primers on the coding sequence (Por4R and Por5F) verified that the amplification products of the expected length (849 bp), were obtained. Sequence analysis of the 1065-bp

amplification product confirmed that the transcript without the exon IA and which uses the first polyadenilation site is present at all developmental stages tested. Mobilization of a P-Element (PlacW) inserted in the *porin* gene at the position 32B3-4 region of 2L chromosome, produced different kinds of mutants that have specific features. In particular, the PlacW element causes the lethal phenotype that can be reverted by precise or almost precise excision of the transposon in the *porin* gene. This experiments showed that exon 1B is not necessary for VDAC synthesis or for fly viability, since the total content of VDAC did not vary after 1B excision; conversely, exon 1A is indispensable because its excision caused the decrease of the total amount of VDAC protein (Aiello et al., 2004).

1.5 The roles of RNA-binding proteins in post-transcriptional functions

In *Drosophila melanogaster* and in many others eukaryotes, gene expression needs a dynamic interplay between proteins and RNAs. The synthesis of RNAs involve the formation of ribonucleoprotein particles (RNPs) (Draper, 1995) ranging from small to large complexes. The interactions between proteins and RNA occur through one or more RNA-binding domains or *via* another protein that is itself directly bound to RNA (Glisovic et al., 2008). NOVA2, PTBP1, U2AF2, and RBFOX2, are examples of proteins that interact with RNA in a largely sequence-specific manner (Lewis et al., 2000; Jin et al., 2003; Kielkopf et al., 2004; Hall et al., 2013). In contrast, the protein SMN, which is involved in snRNP biogenesis, does not have any known RNA-binding domain and interacts with the snRNAs indirectly. RNA-binding proteins (RBPs) play a crucial role in cellular biology of higher eukaryotic organisms. RBPs indeed, participate in several essential post-transcriptional events, including pre mRNA splicing, 3' end formation, RNA localization, turnover and translation (Glisovic et al., 2008). The Fragile X Mental Retardation Protein (FMR1) is one example of a pleiotropic RBP, encoded in *D. melanogaster* by *Fmr1*. FMR1 interacts with components of the RNAi machinery, forming a complex which includes Argonaute 2 (AGO2) of the RISC (RNA-induced silencing complex) complex (Ishizuka et al., 2002). FMR1 also binds ribosomes to block translation by inhibiting tRNA association (Chen et al., 2014a). RBPs recognize their RNA target through RNA-binding domains. In *D. melanogaster* there are common classes of RNA-binding domains, including the RNA-recognition

motif (RRM), the K homology domain (KH), both zinc finger motifs and the double-stranded RNA-binding motif (dsRBM). The difficult to identify functions of RBPs with their RNA-binding domains is due to the fact that there is no one-to-one mapping between domains and functional roles, and many RBPs with characterized functions appear pleiotropic. Many genes involved in post-transcriptional regulation tend to be often regulated post-transcriptionally. Feedback loops are considered the principal idea at the level of a regulatory process. Analysis of RBP and mRNA interaction profiles show ubiquitous interaction with mRNA and proteins products of the same gene; furthermore, RBPs of the same protein complex tend to reciprocally bind the mRNAs of their interaction partners. Post-transcriptional regulation, mediated by protein-RNA interaction, is a common process and constitutes a general mechanism of feedback in the hierarchy of gene regulation (Marcus et al., 2015).

1.6 Example of splicing regulation of *Drosophila melanogaster* genes

Alternative splicing is a mechanism by which multiple mRNA from a single gene can be created, connecting different parts of a pre-mRNA. Alternative splicing can affect 5'- and 3'- untranslated regions of mRNAs modulating translation, stability or localization of mRNA. Also, by modulating insertion and exclusion of coding exons, the percentage of protein diversity dramatically increases. Moreover, using alternative splicing cells can produce functionally different proteins from a single gene in a temporal- or tissue-specific manner. In human, about 95% of gene undergo to an alternative splicing process, but the effects of these events are mostly unknown. Pioneer studies in *Drosophila* have shown the presence of regulatory sequences in the pre-mRNA required for alternative splicing regulation as well as some regulators that bind to them. *Drosophila* is known to use every alternative splicing strategy imaginable and there are a lot of examples as demonstration. The first example is the sex-specific splicing, since in *Drosophila* sex determination is controlled by splicing factors that lead to the sex-specific expression of two different variants of the Doublesex (Dsx) transcription factor. Splicing factors are themselves alternatively spliced, and the Dsx variants are differentially expressed in male and female bodies to control different set of genes. Moreover, the key splicing difference between male and female is the expression in females of the Sex-lethal (Sxl) protein that is expressed in embryos in response to X

chromosomes number, determining female development. In female a full length Sxl protein is expressed, while in males a truncated form of the protein is produced. Sxl is responsible for multiple aspects of female differentiation, governing several sets of genes.

Another important example of alternative splicing is given by the expression of the myosin heavy-chain gene (Mhc), which has in-frame alternative exons in five different regions (exons 3, 7, 9, 11 and 15) and a cassette exon (number 18) encoding the C-terminus. In this case, by multiplying these independent choices, 480 different myosin isoforms could be potentially produced in *Drosophila*, and therefore, different muscle types express specific Mhc isoforms through specific combinations of exons, in order to finely control the contractile properties of each kind of muscle.

Control of the alternative splicing. Usually, it represents an independent recruitment to the pre-mRNA of RNA-binding proteins. Most of them are direct or indirect controllers of one or more alternative splicing events, but not only alternative splicing factors, but also proteins previously considered as constitutive. Many and big differences are found in gene structure between *D. melanogaster* and mammals. For example, in humans, the dimensions of introns are usually much bigger than exons; in *Drosophila* the reverse is true, and also multiple variants of mutually exclusive exons and recursive splicing are not present in mammals. Moreover, the trans-splicing, which is very common in *Caenorhabditis elegans* and in *D. melanogaster*, is not found in mammals. On the other hand, between mammals and insects there is an extensive conservation of alternative splicing patterns. The spliceosome dynamics and composition are very similar between them and most known mammalian splicing factors have orthologous in flies. These include members of SR protein family (Gabut et al., 2007; Blanchette et al., 2005) , the hnRNP/hrp family and other like Tra2, TIAR/Rox, PUF60/pUf68. This means that studies in flies are highly relevant to the mechanisms of alternative splicing in humans and to understand the way that evolution adapts it to its needs.

1.7 The function of RNA structure at 5'UTR in gene regulation mediated by microRNA

The 5' untranslated region (5'UTR) of mRNA is the sequence preceding the start codon of translation, which plays important functions in regulating post-transcriptional events (Davuluri et al., 2000). In the 5'UTR has been found several regulatory elements, such as RNA binding sites for RNA binding proteins (RBPs), upstream open reading frames (uORF) and upstream start codons (uAUGs) that, together with the ability of the 5'UTR to assume a mRNA secondary structure, all these elements have been recognized as a major feature that regulates gene translation (Pickering et al., 2005). For example, in human about 60% of 5'UTRs present a structured RNA near the 5'cap site, which alone is able to block translational initiation. Recently, has been highlighted the role of 5'UTR in mRNA repression mediated by miRNA (Djuranovic et al., 2012), which is a class of non coding RNAs, 20-24 nt in length, that regulate gene expression by base-pairing with complementary sequences in mRNA transcripts. Usually miRNA acts silencing or degrading RNA (Bartel, 2009). The mRNA-miRNA interaction affects expression of the gene target at early stages of translation, i.e., translation initiation. For example, in *Drosophila* S2 cells, gene silencing mediated by miRNA occurs through translational inhibition, by mRNA deadenylation and subsequent decay. In HeLa cells, the function of the eIF4F initiation complex is impaired by mRNA-miRNA interaction confirming that the secondary structure of the 5'UTR is necessary to miRNA-mediated gene silencing. (Meijer et al., 2013). Moreover, Wanjun gu et al., 2015 found that mRNA secondary structure near the 5'cap, rather than the full length 5'UTR is increased to facilitate miRNA-mediated gene regulation, showing a universal trend of increased mRNA stability near the 5'cap in genes with miRNA targets (Wanjun et al., 2015).

2 AIM OF WORK

In *Drosophila melanogaster* the *porin1* gene produces two splice variant transcripts (1A-VDAC and 1B-VDAC) comprising the same VDAC coding sequence, starting from the ATG located just at the beginning of 2nd exon, fused with upstream alternative exon regions (1A- or 1B-exon) containing only the 5'-untranslated (5'-UTR) sequence. The biological significance in *D.m.* of these two forms of VDAC mRNA is unknown. In this work, we have studied the influence of the two 5'-untranslated regions, 1A-5'UTR and 1B-5'UTR, on the expression and translation of the VDAC and reporter genes in yeast, fly and mammalian cells. Preliminary data proved that in flies, the insertion of P elements in the *porin* locus abolishes VDAC expression and produces a lethal phenotype (Oliva et al., 2002). Moreover, the imprecise excision of such P elements showed that deletion of only exon 1B and its flanking introns apparently had no effect on normal development, while the deletion of exon 1A was by itself sufficient to severely reduce the level of the expressed VDAC protein (Oliva et al., 2002). Since the locus carrying the 1A deletion still contained an intact promoter and the entire coding sequence of VDAC, but nevertheless was unable to produce any protein, suggests that protein levels must be regulated post-transcriptionally by alternative splicing of exon 1A and 1B.

Considering that in *D.m.* these two VDAC alternative splice variants are expressed in the same tissues at the same time, previous results left open some questions. The first question is: what is the function of an unproductive VDAC transcript in a cell where a functional protein is always produced from the transcript 1A-VDAC? The second question is: what is the mechanism responsible for the inhibition of 1B-VDAC translation?

In order to answer to these questions, we first scanned the 1A- and 1B-5'UTR sequences searching for any considerable difference, like little uORFs or any sequence able to modify the mRNA translation. Afterward, we produced many mutants from 1A- and 1B-5'UTR sequences whose effects were then assayed by complementation assays of *porin*-null *Δpor1* yeast strain.

We also considered the possible involvement of RNA binding proteins (RBPs) in the translation control mechanism. Specific RBPs interacting only with 1B-5'UTR could regulate the translation of the downward coding sequence by blocking the ribosome recruitment on mRNA or the translation initiation or the ribosome scanning on the mRNA. The RNA Electrophoretic Mobility Shift assay (REMSA) and RNA pull

down experiments were performed to answer to these questions. In addition, bioinformatics analysis was also performed on the sequences of the two alternative mRNAs in order to identify any putative structural motifs.

Another open question is to know whether the two 5'UTRs are able to regulate the expression of other genes as well as *porin1* gene. For this purpose, gene reporters fused to the 5'UTRs were used for transfecting yeast or higher eukaryotic cells.

At the end, the last objective was to confirm data obtained in yeast and in HeLa cells in the homologous organism. So, we studied in *D.m.* cells the expression of constructs carrying the 1A- or 1B-5'UTR fused to the reporter *Firefly Luciferase* gene and also of constructs containing the VDAC coding sequence fused at its 3'-end with a specific tag, in order to distinguish the endogenous protein from the recombinant one.

3 METHODS

3.1 Generation of DNA recombinant constructs of *porin1* gene and 5'UTRs of *Drosophila melanogaster*

In order to test the activity of 5'UTRs of *porin1* gene and its expression level in different organism models, the 5'UTRs and the *porin1* cDNA were cloned in various vectors containing the necessary features to perform the assays. All the typologies of constructs were prepared as indicated below. Following the reaction of ligation, based on the expression [bp vector: 3x(bp insert)=100 ng vector: x ng insert], constructs were amplified in bacterial cells *E.coli*. In particular, XL10GOLD competent cells were transformed with the recombinant DNA molecules and from each transformation plate about 20 colonies were chosen to be screened. Plasmid DNA was extracted from all clones and digested with the restriction enzymes used for cloning inserts into the respective plasmids. Clones containing a sequence of correct size were sequenced and used for other applications.

3.1.1 Cloning of 1B-5'UTR, of *porin1* gene, wild-type and mutant sequences in pYX212 vector.

1B-5'UTR derived from *porin1* gene and all mutant sequences (described in 3.2), were cloned into the pYX212 plasmid, a specific vector for expression in yeast cells. This is a high copy number vector (20-100 copies for cell), characterized by the presence of a *S. cerevisiae* origin of replication 2μ and *ura3* (uracile production) gene necessary for selection of transformed yeasts. It contains also the ColE1 region to allow replication of vector into *E. coli* and the *bla* gene that produces β-lattamase, for selection in bacterial cells. Each sequence 1B-5'UTR-VDAC, inserted in the pBSK- vector, and

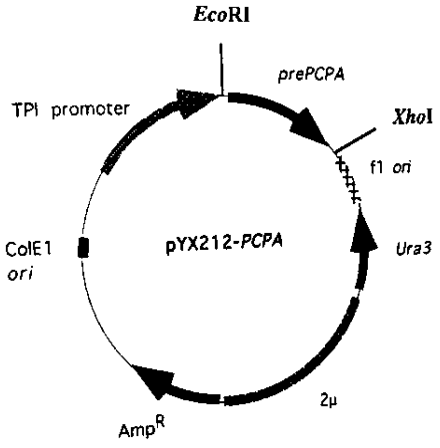

Figure 12: pYX212 vector map

the empty vector pYX212, were digested with the restriction enzymes EcoRI and HindIII and ligated together.
The DNA constructs prepared were used for complementation assay (described in 3.4) in *Δpor1* M22.2 yeast cells lacking of the endogenous Porin.

3.1.2 Cloning of 1A-, 1B, and 1B(Δ16-31)-5'UTR, of *porin1,* in pYX212-GFP vector.

The same vector pYX212 containing Green fluorescent protein (GFP) coding sequence was used to clone 1A-, 1B, and 1B(Δ16-31)-5'UTRs amplified by PCR with primers listed below.

NAME	SEQUENCE
FW_ECOR1_1B	5'-AAAGAATTCTTCCGTTCGTTATCG-3'
REV_ECOR1_1B	5'-AAAGAATTCCTCCCCACATGACC -3'
FW_ECOR1SAL1_1A	5'-AAAGAATTCGTCGACGTGTACGTTTGTCGTGGTGTCTCT-3'
REV_ECOR1_1A	5'-AAAGAATTCTTTGATGAGTTTTAGTTTGGTTAGAGT-3'

Table 1: primers used for cloning 5'UTRs in pYX212-GFP vector.

Amplification conditions, of PCR reaction, were settled based on the annealing temperature of primers and 5'UTRs length. The 5'UTRs were cloned upstream the GFP coding sequence, in order to have 5'UTRs-GFP transcripts. These new constructs were verified by sequencing and used to transform wild type M3 yeast cells strain (described in 3.3). Yeast cells were transformed with the different GFP mutants, lysed and protein extracted to perform western blotting assay (described in 3.7). The pYX212-GFP vector was used as positive control for western blotting.

3.1.3 Cloning of 1A-, 1B-, and 1B(Δ16-31)-5'UTR, of *porin1,* in pEGFP-N1 vector

Expression of reporter genes fused with the *D. melanogaster porin1* UTRs was verified in HeLa cells by western blotting and flow cytometric measurements. For this purpose it was necessary to clone the 5'UTRs into a mammalian expression vector containing the EGFP, the pEGFP-N1 vector (Clontech).

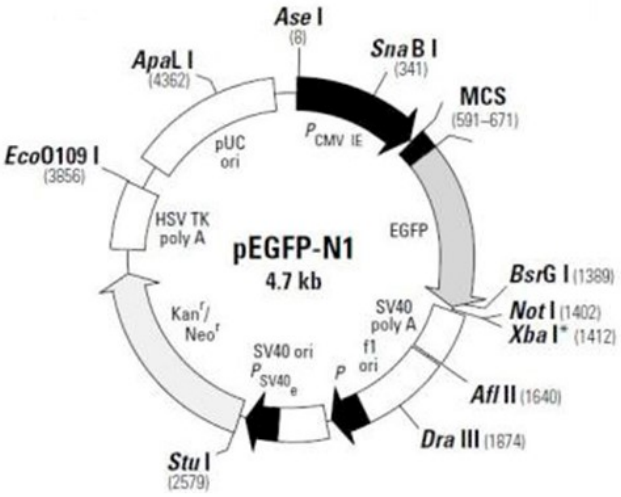

Figure 13: pEGFP-N1 vector map

This is a 4.7 kb in length vector containing the coding sequence of a more brilliant variant of classical GFP, the EGFP (Enhanced GFP). This is characterized by the presence of two mutations, a leucine substitutes a phenylalanin at the position 64, and a threonine substitutes a serine at the position 65. The EGFP sequence is inserted after the multiple cloning site, in order to allow the insertion of other coding sequences in frame with the EGFP, producing EGFP-fused proteins. Cloning was performed using NheI/BamHI enzymes restriction sites, following amplifications of the UTRs sequences using primers reported in table 2:

NAME	SEQUENCE
5'UTR1A-NHE1-FW	5'-AAAGCTAGCGTGTACGTTTGTCGTGGTGTC-3'
5'UTR1A-BAMH1-REV	5'-AAAGGATCCTTTGATGAGTTTTAGTTTGGTTAGA-3'
5'UTR1B-NHE1-FW	5'-AAAGCTAGCTTCCGTTCGTTATCGTCATGT-3'
5'UTR1BΔ16-31-NHE1-FW	5'-AAAGCTAGCTTCCGTTCGTTATCGCAGCG-3'
5'UTR1B-BAMH1-REV	5'-AAAGGATCCCTCCCCACATGACCACAAAC-3'

Table 2: primers for cloning 5'UTRs in pEGFP-N1 vector

Furthermore, another mutant was produced, inserting the 16-31 region of 1B-5'UTR inside the 5'UTR1A by mutagenesis. As template the 1A-pEGFP-N1 was used and the conditions of mutagenesis are reported in 3.2.

3.1.4 Cloning of 1A-, 1B-, and 1B(Δ16-31)-5'UTR, of *porin1,* in pMK26-*Firefly* luciferase vector.

One of the version of pMK26 vector, present in our lab, contains the *Firefly* Luciferase gene which we found suitable to study activity of regulatory sequences by *in*

vivo luciferase assay following transfection in *Drosophila melanogaster* embryonic SL2 cells.

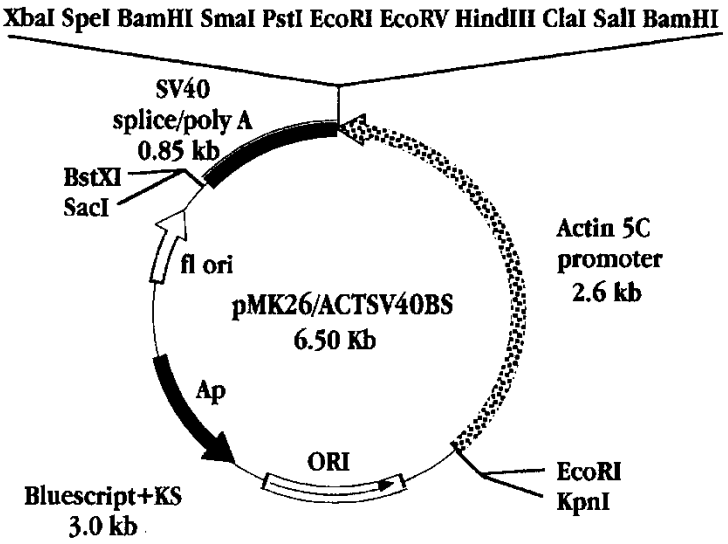

Figure 14: pMK26 vector map

This vector contains the Actin 5C (Ac5) promoter, SV40 splice site and poly(A) signals and a multiple cloning site. The 5'UTRs of *D.melanogaster porin1* gene, 1A, 1B and the mutant 1B(Δ16-31), were amplified by PCR with the insertion of restriction sites PstI or EcoRV, and HindIII. Primers used for amplifications are listed in the table below:

NAME	SEQUENCE
1A-FW_ECORV	5'-AAAGATATCGTGTACGTTTGTCGTGGTGTCTCT-3'
1A-REV_HINDIII	5'-AAAAAGCTTTTTGATGAGTTTTAGTTTGGT-3'
1BΔ16-31-FW_PST1	5'- AAACTGCAGTTCCGTTCGTTATCG-3'
1B-FW_PST1	5'-AAACTGCAGTTCCGTTCGTTATCGT-3'
1B-REV_HINDIII	5'-AAAAAGCTTCTCCCCACATGACCA-3'

Table 3: primers for cloning 5'UTRs in pMK26-F.Luciferase vector

3.1.4 Cloning of 1A-, 1B-, and 1B(Δ16-31)-5'UTR, of *porin1,* linked to *Firefly* luciferase in pBSK-A vector.

In order to perform the *in vitro* transcription, translation and luciferase assay, pBSK-A vector, a generous gift by Fatima Gebauer (F. Gebauer et al., 1994), was used to clone 1A-, 1B, and 1B(Δ16-31)- 5'UTRs linked to *firefly* luciferase derived from

previous mentioned clones generated in pMK26. This vector is characterized by the presence of a poly(a) stretch of 73 residues, that allows the *in vitro* transcription of the inserted gene. The region that goes from T3 promoter to T7 promoter contains the multiple cloning site and the poly(A) tail in the middle of the sequence so that genes of interest can be inserted in both directions.

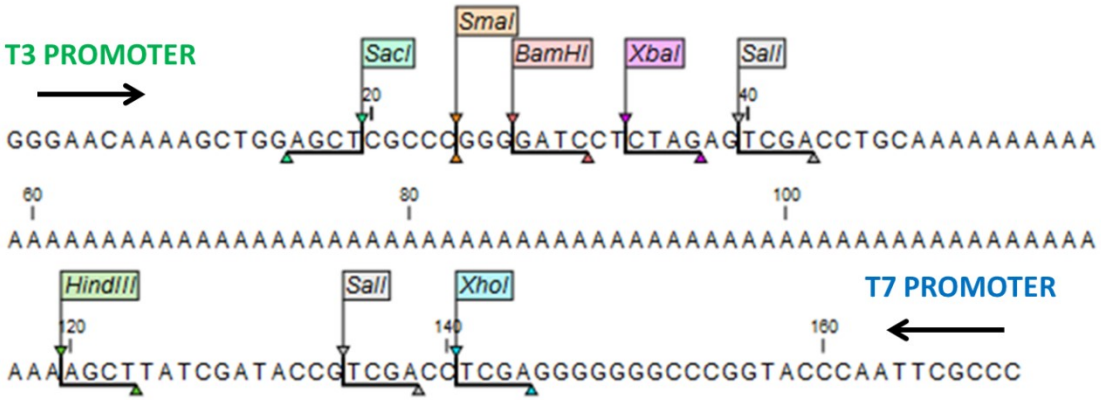

Figure 15: **Sequence from T3 promoter to T7 promoter**

Amplifications of 5'UTRs were performed with primers containing the restriction sites SacI and BamHI, so that amplification products were transcribed by T3 promoter. Primers used for the cloning are those in the table below:

NAME	SEQUENCE
FW:SacI-5'UTR1A	5'-TTTTGAGCTCGTGTACGTTTGTCGTGGTG-3'
FW: SacI-5'UTR1B	5'-TTTTGAGCTCTTCCGTTCGTTATCGTCA-3'
FW: SacI-5'UTR1BΔ16-31	5'-TTTTGAGCTCTTCCGTTCGTTATCGCAGC-3'
REV:F. Luc-BamHI	5'- TTTTGGATCCTTACACGGCGATCTTTCC-3'

Table 4: primers for cloning 5'UTRs-F.Luciferase sequences into the pBSK-A vector

3.1.5 Cloning of 5'UTRs-VDAC-HA constructs in pAc5.1/v5-His vector.

In order to distinguish in *Drosophila* cells the endogenous VDAC protein from the exogenous one, the 1A-, 1B- and 1B(Δ16-31) VDAC sequences were linked to the sequence encoding the HA tag peptide of 9 amino acids YPYDVPDYA*. Insertion was performed with double PCRs to eliminate the stop codon of VDAC and to introduce the HA sequence of 30 nucleotides (TAT CCA TAC GAT GTC CCT GAT TAC GCT

TAA). These constructs, 1A-VDAC-HA, 1B-VDAC-HA and 1B(Δ16-31)-VDAC-HA, were then cloned into the pAc5.1/V5-His vector, to analyse the level of transcription and translation, *in vivo*, of *porin1* gene by western blotting of samples derived from SL2 embryonic cells of *Drosophila melanogaster* transfected with constructs. The 1A-VDAC-HA, 1B-VDAC-HA e 1BΔ16-31-VDAC-HA sequences were amplified by PCR and cloned into the pAc5.1/V5-His or pAc vector, by EcoRI and HindIII restriction sites.

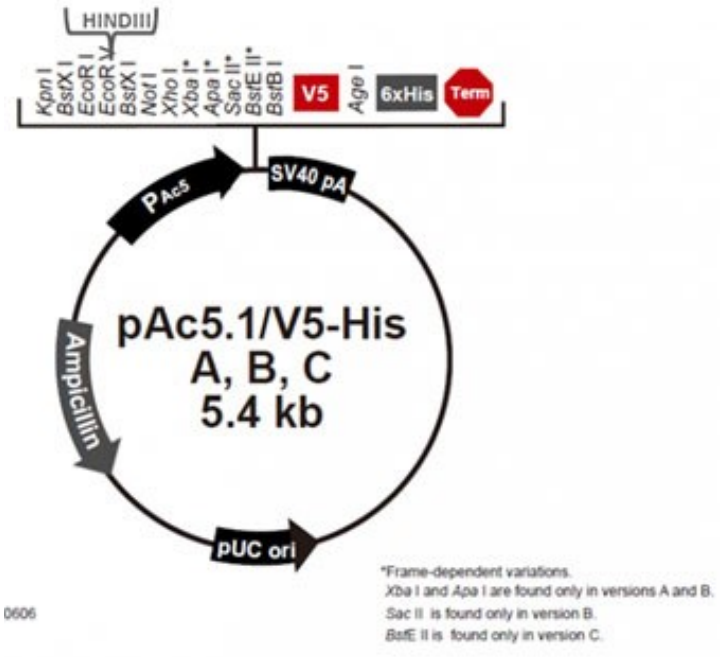

Figure 20: pAC5.1/V5-His (or pAC) vector map

The pAc5.1/V5-His is a 5.4 kb expression vector containing: the *Drosophila* actin 5C (Ac5) promoter for high-level, constitutive expression of the gene of interest in SL2 cells; Multiple cloning site to facilitate cloning of gene of interest; C-terminal containing the V5 epitope and polyhistidine (6xHis) tag for detection and purification of protein of interest; three reading frames to facilitate in-frame cloning with the c-terminal tag; Ampicillin resistance gene for selection of transformants in *E. coli;* same promoter of pMK26, ensuring the same degree of expression. Amplifications of 5'UTRs-VDAC-HA sequences were performed using primers in the table 5.

NAME	SEQUENCE
FW:ECORI-5'UTR-1A	5'-TTTTGAATTC GTGTACGTTTGTCGTGGTGTCT-3'
FW:ECORI-5'UTR-1B	5'- TTTTGAATTCTTCCGTTCGTTATCGTCATGTTG-3'
FW:ECORI-5'UTR-1BΔ16-31	5'- TTTTGAATTC TTCCGTTCGTTATCGCAGCGT-3'
REV:HA-TAG-HINDIII	5'- TTTTAAGCTTTTAAGCGTAATCAGGGACATCG-3'

Table 5: primers for inserting 5'UTR-porin-HA sequences into the pAc5.1/V5-His vector

3.2 Mutagenesis of 1B-5'UTR and 1A-5'UTR of *porin1* gene

Mutagenesis were performed using "QuikChange II XL Site-Directed Mutagenesis Kit" (QIAGEN), consisting of three steps that generate mutants with greater than 80% efficiency. In the first step the mutagenesis is inserted into the region of interest, through a Polymerase chain reaction using the construct to mutagenize as template. Primers used for the PCR must contain the point mutation, or the deletions/insertions, in the middle part of their sequence and they must be designed following the instructions provided by the kit. Mutagenesis of 1B-5'UTR of the 1B-VDAC sequence cloned in pBluescript II KS+ or pBS vector, (3000 bp) by EcoRI/HindIII, were performed. The size of the chosen vector, used for mutagenesis, is the most appropriate to allow the highest fidelity during amplification of the whole plasmid.

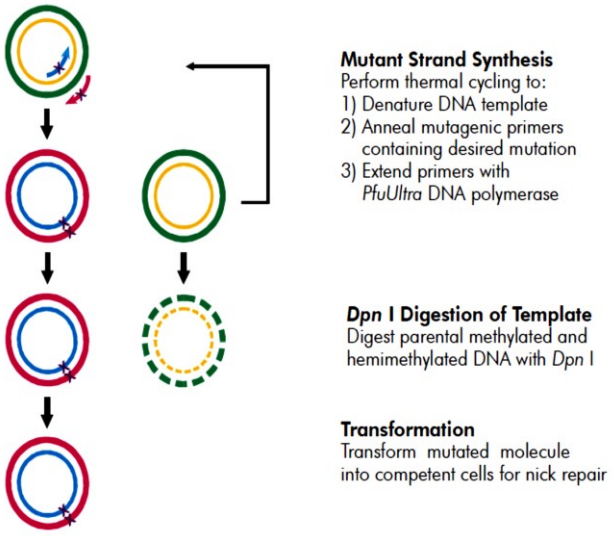

Figure 16: phases of mutagenesis

All the components of the reaction and the cycle used for the amplification are listed below:

AMOUNT	COMPONENTS
5 µl	10X reaction buffer
X µl (16 ng)	dsDNA template
X µl (125 ng)	Forward primer
X µl (125 ng)	Reverse primer
1 µl	10 µMdNTP mix
3 µl	QuickSolution
X µl	H_2O until final volume of 50 µl
1 µl	PfuUltra HF DNA Polymerase (2,5U/ µl)

Table 6: component of mutagenesis PCR reaction

SEGMENT	CYCLES	TEMPERATURE	TIME
1	1	95°C	1 minute
2	18	95°C	50 seconds
		60°C	50 seconds
		68°C	1 minute/ kb plasmid length
3	1	68°C	7 minutes

Table 7: cycle used for amplification reaction

Primers used for producing a deletion in the 1B-5'UTR of *porin1* gene are those in the table 8.

NAME	SEQUENCE
Fw-1BΔ1-15 pBS	5'-GGCTGCAGGAATTCTAGTGATTTCATGTTGCCATCCACCAGCG-3'
Rev-1BΔ1-15 pBS	5'-CGCTGGTGGATGGCAACATGAAATCACTAGAATTCCTGCAGCC-3'
Fw-1BΔ16-31 pBS	5'-GTGATTTTCCGTTCGTTATCGCAGCGTGCAACTCGCTCAATA-3'
Rev-1BΔ16-31 pBS	5'-TATTGAGCGAGTTGCACGCTGCGATAACGAACGGAAAATCAC-3'
Fw-1BΔ32-47 pBS	5'-TCGTCATGTTGCCATCCACCAATAAACATTTTCGATTTC-3'
Rev-1BΔ32-47 pBS	5'-GAAATCGAAAATGTTTATTGGTGGATGGCAACATGACGA-3'
Fw-1BΔ48-62 pBS	5'-CATCCACCAGCGTGCAACTCGCTATTTCACTCTTTACCGTTCTTT-3'
Rev-1BΔ48-62 pBS	5'-AAAGAACGGTAAAGAGTGAAATAGCGAGTTGCACGCTGGTGGATG-3'
Fw-1BΔ63-80 pBS	5'-GCTCGCTCAATAAACATTTTCGCTTTATCGTCGTTTTGTTTG-3'
Rev-1BΔ63-80 pBS	5'-CAAACAAAACGACGATAAAGCGAAAATGTTTATTGAGCGAGC-3'
Fw-1BΔ79-90 pBS	5'-TTTCGATTTCACTCTTTACCGGTTTTGTTTGTTTGTGGTCATGTG-3'
Rev-1BΔ79-90 pBS	5'-CACATGACCACAAACAAACAAAACCGGTAAAGAGTGAAATCGAAA-3'
Fw-1BΔ91-105 pBS	5'-ACTCTTCACCGTTCTTTATCGTCGGTCATGTGGGGAGATGGCTCC-3'
Rev-1BΔ91-105 pBS	5'-GGAGCCATCTCCCCACATGACCGACGATAAAGAACGGTGAAGAGT-3'
Fw-1BΔ106-119 pBS	5'-TTATCGTCGTTTTGTTTGTTTGTATGGCTCCTCCATCATACAGCG-3'
Rev-1BΔ106-119 pBS	5'-CGCTGTATGATGGAGGAGCCATACAAACAAACAAAACGACGATAA-3'
Fw-1BΔ16-28 per pBS	5'-GTGATTTTCCGTTCGTTATCGCACCAGCGTGCAACTCGCTC-3'
Rev-1BΔ16-28 per pBS	5'-GAGCGAGTTGCACGCTGGTGCGATAACGAACGGAAAATCAC-3'
Fw-1BΔ19-31 per pBS	5'-GATTTTCCGTTCGTTATCGTCACAGCGTGCAACTCGCTCAATA-3'
Rev-1BΔ19-31 per pBS	5'-TATTGAGCGAGTTGCACGCTGCGATAACGAACGGAAAAGCTTG-3'
Fw-1BΔ19-28	5'-TTCCGTTCGTTATCGTCACACCAGCGTGCAACTCGC-3'
Rev-1BΔ19-28	5'-GCGAGTTGCACGCTGGTGTGACGATAACGAACGGAA-3'

Table 8: list of primers for mutagenesis of 5'UTR-1B

Mutagenesis of 1A-5'UTR of the 1A-EGFP sequence cloned in the pEGFP-N1 vector by NHEI/BAMHI, was performed. The region 16-31 from 1B-5'UTR was inserted in the 1A-5'UTR sequence, using the method described above. Primers used for this mutagenesis are listed in the table 9:

NAME	SEQUENCE
Fw-1Ains16-31	5'- GTGTACGTTTGTCGTTCATGTTGCCATCCACGGTGTCTCTGTTCCTC-3'
Rev-1Ains16-31	5'-GAGGAACAGAGACACCGTGGATGGCAACATGAACGACAAACGTACAC-3'

Table 9: primers for mutagenesis of 5'UTR-1A

The amplification products were digested with the DpnI enzyme to degrade the methylated parental DNA. Digested DNA was then used to transform XL10GOLD competent bacterial cells and four or five colonies were chosen, from the transformation

plates, for DNA plasmid extraction. The DNA constructs were sequenced to confirm the presence of the inserted mutations.

3.3 Transfection of yeast cells

S. cerevisiae Δ*por1* M22.2 *(MAT*a *lys2 his4 trp1 ade2 leu2 ura3*, *por1*::Leu2) derives from the wild type strain M3 (*MATα lys2 his4 trp1 ade2 leu2 ura3*), and is characterized by the inability to express the VDAC1 protein. The VDAC gene was interrupted by the insertion of a Leucine cassette, creating a null VDAC yeast. These yeast strains were obtained from EUROSCARF (Frankfurt, Germany); they grow on rich medium YP (1% yeast extract, 2% peptone), supplemented with 2% glucose (YPD) or 3% Glycerol (YPY), and minimal medium (0,67% yeast nitrogen base) containing 2% glucose (SD) and supplemented with 10 μg/ml of the appropriate nutritional requirements according to the genotype of the strains. *Δpor1* strain is used for heterologous expression of native or mutant VDACs, cloned into the 2μ multi-copy shuttle vector pYX212 (Novagen) carrying the URA3 gene under the control of the constitutive promoter TPI1.

The protocol of transfection started with an overnight culture of Δ*por1* cells in 10 ml of YPD. The day of transfection, 50 ml of completed medium (YPD) were inoculated with 500 μl of the overnight culture and again incubated at 30°C growing until the OD_{600} will reach 0,6. Yeast were then pelleted and washed twice, first with 10 ml of water and then with 10 ml of 10X TE supplemented with 0,1 M Lithium Acetate pH 7,5. After centrifugation yeast cells were resuspended in 300 μl of the same solution and divided into six aliquots of 50 μl. In each tube, 1 μg of foreign DNA and 15 μg of SSD (Single strand DNA), used as a carrier for the entry of the DNA, were added. The tubes were incubated for 30 minutes at 30°C and then 300 μl of 10x TE - 0,1 M Lithium Acetate pH7,5 - 40% PEG 8000 were added for each tube. A new incubation of 30 minutes at 30°C was provided, which was followed by a 15 minutes heat shock at 42°C. For each sample 50 μl were plated into SD agar medium (yeast nitrogen base 6,7g/L, 2% agar, 2% glucose, 10 μg/ml nutrients), and incubated for 3 or 4 days at 30°C. From each plate one or two colonies were inoculated in 10 ml of liquid SD.

3.4 Drop serial dilutions and complementation assay of yeast cells

To perform yeast complementation assay using the drop serial dilution method, a yeast colony was picked up from the plate and inoculated in 50 ml of minimal medium to grow for two days at 28°C under shaking condition. Two days after, 10^8 cells, calculated by measuring OD_{600} (OD_{600}=1 corresponds to 10^4cell/ml), were harvested and resuspended in 200 µl of water. Starting from this initial concentration of cells, four dilutions (1:10, 1:100, 1:1000 and 1:10000) were prepared, and 2 µl of each dilution were spotted in YPD and YPY agar plates; plates were incubated at 30°C and at 37°C to evaluate if complementation occurs.

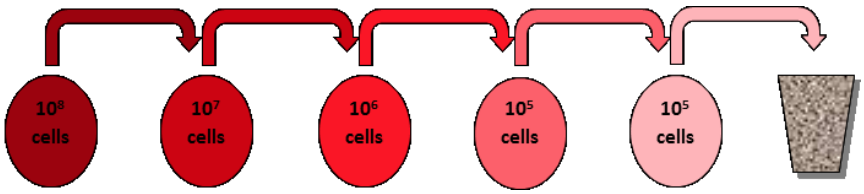

Figure 17 serial dilutions of yeast cells for complementation assay

3.5 Yeast mitochondria and ribosomes preparation

To isolate mitochondria from yeast, cells were grown two days in one liter YP supplemented of 2% Galactose and 0,1% glucose under 200 rpm shaking condition. Solutions for extraction were: BUFFER 1: 100 mM tris/H_2SO_4 pH 9.4 + 10 mM DTT; BUFFER 2: 20 mM KH_2PO_4 pH 7.4 + 1,2 M Sorbitol; BUFFER 3: 0,6 M Sorbitol + 10 mM tris/HCl pH 7.4 + PMSF 1 mM + 1 mM EDTA pH 7.4; BUFFER 4: 0,25 M Sucrose + 20 mM tris/HCl pH 7.4 + 1 mM EDTA pH 7.4. The day of extraction, the saturated yeast culture was harvested by centrifugation at 6000 x g for 5 minutes and washed twice with sterile water. Yeast cells were then resuspended in buffer 1 (2ml/g) and subjected to shaking condition at 70 rpm for 20 minutes at 30°C. The buffer 1 was eliminated with a centrifugation of 5 minutes at 3000 x g at room temperature and the cells were resuspended in 1,2 M sorbitol, with an amount sufficient to cover the pellet, and centrifuged for 5 minutes at 3000 x g at room temperature. In order to obtain spheroplasts, the pellet was resuspended in buffer 2 (7ml/g) with the addition of Zymolyase (1mg/g) and shaked into a glass flask at 70 rpm for at least 1 hour at 30°C. Spheroplasts were harvested at 2200 x g for 8 minutes at 4°C and then placed in ice and

cleaned twice with 1,2 M sorbitol. Each wash step was performed by centrifugations at 2200 x g of 8 minutes at 4°C. The pellet was weighed and resuspended in cold buffer 3 (6,5 ml/g) with the addition of 260 µl of 25x /6,5 ml PMSF. The suspension was transferred into the potter and homogenized. Three centrifugation steps were performed to separate mitochondria from the other cell components. First centrifugation was carried out at 1500 rpm for 5 minutes at 4°C and the supernatant was collected and subjected to the second centrifugation at 3000 rpm for 5 minutes at 4°C. The third centrifugation was performed with the previous supernatant. The pellet enriched of mitochondria was obtained with a centrifugation at 12000 x g for 15 minutes at 4°C and was resuspended in 4-5 ml of buffer 4 and homogenized again. 30 ml of buffer 4 were added to this homogenate and centrifuged at 3000 x g for 5 minutes at 4°C. The supernatant was re-centrifuged at 12000 x g for 20 minutes at 4°C and the mitochondrial pellet obtained was resuspended in 0,5 ml of buffer 4 and stored at -20°C.

Crude ribosomal fraction was prepared from two litres of yeast cells at exponential phase cultured in SD-Ura containing 2% glucose. Spheroplasts were prepared as described above and finally broken by mechanic disruption. Debris was separated by centrifugation at 8000 x g for 10 min at 4°C. The supernatant, containing the cytoplasm and the ribosomes was centrifuged for 1h and 15' at 50000 rpm at 4°C in an ultracentrifuge TL-100 (Beckman), using a rotor TL100.3. The supernatant was removed and the pellet was washed twice with the homogenisation buffer containing diethylpyrocarbonate.

3.6 Production of anti-*D.m*. porin1 antibody

Anti-*D.melanogaster* porin1 polyclonal antibody was generated in rabbits by using purified *D.melanogaster* recombinant VDAC protein as antigen. The recombinant protein was expressed in bacteria and purified by a Ni-NTA affinity chromatography.
Cells transformed by pQE30DmVDAC1 were grown to 0.6 $O.D._{600nm}$ and IPTG was added to the culture in a final concentration of 1 mM to induce expression of recombinant VDAC. The cells were harvested after growth for another 5 hours by centrifugation. The pellet was lysed in a denaturing buffer. His-bind Resin Buffer from Novagen was used to purify the recombinant porin. Adsorption of the recombinant protein to the Ni-NTA resin was obtained by gentle shaking for 1 h at 4°C. After washing steps the protein was isolated by incubation for 1 h at 4°C with the elution

buffer containing 250 mM imidazole, pH 8.0. The sample was extensively dialysed and the protein concentration measured by the BCA Protein Assay Reagent (Pierce).
Rabbits were immunized three times, following standard protocols. 100 µg of purified VDAC proteins were used in any booster. After three immunization cycles, blood was collected and the serum was obtained.

3.7 Immunoblotting assay of VDAC proteins extracted from yeast mitochondria

For each sample, mitochondria were harvested at 14000 rpm for 30 minutes at 4°C, resuspended in 500 µl of lysis buffer (triton 1%, 10 mM Tris/HCl pH 7.0, 1 mM EDTA) and incubated in ice for 1h. A centrifugation step followed at 14000 rpm for 30 minutes at 25°C and the supernatants were collected and precipitated with 5 volumes of acetone. Protein pellets were then resuspended in 20 µl of SDS loading buffer 1X and loaded into a 12% polyacrylamide gel for SDS page. After the electrophoresis, proteins were transferred from the gel into a nitrocellulose membrane. This was blocked with 5% milk in 1X PBS-Tween (T-PBS) for 1 hour and blotted overnight with a home made primary antibody, named anti-DM porin1 (rabbit) at the dilution 1:100 in 2% milk-T-PBS. The membrane was then washed three times with T-PBS 1X and blotted again with the secondary antibody anti-rabbit (Invitrogen) 1:10000 for 1 hour. The membrane was exposed to ECL solution and the signal generated was revealed by autoradiography on X-Ray film.

3.8 Immunoblotting assay of proteins extracted from yeast transfected with 5'UTRs-GFP constructs

In order to evaluate the expression levels of GFP from wild type yeast cells transfected with GFP, 1A-GFP, 1B-GPF and 1B(Δ16-31)-GFP, immunoblotting assay was performed. Proteins were extracted from yeast cells cultured overnight at 30°C under shaking condition, in 50 ml of YPD medium. The saturated culture was pelleted at 3000 x g for 5 minutes at 25°C. 400 µl of lysis buffer without detergents (0,1 M tris/ HCl pH7,5; 5 mM EDTA; 0,15M NaCl), were added to the pellet together with an equal amount of glass beads. For breaking up the cell wall, yeast and beads were mixed for 1 minute with vortex and then incubated in ice for another minute. This cycle was

repeated at least ten times. Once that the cell walls were disrupted, the lysate was separated from the beads by a soft centrifugation and the supernatant was collected to be centrifuged again at 13000 rpm for 20 minutes at 4 °C. The new supernatant was collected and protein concentration was measured by Lowry method.

55 µg of GFP and 1A-GFP, and 360 µg of 1B-GFP and 1BΔ16-31-GFP were loaded into a 12% polyacrylamide gel for SDS-PAGE. After electrophoresis proteins were transferred onto a nitrocellulose membrane and blotted with the primary antibody anti-GFP (Roche) used at the dilution 1:1000 in 5% milk in T-PBS 1X, and with the secondary antibody anti-Mouse 1:10000. The membrane was exposed to ECL solution and the signal generated was revealed by autoradiography on X-Ray film.

3.9 RNA Electrophoresis Mobility Shift Assay (REMSA)

REMSA assay was performed using the protocol provided by Thermo Fisher Scientific with some modification. The Biotinylated RNA probe was used at final concentration of 0,5 nM, while the not-Biotinylated competitor was used at final concentration of 6 µM. The interactions were conducted in a reaction buffer containing the REMSA buffer 1X composed by 5% Glycerol, 200 mM KCl, tRNA 7 µg, Heparin 31µg, Nuclease-Free water. As control a Biotinylated RNA corresponding to a different sequence was used. Its final concentration in the reaction buffer was 2 nM while the not-Biotinylated RNA competitor had a final concentration of 6µM. Three sample were prepared for each reaction. The first sample was prepared only with the Biotinylated RNA, to control the migration of the naked RNA. The second sample was prepared adding the total yeast lysate of M3 wild type strain (prepared as described in 3.7) to the Biotinylated RNA probe, to verify the proteins-RNA interactions. To validate these interactions, the not-Biotinylated RNA competitor was added to the third sample. These three samples were loaded into a native 0,6% polyacrylamide gel prepared into 0,5 X TBE and subjected to a constant voltage of 100V. The electrophoresis was stopped when 3/4 of gel length was reached by the bromophenol blue. All solutions were prepared with RNAse free water.

Transfer, cross linking and detection methods.

Separated samples were transferred by semidry blotting onto a nylon membrane, applying 400 mA for 45 minutes and then the membrane was cross-linked for 50 seconds using UV-light. To detect the biotinylated RNA molecules, the REMSA kit

provided a solution of Stabilized Streptavidin-Horseradish Peroxidase Conjugate, which binds biotinylated molecules, and the other solutions to perform the detection using X-ray films.

3.10 RNA pull down assay

In order to isolate proteins interacting with a specific sequence of RNA, RNA pull down assay was performed using 160 µg of total yeast lysate obtained as described in 3.7, 400 pmol of biotinylated oligo-RNAs and 200 µg of streptavidin-conjugated magnetic beads *Dynabeads MyOne Streptavidin C1* (Invitrogen). First of all, 200 µg (20 µl) of pre-washed beads were incubated with 26 µl of 10 µM biotinylated oligo RNA (146 ng/ µl) and 40 µl of Binding and Washing Buffer 2X (10 mM tris HCl pH7,5; 1 mM EDTA and 2M NaCl), for 1 hour under soft shaking at room temperature. The supernatant was taken out and the amount of unbound RNA was measured to calculate the remaining RNA. The RNA-conjugated beads were washed three times with 100 µl of Binding and Washing Buffer 1X and then were resuspended in 40 µl of Binding and Washing Buffer 1X . In another tube the total yeast lysate was pre-incubated with Dynabeads to eliminate background caused by proteins interacting not specifically with beads. 25 µl of total yeast lysate, corresponding to 160 µg of proteins, were mixed with 20 µl of REMSA buffer 10X (100mM HEPES pH 7.3, 200mM KCl, 10mM MgCl2, 10mM DTT), 2 µl 100 mM DTT, 3 µl tRNA (10 µg/ µl) and 100 µl DEPC water. This mix was incubated with 10 µl of pre-washed beads for 1 hour under soft shaking. The proteins unbound to the beads were then added to the RNA-beads complexes reaching a final volume of 200 µl. The mix was softly shaken for 1 hour. The supernatant was saved while the beads were boiled with 1X LDS to detach the protein-RNA complexes from the beads. The same protocol was used with the RNA control, using 40 µl (95ng/ µl), corresponding to 400 pmol.

3.11 Mass spectrometry analysis

Mass spectrometry analysis was performed by the Mass Spectrometry Facility center at University of St Andrews. The proteins detached from the beads with LDS 1X were loaded into a 12% polyacrylamide gel for electrophoresis. The gel was stained with Comassie Blue and the lane of proteins was cut into 0,5 cm slices, containing each

protein band. These were then subjected to in-gel digestion, using a ProGestInvestigator in-gel digestion robot (Genomic Solutions, Ann Arbor, MI) using standard protocols. Briefly the gel cubes were destained by washing with acetonitrile and subjected to reduction and alkylation before digestion with trypsin at 37°C. The peptides were extracted with 10% formic acid and concentrated down to 20 ml using a SpeedVac (ThermoSavant). They were then separated using an UltiMate nanoLC (LC Packings, Amsterdam) equipped with a PepMap C18 trap & column, using a 60 min elution profile, with a gradient of increasing acetonitrile, containing 0.1% formic acid, to elute the peptides (5–35% acetonitrile in 18 min, 35–50% in a further 7 min, followed by 95% acetonitrile to clean the column, before reequilibration to 5% acetonitrile). The eluent was sprayed into a Q-Star XL tandem mass spectrometer (Applied Biosystems, Foster City, CA) and analysed in Information Dependent Acquisition (IDA) mode, performing 1 s of MS followed by 3 s MSMS analyses of the 2 most intense peaks seen by MS. These masses are then excluded from analysis for the next 60 s. MS/MS data for doubly and triply charged precursor ions was converted to centroid data, without smoothing, using the Analyst QS1.1 mascot.dll data import filter with default settings. The MS/MS data file generated was analysed using the Mascot 2.1 search engine (Matrix Science, London, UK) against UniProt with no species restriction. Data was searched with tolerances of 0.2 Da for the precursor and fragment ions, trypsin as the cleavage enzyme, one missed cleavage, carbamidomethyl modification of cysteines as a fixed modification and methionine oxidation selected as a variable modification. The Mascot search results were accepted if a protein hit included at least one peptide with a score above the homology threshold.

3.12 Bioinformatics analysis

Bioinformatics analysis were performed for three purposes and three different software were used. (1) In order to predict interactions between yeast 18S rRNA and 1B-VDAC/1A-VDAC/1B(Δ16-31)-VDAC, we used the “IntaRNA” software, by which we could be able to calculate the hybridation energy, and the total energy of the interaction during the reaction. This software also showed the nucleotide positions of interaction allowing to establish which regions of rRNA are involved in the reaction. (2) For the second purpose, the analysis of the 1A- and 1B- 5UTR sequences for the presence of RNA-binding motifs, we used the online free “RBPMap” software, which

gave a precise prediction of potential RNA binding proteins that could interact with the two sequences. (3) Finally, for verifying if the two 5'UTRs are conserved sequences in the *Drosophila* genus, the nucleotide BLAST tool from FlyBase Database was used.

3.13 Transfection of HeLa cells

HeLa cells derive from one cell grown from the cervical cancer of a young African-American woman, **He**nrietta **La**cks and represent the first human cells to be continuously grown in culture. The cells appear "immortal" and are still used in medical research today.

0,5 x 10^6 HeLa cells were seeded into a 6-well plate and incubated at 37°C with 5% CO_2 for 24 hours. Transfection was performed using the *"Lipofectamine 3000 transfection kit"* (Invitrogen), based on the formation of lipid/DNA complexes with a positive charge that facilitate the entry in the cells. 2,5 µg of each plasmid DNA were used for transfection. Two mixes were prepared: in the first one 3,75 µl of Lipofectamine 3000 were added to 125 µl of DMEM without serum; in the second, DNA and 5 µl of P3000 Reagent were mixed with 125 µl of DMEM. The first mix was added to second one and incubated 5 minutes at room temperature. Finally the mix was added drop to drop to the cells in the wells and incubated at 37°C + 5% CO_2 for 48 hours.

3.13.1 Immunoblotting assay of proteins extracted from transfected HeLa cells with 5'UTRs-EGFP constructs

After the incubation, the medium was removed from the wells and cells were washed with PBS 1X and detached with 1 mM EDTA in PBS 1X. Cells were pelleted into a 1,5 ml tube for 5 minutes at 1500 rpm. Pellets were resuspended in 50 µl of lysis buffer (NaCl 150mM, 1% triton, 50 mM Tris HCl pH8, Protease Inhibitor 1X) and incubated in ice for 90 minutes. Tubes were then centrifuged at 13000 rpm at 4°C for 30 minutes and supernatant was collected. Protein concentration was measured with Lowry methods and 50 µg proteins were loaded into a 12% polyacrylamide gel for SDS Page. Proteins were then transferred onto a nitrocellulose membrane and blotted with the primary antibody anti-GFP (Roche) used at the dilution 1:1000 and with the secondary

antibody anti-Mouse 1:10000. The membrane was exposed to ECL solution and the signal generated was revealed by autoradiography on X-Ray film. The membrane was then stripped and blotted again with anti-actin antibody (Sigma) to detect actin as loading control.

3.13.2 Flow cytometry assay

Cytofluorimetric assay was performed in order to evaluate the expression of the 5'UTRs-EGFP by HeLa cells. The *CyFlow® ML flow cytometer* (*Partec*) system was used for all experiments. It is equipped with three laser sources and 10 optical parameters with dedicated filter setting, and a high numerical aperture microscope objective (50× NA 0.82) for the detection of different scatter and fluorescence signals. Around 20.000 cells per sample were analyzed and each experiment was repeated at least twice in triplicate. The cells were excited by an air-cooled argon 488 nm laser and the signal from fluorescent probes was detected. Two region were analyzed M1 (low fluorescence) and M2 (high fluorescence), to evaluate two degree of fluorescence. Data obtained were acquired, gated, compensated, and analysed using the *FlowMax* software (*Partec*). Each experiment was repeated three times in triplicate. Data were statistically analyzed by one-way ANOVA with Tukey's post hoc test. A $p < 0.05$ was taken as significant.

3.14 *In vitro* transcription assay

The *in vitro* transcription assay was performed in order to evaluate the translation levels of Firefly Luciferase linked to 5'UTRs sequences of *porin1*. The pBSK-A vector with 5'UTRs-F.Luciferase sequences were digested with the enzyme XhoI that cuts after the poly(A) tail, in order to have a linearized vector, where the RNA polymerase T3 could start and finish the transcription. Components for in vitro transcription are:

- 5X transcription buffer,
- Arca $Gpppm^7$ 40mM,
- DTT 100 mM,
- CTP-ATP-UTP 20mM,
- RNA polymerase T3(80 U/µl),
- RNAsin
- water till 16,9 µl.

To this mix 5 µl of digested DNA (1 µg/ µl) were added and samples incubated a 37°C for 5 minutes. Following addition of 1 µl of GTP 10mM and incubation of 1 hour at 37°C, degradation of the remaining DNA was performed with 1 µl of RQ-DNASE for 20 minutes in a 37°C bath. Finally to purify the mRNA, 80 µl of water and 100 µl of phenol (pH4,5) were added to the sample and then centrifuged at 12000 x g for three minutes. The upper phase, containing RNA, was taken out and mixed with 100 µl of phenol/chlorophorm and samples were again centrifuged and the removed supernatant was loaded into a G_{50} columns to remove the 5'capping. This purification step was repeated two times. RNA was precipitated with 0,3M sodium acetate and 2,5 volumes of Etanol 100% and incubated 30 minutes at -20°C. Samples were centrifuged at 1300 rpm for 15 minutes at 4°C. Following washing with etanol 70% RNA pellet was left to dry and then resuspended in 20 µl of RNAse free water. RNA samples were loaded in 1% agarose gel with a marker of concentration and RNA concentration was assessed measuring absorbance at 260/230 nm and 260/280 nm.

3.15 *In vitro* translation assay

The cell free system of mRNA translation was performed using 4 ng of the in vitro transcribed RNA. Components of reaction are:

- 0,07 mM aminoacids;
- 0,017M creatine phosphate;
- 0,087 mg/ml creatine phosphokinase;
- 0,6mM DTT;
- 0,026M Hepes pH7.5;
- 0,43mM Magnesium Acetate; ,
- 0,5 M Potassium Acetate;
- 1 ng *Renilla* Luciferase mRNA;
- 5 µl (25 mg/ml) Embryo extracts 90 minutes
- water till 11,5 µl.

The reaction was incubated at 25°C for 120 minutes and stored at -20°C. *Firefly* and *Renilla* Luciferases *in vitro* translated were used for measuring their enzymatic activity.

3.16 Dual Luciferase Reporter Assay System

The *in vitro* translated proteins, *Firefly* Luciferase and *Renilla* Luciferase, were used for a luminescence assay using the Dual-Luciferase Reporter Assay System (Promega).

Firefly and *Renilla* Luciferase, because of their distinct evolutionary origins, have different enzyme structures and substrate requirements. Thanks to these differences it is possible to discriminate between their respective bioluminescent reactions. Using Dual-Luciferase Reporter Assay System makes possible to quench the *Firefly* luciferase reaction while simultaneously activate the luminescent reaction of *Renilla* luciferase. *Firefly* Luciferase, is a 61 kDa monomeric protein that does not require post-translational processing for enzymatic activity, and it functions as a genetic reporter immediately upon translation. Photon emission is achieved through oxidation of beetle luciferin in a reaction requiring ATP, Mg^{2+} and O_2. The oxidation under normal condition occurs through a luciferyl-AMP intermediate that turns over very slowly. This reaction generates a "flash" of light that decays after the substrate and enzyme are mixed.

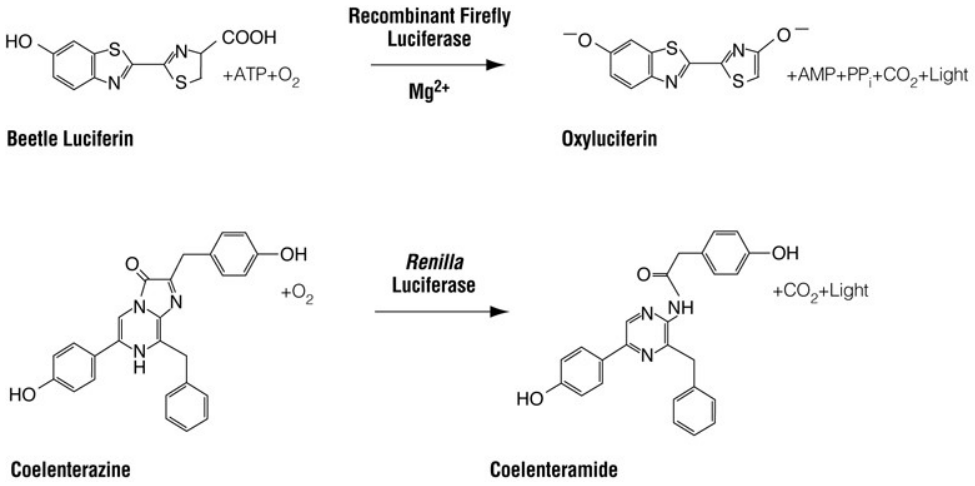

Figure 23: Firefly and Renilla Luciferase enzymatic activity

The presence of coenzyme A (CoA) that is incorporated in the reagents to quantitating the *Firefly* Luciferase, yields stabilized luminescence signals with significantly greater intensity. *Renilla* Luciferase is a 36 kDa monomeric protein composed of 3% carbohydrate when purified from its natural source, *Renilla reniformis*. However, like *Firefly* luciferase, post-translation modification are not required and it may function as a genetic reporter immediately after translation. The luminescent reaction catalysed by *Renilla* Luciferase utilize O_2 and coelenterate-luciferin (coelenterazine).

Each sample were diluted 1:100 in 1X passive lysis buffer and placed in triplicate into a 96-wells plate. 100 µl of Luciferase Assay Reagent were dispensed to the samples and the *Firefly* Luciferase luminescence was measured, following addition of 100 µl of STOP&GLO reagent and measurement of *Renilla* Luciferase activity. Varioskan Flash Multimode Reader was used for luminometric assay. Each experiment was repeated three times in triplicate. Data were statistically analyzed by one-way ANOVA with Tukey's post hoc test. A $p< 0.05$ was taken as significant.

3.17 SL2 cells culture and transfection protocol

SL2 cells, or Schneider 2 cells, are one of the most commonly used *Drosophila melanogaster* cell line. SL2 cells were derived from a primary culture of late stage embryonic cells (20-24 hours). They grow in suspension or loosely adherent in Schneider's medium + L-glutamine (Gibco), supplemented with 10% Fetal Bovine serum, penicillin (50 IU/ml) and streptomycin (50 IU/ml) at 25°C without CO_2.

Cells were seeded 18-24 hours before transfection into 6-well plates in order to have 3 x 10^6 cell per 2 ml/well complete medium and were incubated at 25°C to reach 50-80% confluency. The day of transfection, cells were co-transfected with the *Renilla* Luciferase reporter in pAc5.1 vector and 5'UTRs-F.Luciferase constructs in pMK26, or 5'UTRs-VDAC-HA in pAc5.1 vector. 300 ng of Luciferase/VDAC-HA and 20 ng of *Renilla* reporter were used for transfection. Lipofectamine 3000 (Invitrogen) was used as transfection reagent.

3.18 Measurements of luciferase activity in total SL2 lysates

Cells were detached from the plate and harvested at 0,4 x g for 5 minute at room temperature 48 hours after transfection. Pellets were washed with sterile 1X PBS and centrifuged again. Cellular pellets were resuspended in 40 µl of 1X passive lysis buffer from Dual Luciferase Reporter Assay System (Promega). Each lysate was diluted ten times and 20 µl of the dilution were plated into a 96-well plate. Enzymatic activity of both Luciferases, *Firefly* and *Renilla* Luciferase, was assayed as described in 3.15.

3.19 Immunoblotting assay of protein extracted from transfected SL2 cells

Transfection of SL2 cells was performed as described in 3.17.1. 48 hours after transfection, cells were detached from the plate and harvested at 0,4 x g for 5 minutes. Pellets were washed with sterile 1X PBS and centrifuged again. Cells were lysed in RIPA buffer, incubated 20 minutes in ice and then centrifuged 30 minutes at 13000 rpm. Supernatant was collected and protein concentration measured using the LOWRY method. For western blotting 50 µg of total lysate were loaded into a 12% or 15% polyacrylamide gel for SDS-PAGE. After electrophoresis proteins were transferred from the gel to a nitrocellulose membrane. The membrane was first stained with Ponceau Red solution, to observe the correct transfer of proteins, and then blocked overnight with the Odyssey Blocking Buffer. The membrane was blotted with a primary antibody anti-HA (Santa Cruz), diluted 1:100 in Odyssey Blocking Buffer or with polyclonal antibody anti-*Dm*porin1 (1:200) generated in rabbit against the recombinant protein. Incubation lasted one hour. The membrane was washed three times with T-PBS 1X and incubated for 1h with the rabbit secondary antibody (800 nm) diluted 1:25000 in Odyssey Blocking Buffer. The membrane was then stripped and blotted again with the primary antibody mouse anti α-Tubulin (SIGMA) diluted 1:500, for detection of Tubulin as loading control.

3.20 Semi-quantitative PCR

Semi-quantitative PCR was performed on a cDNA library from testis and a cDNA library from ovary cloned in lambda ZapII (Stratagene) (a kind gift of Tulle Hazelrigge, Columbia University, NY, 28). 3 x 10^6 pfu from each library were diluted to 74 µl with water and heated at 70°C for 5 min and subsequently chilled on ice. The PCR reaction was performed in 100 µl final volume with primers Fw1A and RevDmPorin 167 (1 µM) with the following conditions: 94°C 1'20'', 50°C 1'20'', 72°C 45''. 10 µl aliquots were taken from the reaction after 15, 20, 25, 30 and 35 cycles and electrophoresed in 2% agarose. Similarly for 1B-VDAC 1.5 x 10^7 pfu of each library were used. After denaturing steps as described above, the PCR reaction was performed with primers Fw1B and RevDmPorin43 (1 µM) with the following conditions: 94°C 1'20'', 55°C 1'20'', 72°C 45''. 10 µl aliquots were taken as described and electrophoresed. Etidium

bromide stain was quantitated by scan densitometry of the stained band from the picture taken under UV light. Primers used for the RT-PCR are listed below:

NAME	SEQUENCE
FW-DmTubulin	5′-CGTGAATGTATCTCTATC-3′
REV-DmTubulin	5′-TTAGTACTCCTCAGCGCC-3′
FW 1A	5′-GTTTGTCGTGGTGTCTCTGTT-3′
REV-DmPorin 167	5′-TCTTCAGATCGAGCTTCCACA-3′
FW 1B	5′-TTCGTTATCGTCATGTTGCCA-3′
REV-DmPorin 43	5′-TGTTTGCCCAAATCGCTGTAT-3′

Tabella 10: primers used for RT-PCR

3.20.1 RNA extraction from yeast cells

RNA extraction was performed using the RNeasy Mini Kit (Qiagen). Cells were grown in 20 ml of appropriate media at 30°C with shaking until they reached the exponential phase and spheroplasts were produced by enzymatic digestion as described above. RNA concentration was measured at 260 nm (1 OD_{260} = 40 µg/ml). Total RNA was extracted also from the ribosomal and polysomal fractions obtained as described above. In RT-PCR experiments the cDNA was synthesized from total RNA by using the First Strand cDNA Synthesis Kit (MBI Fermentas).

3.20.2 RNA extraction from transfected SL2 cells and qPCR analysis

Transfection of SL2 cells was performed as described in 3.17.1. 48 hours after transfection, cells were detached from the plate and harvested at 0,4 x g for 5 minutes. Pellets were washed with sterile 1X PBS and centrifuged again. RNA extraction was performed using ReliaPrep RNA Cell Mini Prep System (Promega). RNA concentration was measured at 260 nm (1 OD_{260} = 40 µg/ml) and 2000 ng of RNA were used for cDNA synthesis, by using QuantiTec Reverse Transcription Kit (Qiagen). 2µl of each RNA sample were used as template for qPCR using QuantiFast SYBR Green PCR kit (QIAGEN). qPCR reaction was performed with the couple of primers, FW1A/Rev-DmPorin167, FW1B/Rev-DmPorin43, and FW-DmActin/Rev-DmActin (FW_DmActin: 5’-ACGAGTTGCCCGATGGACAG-3’; REV_DmActin: 5’-GCACAGTGTTGGCGTACAGA-3’), with the following conditions: 95°C 15’’, 60°C

20’’, 68°C 30’’ (45 cycles). Three independent experiments were performed in triplicate and data were statistically analyzed by one-way ANOVA with Tukey's post hoc test. A $p< 0.05$ was taken as significant.

4 RESULTS

4.1 Semi-quantitative PCR: Two splice variants of the mRNA coding for VDAC are present in *D. melanogaster* cells in different amounts.

To gain insights into the biological relevance of the two splice isoforms of *D. melanogaster* VDAC mRNA, we compared their levels in two different tissues, testis and ovary, by performing semi-quantitative PCR on tissue specific cDNA libraries. The RT-PCR amplification was performed with primers specific for each alternative 5'UTR. Figure 24A shows that both mRNAs are transcribed in the two libraries as also observed in other fly tissues (De Pinto et al., 2010). To quantify the levels of the two spliced forms PCRs were performed with different number of amplification cycles, from 15 to 35. The PCR products were loaded on an agarose gel and quantified by scan densitometry. The data clearly show that the splice variant 1B-VDAC is present at much lower levels than 1A-VDAC (Figure 24A). A control experiment performed with a-tubulin or rp49 primers indicated that 1A-VDAC is transcribed similarly to other housekeeping genes (not shown). In contrast, the 1B-VDAC form could be only detected using a higher concentration of template (5 fold) than the one used for the detection of the 1A-VDAC form. Even in this condition, the ratio 1A-VDAC:1B-VDAC at the plateau is about 10 (Fig. 24B). Thus, the levels of 1B-VDAC form are approximately 50 fold less than the ones of 1A-VDAC.

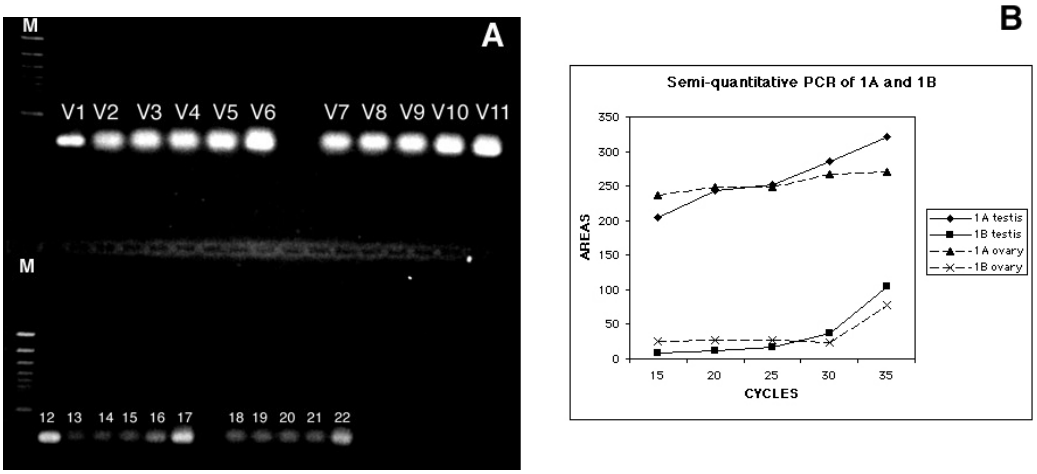

Figure 24: Semiquantitative analysis of the alternative transcripts 1A-VDAC and 1B-VDAC in D.melanogaster cDNA libraries. A) 1 µl of a cDNA library from *D.melanogaster* testis or ovary were used for amplification with primers specific for 1A-VDAC. Alternatively 7.5 µl of the same cDNA libraries were amplified with primers specific for 1B-VDAC. After the indicated PCR cycles, 10 µl aliquots were collected. They were electrophoresed and the etidium bromide staining per band was quantitated by densitometry. A) agarose gel of PCR-amplified DNA obtained from testis library (lanes V2-V6 and 13-17) or from ovary library (lanes V7-V11 and 18-22). In lanes V1-V11 1A-VDAC amplifications are reported, in lanes 12-22 1B-VDAC amplifications. The DNA was obtained after 15, 20, 25, 30 and 35 PCR cycles as described in Methods. V1 and 12 are standard amplification of 1A-VDAC and 1B-VDAC reported as control for gel migration. M are ladder markers GeneRuler 100 bp (Fermentas). B) densitometric areas of the bands reported in panel A were charted against the PCR number of cycles.

4.2 Expression of *D.m*. VDAC in yeast lacking of *por1* gene

The alternative full-length cDNAs for *D. melanogaster* VDAC (*Dm*VDAC) used in this work were already available in our laboratory (Messina et al. 1996, Oliva et al., 1998) as plasmids cloned in *E. coli*. In this work, 1A-VDAC and 1B-VDAC cDNAs were amplified by PCR and sub-cloned in yeast pYX212 plasmid at EcoRI and HindIII restriction sites. These constructs were then used in the complementation analysis of a Δ*por1* yeast strain, a yeast lacking the major VDAC gene, named *por1*. This analysis was performed in order to elucidate whether:

1. 1B-VDAC mRNA is not translated in yeast as in *Drosophila*;
2. *Dm*VDAC could substitute for the yeast *por1* gene, producing a functional VDAC protein.

Yeast cells lacking the *por1* gene are unable to use mitochondria and thus to perform correct respiration. Therefore, when Δ*por1* yeast cells are maintained on not fermentable carbon source (like YPY, a glycerol-based media) they are not able to grow at 37°C (not permissive temperature) (Blachly-Dyson et al., 1990). These mutant cells also grow slowly at 28-30°C, the normal growth temperature, while yeast with a wild-type *por1* gene grow at both temperatures. We used this Δ*por1* mutant yeast because its defective phenotype can be recovered by heterologous expression of native VDACs **(**Blachly-Dyson et al., 1993; Sampson M. J. et al., 1997). It is known that human and mouse VDAC1 and VDAC2 isoforms are able to complement the VDAC deficiency of Δ*por1* yeast, while VDAC3 is unable to completely rescue this phenotype (De Pinto et al., 2010). Therefore, the Δ*por1* yeast failure to grow on YPY at 37°C following transformation with heterologous genes can indicate that either the recombinant protein cannot functionally substitute for the yeast VDAC or the recombinant protein is not expressed at all.

Results from our analysis show different degrees of Δ*por1* yeast complementation in 3% glycerol and at 37°C, after transfection with constructs containing alternatively 1A- or 1B-VDAC mRNA. These complementation assays were performed using drop serial dilutions of yeast cells, spotted on plates containing glucose (YPD) or glycerol (YPY) as carbon source, and then incubated at 28°C or 37°C.

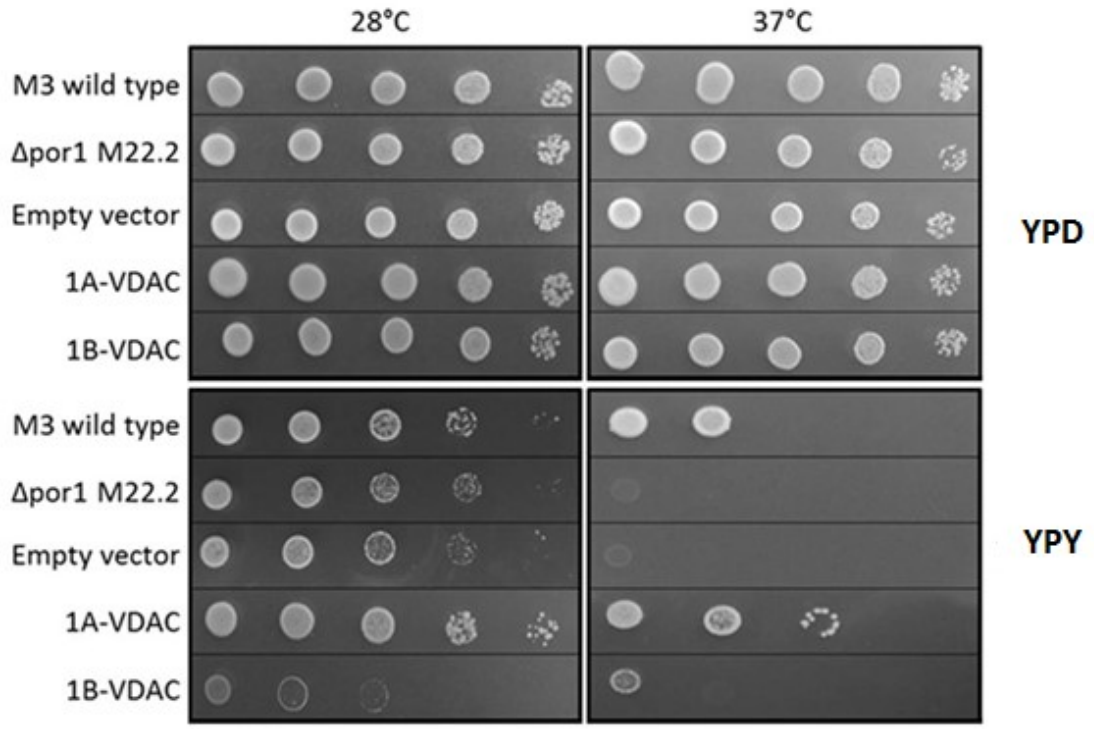

Figure 25: Complementation assay of M22.2 yeast strain lacking of the endogenous VDAC, transfected with *D. melanogaster* 1A- and 1B-VDAC variants, and spotted on YPD (Glucose) or YPY (Glycerol) at 28 and 37°C.

As shown in Fig 25, all tested yeast strains (wild type; Δ*por1* not transfected; Δ*por1* transfected with empty vector, 1A-VDAC or 1B-VDAC) were able to grow on glucose both at 28°C or 37°C, at any dilutions. In YP + 3% glycerol (YPY) not all probed strains grew at similar levels. In particular, on YPY at 28°C, yeast cells transformed with 1B-VDAC did not grow much, and they are visible only until the third dilution of the transfected cell. Instead, yeast transfected with 1A-VDAC grew on YPY at 28°C, and it is visible at any dilution. Moreover, all strains grew slowly on YPY at 37°C and only the wild type M3 and the 1A-VDAC transfected yeasts are present at the second and the third dilution, respectively.

These overall results suggest that fly 1A-VDAC mRNA is properly translated in a functional VDAC protein able to recover the mitochondrial activity in Δ*por1* yeast. Conversely, the 1B-VDAC mRNA does not produce in yeast a functional VDAC, probably because it is not translated.

4.2.1 Mutagenesis of uORF located into 1B-5'UTR

The 1A-VDAC and 1B-VDAC transcripts diverge only for the different 5'-UTR sequence. Therefore, the 1B-5'UTR sequence must contains sufficient information to determine the inhibitory effect on the translation of the coding region linked to it. We used different strategies to identify any useful data into 1B-5'UTR sequence. Scanning the 1B sequence we observed the presence of a single uORF localized at nucleotide stretch 18-51.

Figure 26: A little uORF is located in the 1B-5'UTR sequence at the positions 18 and 51.

We hypothesized that this uORF could be recognized by ribosomes preventing thus the translation of the next main coding sequence. For this reason, the ATG and TAA of uORF were mutagenized by exchanging one nucleotide of each triplet with another, removing thus these start and stop codons. The mutants, called mutATG and mutTAA, were transfected into Δ*por1* strain for complementation assay.

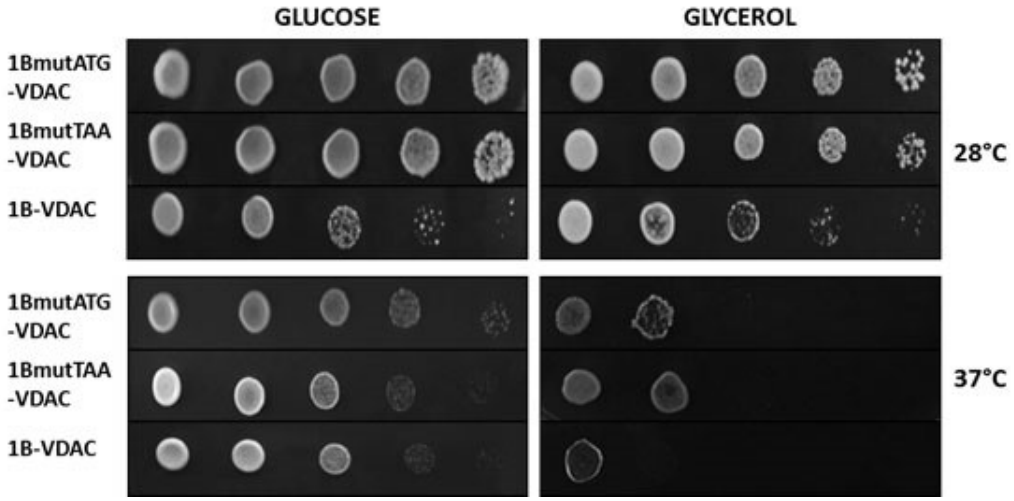

Figure 27: Complementation assay of Δ*por1* yeast transformed with uORF mutants, mutATG and mutTAA, on YPD (Glucose) or YPY (Glycerol) at 28 and 37°C.

Our results show that Δ*por1* yeast strain transfected with the uORF mutants (mutATG or mutTAA) can grow on glycerol at 37°C although the transfected yeasts do not complement the defective phenotype as much as the 1A-VDAC (Figure 25). We thus concluded that uORF in the 1B-5'UTR is not involved in the mechanism causing the block of the coding translation.

4.2.2 Characterization of 1B-VDAC mutants in yeast

In order to identify one or more putative signal sequences located in the 1B-5'UTR we performed a mutagenesis scanning experiment and produced eight mutants, each carrying the deletion of an internal sequence of 15 nucleotides in length. Each mutant was next cloned in pYX212 vector and used in complementation assays of Δ*por1* yeast.

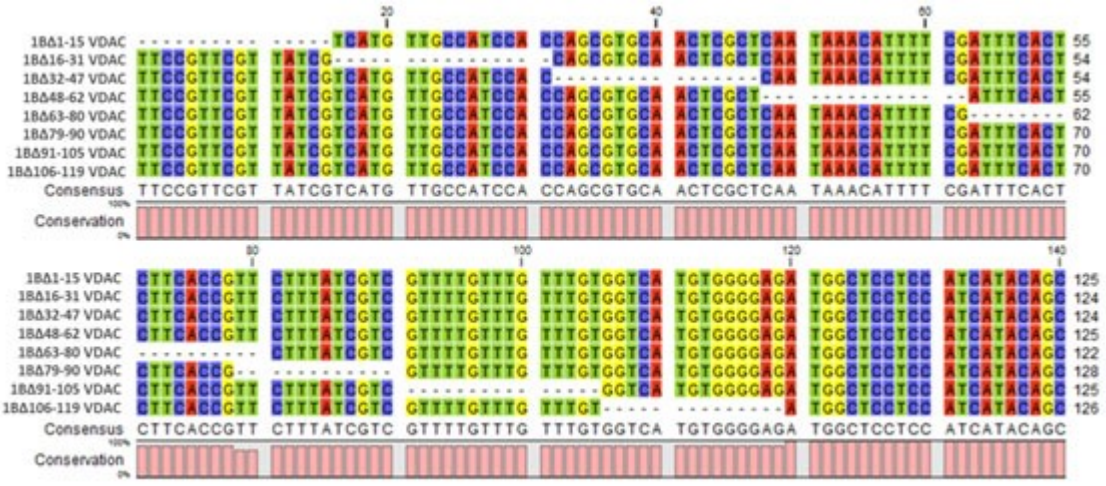

Figure 28: Multiple alignment of mutant 1B- 5'UTRs of *D. melanogaster* VDAC

In Figure 28 is reported a multiple sequence alignment among the eight 1B-5'UTR mutant sequences and the 1B-5'UTR wild-type sequence.

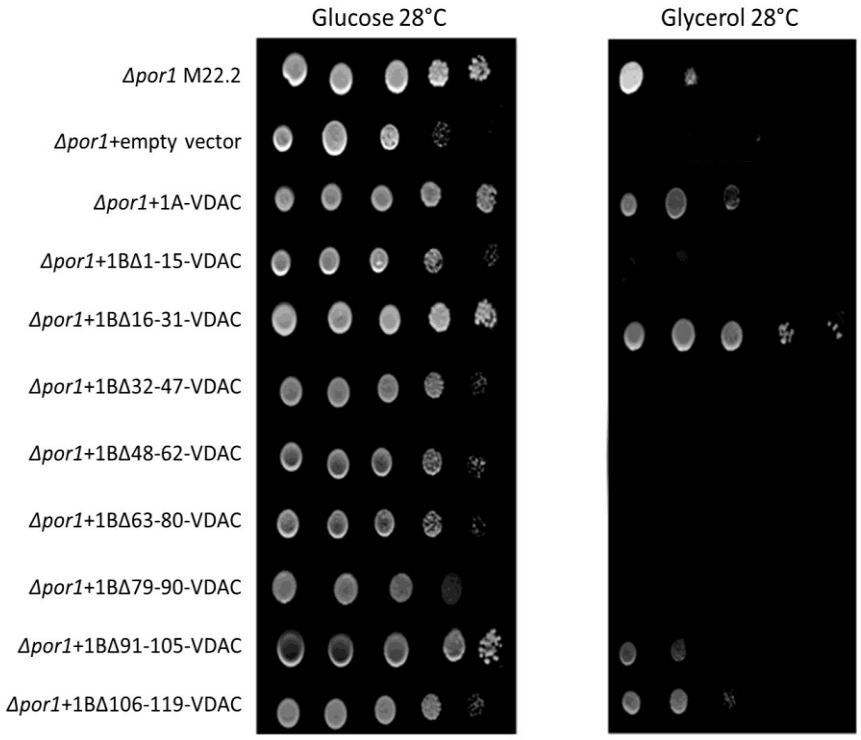

Figure 29: Microtiter assay with 1B-5'UTR mutants conducted at 28°C on plates containing glucose (YPD) or glycerol (YPY).

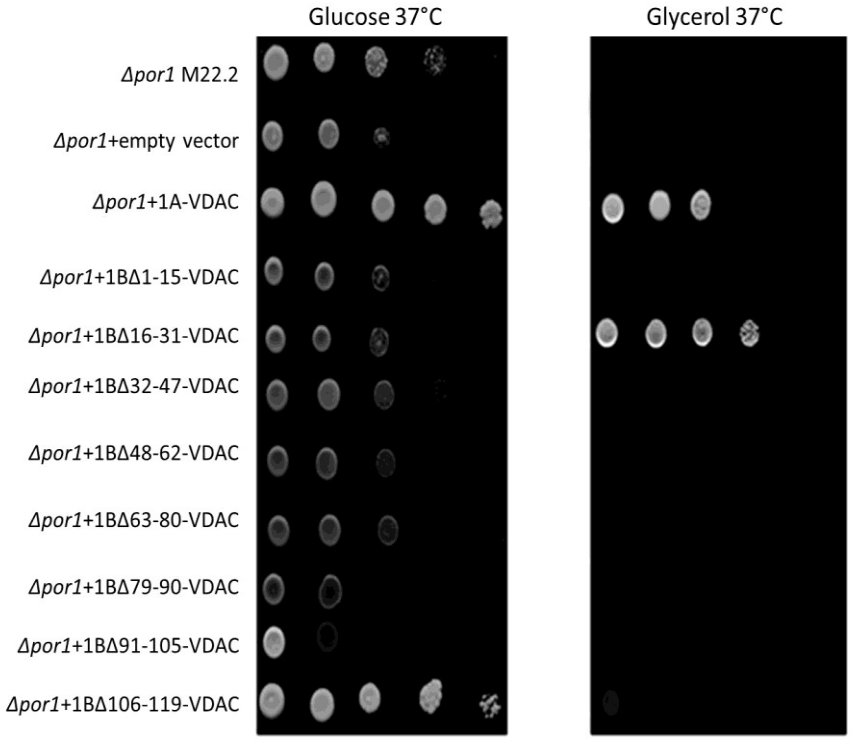

Figure 30: Microtiter assay with 1B-5'UTR mutants conduct at 37°C on plates containing glucose (YPD) or glycerol (YPY).

In the complementation assays, Δ*por1* yeast transfected with 1A-VDAC was used as positive control while not transformed Δ*por1* yeast and Δ*por1* yeast transformed only with the pYX212 empty vector, were used as negative controls. The 1B-5'UTR mutant cells, seeded on glycerol and incubated at 28°C, displayed a great difficulty to grow (Fig. 29). This behavior becomes more evident when cells grew on glycerol at 37°C (Fig. 30). In particular, the only 1B-5'UTR mutant, able to complement the Δ*por1* yeast was the 1B(Δ16-31)-VDAC mutant. This mutant recovered the Δ*por1* growth defect as well as yeast transformed with 1A-VDAC. The 1B-5'UTR mutant 1B(Δ106-119)-VDAC grew weakly on glycerol at 37°C and transfected cells did not complement the defective phenotype as much as the 1A-VDAC; the other mutants did not grow on glycerol at 37°C. Therefore, we started to focus our interest on the analysis of 1B(Δ16-31)-VDAC mutant.

Next, we determined the levels of transcriptional and translational products of 1A-VDAC and 1B-VDAC in M22.2 yeast cells. M22.2 cells transformed with 1A-VDAC or 1B-VDAC were harvested and the total RNA was extracted and used as a template for RT-PCR. Similar levels of the VDAC transcripts were observed (Fig. 31A-B-C). Cellular fractionation experiments showed, by means of a specific polyclonal antiserum, that the *D.melanogaster* VDAC is localized in mitochondria of yeast cells transformed with 1A-VDAC carrying plasmid, while no VDAC was detected in the soluble post-mitochondrial fraction (Figure 31D). These data show that the protein expressed by 1A-VDAC is correctly targeted to mitochondria. Figure 31E shows a Western blot of protein extracted from mitochondria of M22.2 cells transformed with 1A-VDAC or with 1B-VDAC. The immunostaining showed a strong reaction in the lane corresponding to the protein obtained from M22.2 carrying 1A-VDAC (lane 2), while no protein band was detected in the cells carrying the transcript 1B-VDAC (lane 4), despite the fact that its gene was present and transcribed in these cells.

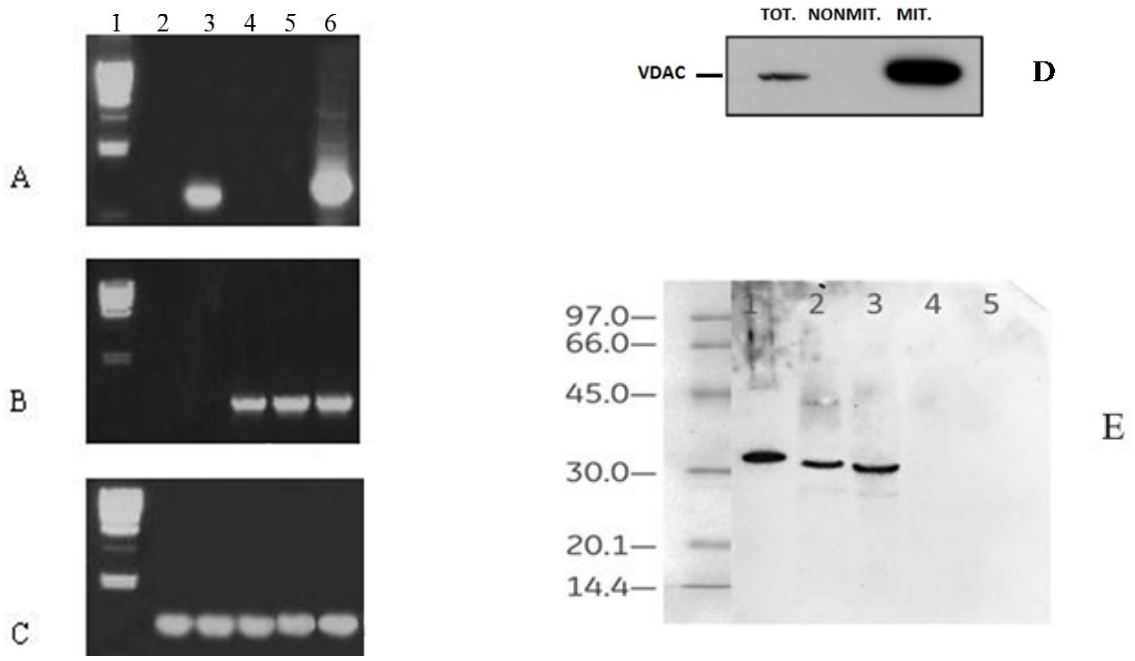

Figure 31: Both 1A-VDAC and 1B-VDAC are transcribed in VDAC-deleted yeast strain M22.2, but only 1A-VDAC is translated and its product targeted to mitochondria.
(A)RNA from M22.2 Δ*por1* yeast (lane 2) and from the same strain transformed with 1A-VDAC (lane 3), 1B-VDAC (lane 4) or 1B(Δ16-31)-VDAC (lane 5) were reverse transcribed and used in PCR reactions specific for 1A-VDAC; as a positive control (lane 6.A) the plasmid pYX212 carrying 1A-VDAC was amplified; in lane 1 a λ-HindIII molecular weight marker. B) The same templates were used for PCR amplifications specific for 1B-VDAC; as a positive control the plasmid pYX212 carrying 1B-VDAC was used in lane 6.B). C) The same templates were used for a control PCR reaction with primers specific for YMC2 (Yeast Mitochondrial Carrier YBR104W), a housekeeping yeast gene; as a positive control the plasmid pYX212 carrying YMC2 was used (lane 6.C). D) *D. melanogaster* VDAC encoded by the plasmid pYX212 carrying the construct 1A-VDAC is targeted to yeast mitochondria. M22.2 yeast cells carrying pYX212-1AVDAC were grown at the exponential phase and a mitochondrial and a cytoplasm fractions were separated. 100 µg of protein fractions were electrophoresed, blotted and immuno-decorated with anti-*D. m.* porin antibody (1:1000 dilution). E) Western blot analysis of mitochondrial protein extracts from M22.2 yeast strain carrying 1A-VDAC (lane 2), 1B(Δ16-31)-VDAC (lane 3) or 1B-VDAC (lane 4); lane 1: recombinant 7T21 *D. melanogaster* VDAC protein; lane 5 M22.2 Δ*por1* untransfected In each lane 100 µg of protein fractions were electrophoresed, blotted and immuno-decorated with anti-*D. m* porin antibody (1:1000 dilution).

4.2.3 Western blotting on yeast mitochondrial lysates

Western blotting analysis was performed to test the *Dm*VDAC expression in mitochondrial lysates from yeast cells transformed with 1A- 1B- or 1B(Δ16-31)-VDAC coding sequences (Figure 31E). In these experiments, we used the recombinant *D. melanogaster* VDAC as a positive control and an antibody against the *D. melanogaster* VDAC produced in rabbit in our laboratory (Oliva et al., 2002).

Western Blotting revealed that VDAC was only expressed in yeast cells transformed with 1A-VDAC (lane 2) or 1B(Δ16-31)-VDAC (lane 3). No VDAC protein was detected in the mitochondrial samples from yeast transformed with 1B-VDAC or empty vector (lane 4-5).

These results suggest that:

- VDAC protein is not expressed from 1B-VDAC mRNA in yeast cells, explaining the inability of 1B-VDAC mRNA to restore the growth defects of Δ*por1* yeast.
- the 16-31 nt stretch in the 1B-5'UTR is certainly involved in the translation control mechanism of 1B-VDAC mRNA in yeast.

4.2.4 Analysis of bound 1A-VDAC and 1B-VDAC mRNAs to ribosomes of VDAC-deleted yeast strain

To evaluate whether 1B-5'UTR affects translation by interfering with the binding of the transcript to the ribosomes, M22.2 yeast cells transformed with 1A-VDAC or with 1B-VDAC carrying plasmids were grown, harvested and the ribosomal fraction purified and analysed. The results presented in Fig. 32 clearly show that both 1A-VDAC and 1B-VDAC mRNAs were bound to ribosomes. Thus, in yeast cells, the lack of translation of the 1B-VDAC mRNA is not due to the inefficiency of ribosomal binding, but possibly to interference with other components of translation machinery.

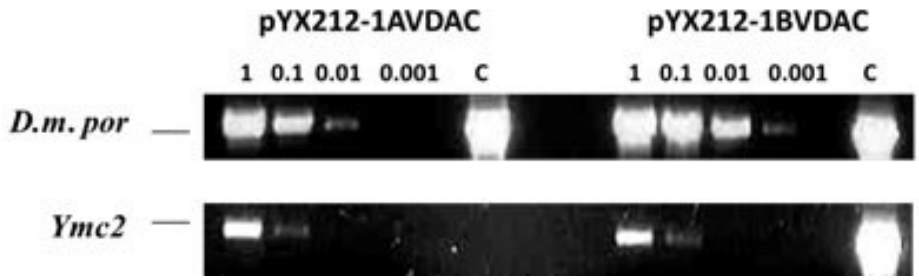

Figure 32: Either 1A-VDAC and 1B-VDAC transcripts bind to ribosomes in VDAC-deleted yeast strain. The ribosomal fraction from M22.2 Δ*por1* cells transformed with 1A-VDAC or 1B-VDAC was isolated by ultracentrifugation. RNA associated to the ribosomal fraction was extracted and RT-PCR was performed with primers specific for 1A-VDAC or for 1B-VDAC. The samples in each lane contain respectively 2 µl of total cDNA, and 1:10, 1:100 and 1:1000 dilutions of the same template. C is a positive control. Every reaction was repeated with primers specific for YMC2, a housekeeping yeast gene.

4.2.5 RNA Electrophoresis Mobility Shift Assay (REMSA)

It is well known that many RNA Binding Proteins (RBPs) interact with mRNAs via a set of modular RNA-binding domains (RBDs), including the RNA recognition motif (RRM), the heterogeneous nuclear RNP K-homology domain (KH), zinc fingers (Znf), etc. (Lunde et al., 2007). These motifs have been included in bioinformatics algorithms designed to identify other proteins harboring similar signatures and classify putative additional RBPs (Anantharaman et al., 2002). However, numerous

noncanonical RBDs have been reported (Lee and Hong, 2004; Niessing et al., 2004; Rammelt et al., 2011; Zalfa et al., 2005), reflecting limitations in the scope of computational predictions. More recently, two studies using protein microarrays and RNA probes identified about 200 RBPs from budding yeast, including several novel candidates (Scherrer et al., 2010; Tsvetanova et al., 2010).

By sequence scanning the 16-31 nt region from 1B-5'UTR we did not recognize any known RNA-binding domain. We thus performed a RNA electrophoresis mobility shift assay (REMSA) on a little synthetic RNA sequence corresponding to the 16-31 region from 1B-5'UTR. In REMSA, naked RNA and protein-RNA complexes can be distinguished because they have different migration on gel electrophoresis. Therefore, we tested the ability of our RNA samples to interact with putative yeast RBPs in total extracts from wild-type M3 yeast strain.

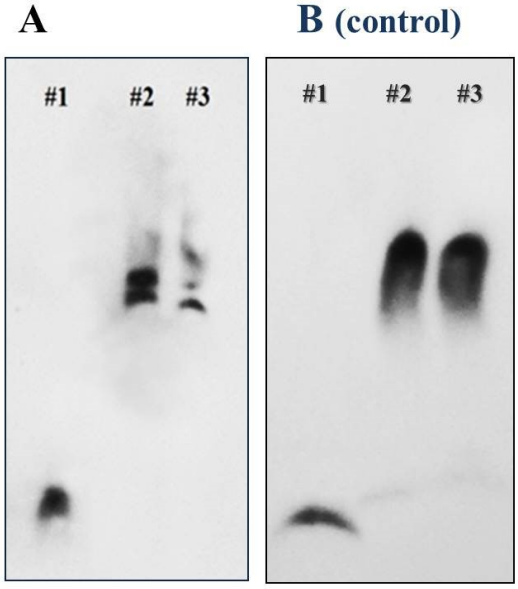

Figure 33: REMSA assays performed with two different oligo RNAs. Panel A; #1) 0,5 nM Biotinylated RNA 10-37; #2) 0,5 nM Biotinylated RNA 10-37 + total yeast lysate; #3) 0,5 nM Biotinylated RNA 10-37 + total yeast lysate + 6 µM not biotinylated RNA competitor. Panel B: #1) 2 nM Biotinylated RNA 74-95; #2) 2 nM Biotinylated RNA 74-95 + total yeast lysate; #3)2 nM Biotinylated RNA 74-95 + total yeast lysate + 6 µM not biotinylated RNA competitor.

We carried out REMSA assays by using as sample a RNA oligonucleotide (named 10-37) with a sequence corresponding to the 10-37 nt region of 1B-5'UTR, including thus the 16-31 nt sequence. In the same experiment, another RNA oligo, named 74-95, having the sequence 74-95 of 1B-5'UTR, was used as a negative control. To improve the binding between RNA and yeast proteins, Heparin was added to the reaction mix. Results from REMSA experiments are reported in Figure 33 where panel A reveals that yeast proteins are able to establish specific interactions with our RNA sample. Indeed, a strong signal was obtained with the biotinylated RNA 10-37 (lane #2) and this signal

diminished by adding a molar excess of the specific competitor RNA (non-biotinylated RNA 10-37) (lane #3). The specific competitor works stealing the proteins from the formed ribonucleoprotein complex, proving thus that protein binding to RNA 10-37 is specific. Exactly, at lane #2, two bands are visible; these could be produced by interaction of two different RBPs with different RRM into the target RNA 10-37.
Figure 33-B shows the results of REMSA on RNA 74-95, used as bait molecule. In this case, we obtained a similar strong signal using the biotinylated RNA 74-95 alone (lane #2) or together with a specific competitor RNA (non-biotinylated RNA 74-95) (lane #3). Consequently, in this reaction the RNA competitor does not interfere with the formed ribonucleoprotein complex, suggesting that these RBPs bind the RNA 74-95 only by aspecific interactions.

4.2.6 RNA pull down assay and mass spectrometry

Experiments of RNA pull down (RPD) were performed to isolate ribonucleoprotein complexes formed between the RNA 10-37 and the yeast total proteins. In the RPD assay, streptavidin-conjugated magnetic beads were used to capture biotinylated RNA–protein complexes. These ribonucleoprotein complexes were eluted from beads with sample buffer 1X (see Methods Section) and, after incubation at 95°C for 3 min, samples were analyzed by SDS-PAGE (Fig. 34, lane 2). After gel staining, each protein pattern in each lane was excised from gel and cut in very thin slices. Exactly, we cut out 9 slices from sample of RNA10-37 binding proteins and 9 slices from sample of RNA-control binding proteins (RNA 74-95) (Fig. 35) Proteins in each slice were then identified by Mass spectrometry analysis. Mass spectrometry analysis was performed with a Q-Star XL tandem mass spectrometer (Applied Biosystems, Foster City, CA). The MS/MS data files generated were analysed using the Mascot 2.1 search engine (Matrix Science, London, UK) against UniProt with yeast species restriction. The Mascot search results were accepted if a protein hit included at least one peptide with a score above the homology threshold.

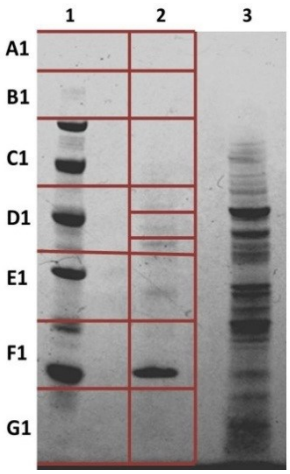

Figure 34: proteins interacting with oligo RNA 10-37 and subjected to mass spectrometry analysis. Lane 1: Protein ladder; lane 2: Biotinylated RNA 10-37-protein complexes; lane 3: unbound proteins

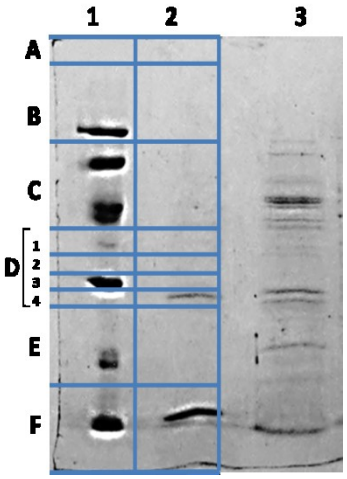

Figura 35 proteins interacting with oligo RNA 74-95 and subjected to mass spectrometry analysis. Lane 1: Protein ladder; lane 2: Biotinylated RNA 74-95-protein complexes; lane 3: unbound proteins

TABLE 1. List of proteins interacting with 16-31nt-1B RNA identified by MS-SPEC.

MW	PI	Protein name/Symbol	score	Cover %	UniProt ID	GO biological process	Loc.
42,3	7,68	K7_Arc1p	707	45	G2WDZ5	tRNA binding	cyt
96,7	5,66	Valyl-tRNA synthetase (Vas1p)	627	14	E7NHX9	tRNA ligase activity	cyt
48,72	5,89	Met17p	473	24	E7Q715	methionine biosynthesis	cyt
66,6	5,37	Hsp70 ATPase SSB2 (Hsp76)	415	19	P40150	regulation of translational fidelity	cyt
83,0	8,30	Gus1p	413	17	J8Q5E4	Nucleotide binding	cyt
44,9	6,13	Oye2p	292	14	E7KDJ6	oxidoreductase activity	cyt
44,48	5,02	eIF4A	690	27	P10081	regulation of translational initiation / unwinds RNA secondary structures	cyt
34,7	5,64	Guanine nucleotide-binding protein subunit beta-like protein (Asc1)	203	22	P38011	Negative regulation of translation / Bound to the 40S ribosome near to exit channel for mRNA	cyt
25,12	6,52	Gsp2p /Ran-GTPase	659	30	E7M0I0	Transport of mRNA from nucleus to cytosol	nc
14,67	9,94	S22A	245	32	A6ZQE6	ribosomal 40S subunit protein	cyt
11,68	5,43	Hsp12p	255	43	E7KM26	Heat shock protein	cyt

Table 11: list of proteins interacting with the 10-37 region of 1B-5'UTR

Proteins in Table 11 are significantly engaged in the binding of RNA 10-37. Their activity is tightly linked to mechanisms correlated with the translation. In particular, eIF4A and Asc1 could be highly involved. eIF4A is a RNA helicase that works as a subunit of eIF4F, a complex composed of eIF4G and eIF4E. The yeast ribosomal protein Asc1 is the homologue of RACK1 and it is required for an efficient translation of housekeeping mRNA with a short open reading frame.

4.2.7 5'UTR of 1B-VDAC mRNA strongly interacts with the helix 34 of yeast 18S rRNA

The "IntaRNA" (http://rna.informatik.uni-freiburg.de/IntaRNA/Input.jsp) is a free software for the accurate prediction of interactions between two RNA molecules. It has been designed to predict mRNA target sites for given non-coding RNAs. We used IntaRNA program to predict interactions between yeast 18S ribosomal RNA and *Dm porin1* mRNAs (1A-VDAC, 1B-VDAC and mutant 1B-Δ16-31-VDAC) assayed in this work. This analysis predicts that the 2-115 sequence on 1B-VDAC mRNA targets to 1.209—1.331 sequence of yeast 18S rRNA, producing a long dsRNA stretch with an hybridation energy of -76,0 Kcal/mol (Fig. 36).

Conversely, the 1712-1734 sequence from 18S rRNA it is able to complement with the 7-28 stretch on 1A-VDAC mRNA, forming thus a short dsRNA with an hybridation energy of -22,3 Kcal/mol (Fig. 37). Similary, 1B(Δ16-31)-VDAC mRNA can interact with 18S rRNA producing only short dsRNA stretch, with a low hybridation energy value (Fig. 38).

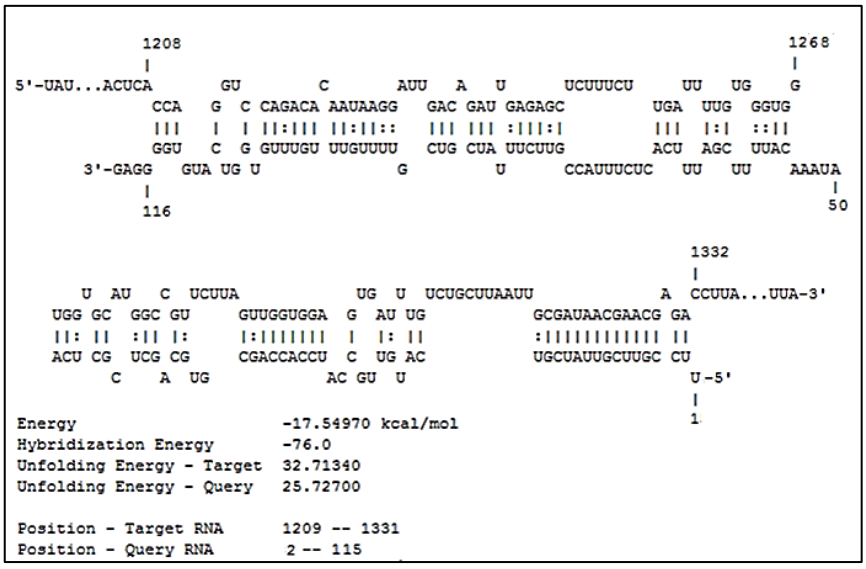

Figure 36: interaction between 5'UTR 1B and 18S rRNA

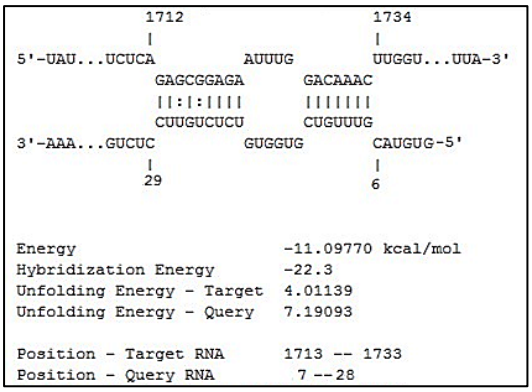

Figure 37: interaction 5'UTR1A - 18SrRNA

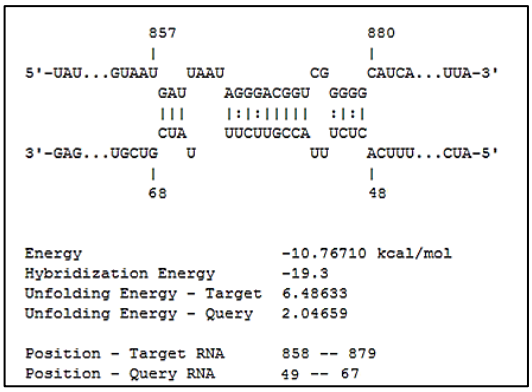

Figure 38: interaction 5'UTR 1B(Δ16-31) - 18S rRNA

Interestingly, we found that the region of 1B-VDAC mRNA interacting with 18S rRNA corresponds to the whole 1B-5'UTR sequence. Moreover, it is highly considerable that the sequences of 18S rRNA forming dsRNA by interaction with 1B-5'UTR correspond to solvent-exposed rRNA regions. In particular, the helix h34 of 18S RNA, a domain highly involved in the interaction with the 1B-5'UTR sequence, is usually used by the ribosome to latch the transcript into the mRNA entry channel of 40S ribosomal subunit (Fig.39).

Figure 39: h34 helix of yeast 18S rRNA

Overall, our results from RNA:RNA prediction analysis together with MS data suggest that in yeast some different mechanisms could be involved in the translation control of 1B-VDAC transcript from *D. melanogaster*.

4.3 Expression of reporter genes fused to *D. melanogaster* 1A- or 1B-5'UTR sequences

After demonstration in *Drosophila melanogaster* as in yeast that alternative *D. melanogaster* 1A-VDAC and 1B-VDAC mRNAs are subject to a different translational

control, we wanted to assay if corresponding 1A- and 1B-5'UTRs can influence the expression of any coding sequence fused to it or if they act only on the corresponding VDAC mRNA. For this purpose, we designed experiments where constructs carrying different reporter genes [(Green Fluorescent Protein (GFP) and Luciferase (Luc)] were expressed *in vitro* in various cell models (yeast, human and *D. melanogaster* cells).

4.3.1 Expression in yeast of GFP fused to wild type or mutant 5'UTRs from *D. melanogaster porin1* gene

The 1A-, 1B- or 1B(Δ16-31)-5'UTR sequences were cloned in the pYX212 expression vector, upstream of the GFP sequence. These constructs, producing transcripts with a GFP coding sequence fused to one of tested 5'UTR, were used to transform the M3 wild-type yeast strain. M3 cells transformed with 1A-, 1B-, or 1B(Δ16-31)-GFP were harvested and the total RNA was extracted and used as a template for RT-PCR. Proteins in total lysates from the same cells were analyzed by western blotting (WB) using an antibody against the GFP protein.

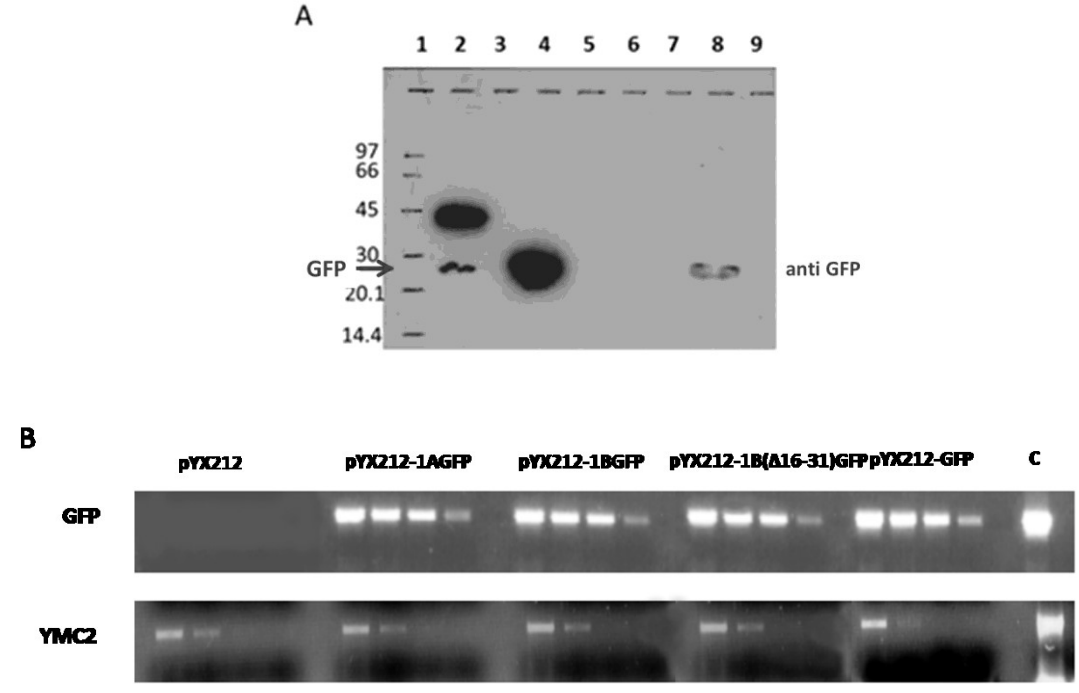

Figura 40: The 5'-UTR sequence 1B has an inhibitory effect upon translation of downward coding sequences.
A) Western blot analysis of protein extracts from M3 yeast strain carrying 1A-GFP (lane 4), 1B-GFP (lane 6), 1B(Δ16-31)-GFP (lane 8) or as a positive control the wt-GFP (lane 2). In lanes 2 and 4 were loaded 55 µg of protein fractions, while in lanes 6 and 8, 360 µg of total lysates were electrophoresed, blotted and immuno-decorated with anti-GFP antibody (1:1000 dilution). In lane 1were loaded a molecular weight marker while lanes 3, 5, 7 and 9 were empty. B) RT-PCR performed starting from RNA of the same strains in (A). 2 µl of total cDNA, and 1:10, 1:100 and 1:1000 dilutions of the same templates were amplified with primers specific for GFP. Lane C shows the amplification upon pYX212-GFP as a control. Every reaction was repeated with primers specific for YMC2, a housekeeping yeast gene, as a loading control (FW YMC2: 5'-ATGAGTGAAGAATTTCCTA-3'; REV YMC2: 5'-CTACTCTTCCCCCAGAAATC-3'

In Fig. 40A is displayed a WB experiment, carried out with an anti-GFP antibody, of total extracts from yeasts transformed with constructs for wt-GFP, 1A-GFP, 1B-GFP or 1B(Δ16-31)-GFP transcripts. Our results highlighted that GFP was highly expressed from transcripts corresponding to 1A-GFP sequence (Fig. 40, lane 4). Conversely, GFP was not expressed from transcripts with 1B-5'UTR sequence (Fig. 40, lane 6), despite the protein extract was overloaded (360 µg) in the corresponding gel lane, while a lower amount (55 µg) of 1A-GFP sample was present in the other lane in the same gel. In yeast transformed with the construct carrying 1B(Δ16-31)-GFP transcript the translation of GFP coding sequence was still subject to inhibition (Fig. 40, lane 8).

Altogether, these results prove that in yeast: 1) the 1B-5'UTR sequence inhibits the translation of any coding sequence fused to it; 2) the deletion of the sequence 16-31 nt from 1B-5'UTR is not able to recover its inhibitory effect; 3) the 1A-5'UTR sequence contains all essential information to start the translation of any coding sequence.

4.3.2 Expression in HeLa cells of GFP fused to wild-type or mutant 5'UTRs from *D. melanogaster porin1* gene

The 1A-, 1B-, 1B(Δ16-31)-5'UTR, and 1A(ins16-31)-5'UTR sequences were cloned in pEGFP-N1 vector in frame with the coding sequence for EGFP, a more brilliant (Enhanced-GFP) GFP protein. The mutant 1A(ins16-31)-5'UTR sequence was obtained by insertion of the sequence 16-31 from *D.m.* 1B-5'UTR into the 1A-5'UTR sequence. This mutant was produced for testing if the sequence 16-31 nt is able to reduce the translation of a reporter gene when inserted into the 5'UTR fused to it. All recombinant vectors produced were used to transfect HeLa cells.

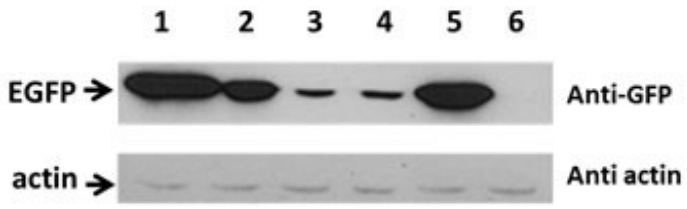

Figure 41: Western blotting with anti-GFP ab, of total lysates from HeLa cells transfected with EGFP constructs carrying wt or mutant *Dm porin1* 5'UTRs. Lane 1: wt EGFP; lane 2: 1A-EGFP; lane 3: 1B-EGFP; lane 4: 1B(Δ16-31)-EGFP; lane 5: 1A-ins16-31-EGFP; lane 6: untransfected cells. 5 x 10^6 HeLa cells were seeded into a 6-well plate and incubated at 37°C with 5% CO_2 for 24 hours. Transfection was performed using the *"Lipofectamine 3000 transfection kit"* (Invitrogen) with 2,5 µg of each plasmid DNA. 48 h later, cells were collected and lysed. 50 µg of each lysate were electrophoresed for SDS-PAGE. WB was performed using anti-GFP (Roche 1:1000) and anti actin 1:1000 as loading control.

In the Fig. 41 is shown a WB from total lysates of HeLa cells transfected with EGFP constructs. The EGFP expression was revealed by using a commercial, usual anti-GFP (Roche) antibody. Results display that 1B(Δ16-31)-EGFP sample has a very low expression level of EGFP as well as 1B-EGFP sample, while 1A(ins16-31)-EGFP sample has an high expression level of EGFP, like 1A-EGFP sample. To confirm these results, we conducted on the same samples a flow cytometry assay.

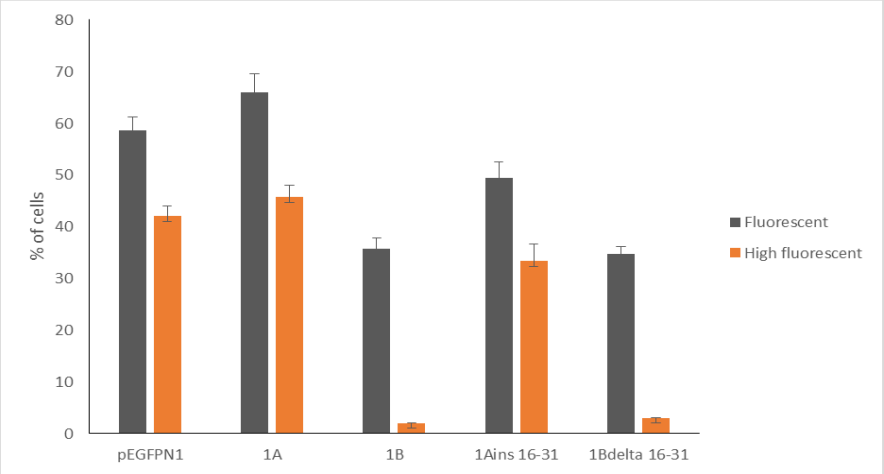

Figure 42: Percentage of fluorescent HeLa cells transfected with EGFP constructs.

In Fig. 42, the histograms represent the percentages of cells expressing EGFP, on the total amount of 20.000 cells for each sample and two gates of fluorescence were analyzed. So, expression data obtained by this analysis are very careful and thus more reliable than the corresponding WB results. In particular, our flow cytometry assays demonstrated that 1A-EGFP transcript highly synthesizes EGFP, approximately 10% more than a transcript containing only EGFP and without any 5'UTR fused to it. This result confirms that 1A-5'UTR is highly efficient to promote the translation of any linked coding sequence. Conversely, 1B-EGFP or 1B(Δ16-31)-EGFP samples showed a low percentage, 3-5%, of cells expressing EGFP. Interestingly, in the 1A(ins16-31)-EGFP sample there was a decreased GFP expression of 15%, probably related to the insertion of 16-31 sequence.

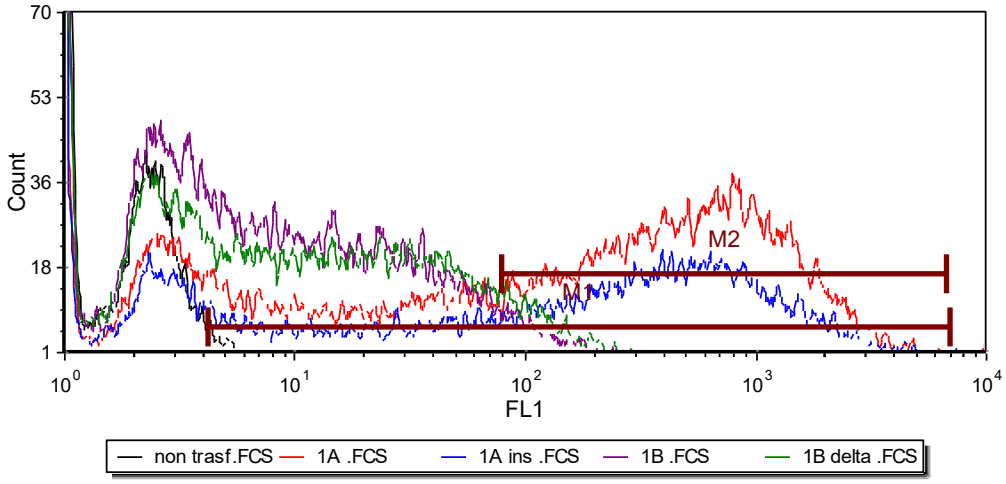

Figure 43: Flow cytometry assay of HeLa cells expressing EGFP fused to wild type or mutant 1A- or 1B-5'UTRs

4.4 *In vitro* transcription and translation experiments in *D. melanogaster* embryonic extracts

The *Firefly* Luciferase (Luc) coding sequence was fused to wt or mutant 5'UTRs from *D.melanogaster porin1* gene and then inserted in the modified pBSK- vector (F. Gebauer et al., 1994). The pBSKA-5'UTR-Luc constructs were digested with a restriction enzyme cutting after the poly(A) tail. These linearized constructs were used in *in vitro* transcription assays with the T3 RNA polymerase. The RNA concentration was evaluated both by microvolume measurements in a NanoDrop spectrophotometer and by visual estimate of the electrophoretic staining from each samples after migration in 1% agarose gel with 2X formaldehyde gel-loading buffer. Next, 4 ng of mRNA from each sample were used in *in vitro* translation analysis with 25 µg of *D. melanogaster* embryo extracts.

4.4.1 Measurements of Luciferase activity after *in vitro* translation of 5'UTRs-Luc constructs

The 1A-Luc, 1B-Luc and 1B(Δ16-31)-Luc mRNAs were translated *in vitro* together with the *Renilla* Luciferase mRNA (RLuc). The measurement of Luc and RLuc activities was performed using a Dual Luciferase Reporter (DLR) assay (Promega). In this assay, the activities of Firefly (*Photinus pyralis*) and Renilla (*Renilla reniformis*)

Luciferases are measured sequentially from a single sample. Three replicas of each sample were measured, and each assay was repeated three times. The graph in Fig. 44 shows results from these *in vitro* translation experiments, where we can see that 1A-Luc was five times more expressed than 1B-Luc, in *Dm* embryonic extracts. The embryonic extracts contain all cellular components and thus also the factors that *in vivo* recognize each 5'UTR, controlling the mRNA translation. The 1B(Δ16-31)-Luc construct was translated at the same level of 1B-Luc, showing that, also in this cell model, the lacking sequence 16-31 nt does not modify the ORF expression level.

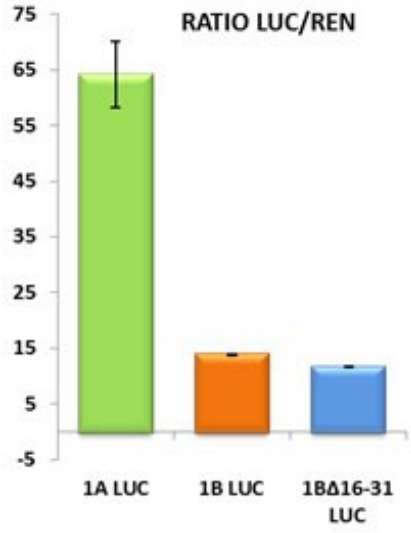

Figure 44: Firely Luciferase (Luc) and Renilla Luciferase (RLuc) activities from Luc constructs with wt or mutant 5'UTRs. Luciferase constructs *in vitro* translated, in the presence of Embryo extracts, were diluted 1:100 in Passive Lysis Buffer 1X. Luciferase activity was measured by Dual Luciferase Reporter Assay System.

4.5 Analysis of *in vivo* expression in *D. melanogaster* embryonic SL2 cells

4.5.1 Expression in SL2 cells of constructs carrying wild type or mutant 5'UTRs linked to Luciferase reporter genes

Previous results obtained by *in vitro* translation experiments, to be considered sure, had to be confirmed in a suitable cell model. Therefore, we performed *in vivo* expression analysis in *Drosophila melanogaster* embryonic SL2 cells, the most used cells for *D.m.* expression analysis. SL2 cells were transfected with the *Dm* 5'UTRs-Luc constructs cloned in the pMK26 vector. The pMK26-Luc was also used as a positive control in our experiments. Moreover, SL2 cells were also co-transfected with a construct (pAc-Rluc) containing the *Renilla* Luciferase reporter gene inserted in a pAc

vector (pAc5.1/V5-His, Invitrogen), as a control of transfection. Luciferase activity in transfected SL2 cells was then measured with a DLR assay (as in 4.4.1).

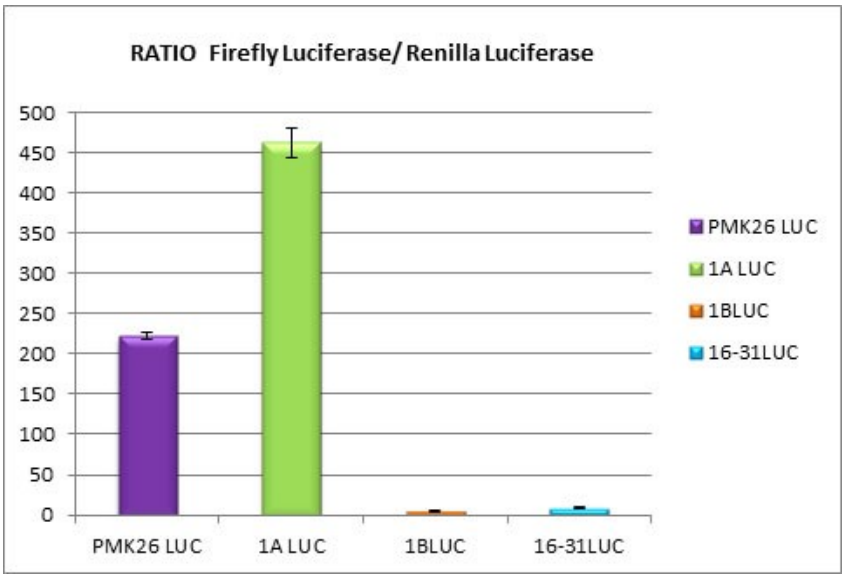

Figure 45: Luciferase activity assay in SL2 cells expressing 5'UTRs-Luc constructs. . $3x10^6$ SL2 cells were seeded in $10cm^2$ plates (6well plates) in 10% FBS Schneider's Drosophila medium. After 24h the cells were transfected by Lipofectamine 3000 with 20 ng of Renilla construct, and 300 ng of 1A, 1B- and 1B(Δ16-31)-Luciferase in pMK26 vector. 48h post-transfection cells were collected and lysed with Passive Lysis buffer 1X. Luciferase activity was measured by Dual Luciferase Reporter Assay System(Promega)

Data obtained from these experiments (Fig. 45) show that Luc activity of the 1A-Luc sample is twice higher than the pMK26-Luc positive control and 450 times higher than the 1B-Luc or the 1B(Δ16-31)-Luc samples. Therefore, these results prove that: a) the 1B-5'UTR sequence or its mutant 1B(Δ16-31)-5'UTR are able to inhibit the translation of the Luciferase coding sequence; b) the 1A-5'UTR sequence considerably stimulates the translation of the gene reporter.

4.5.2 Expression in SL2 cells of constructs carrying the *D. melanogaster porin1* coding sequence fused to the wild type or mutant 5'UTRs

The constructs 1A-VDAC-HA, 1B-VDAC-HA and 1B(Δ16-31)-VDAC-HA used for this analysis, after cloning in the pAc vector, were co-transfected with the pAc-Rluc (as transfection control) in SL2 cells as described in 3.17. These VDAC constructs carried a wt (1A- or 1B-) or mutant (1BΔ16-31) 5'UTR sequence linked to the *D.m. porin1* coding sequence, in frame with the Hemagglutinin (HA) tag. The expression of the HA-tag sequence from any VDAC construct allowed us to distinguish in SL2 cells

between the endogenous VDAC (revealed only by a home-made anti-*Dm*Porin1 antibody) and the recombinant VDAC (revealed also by an anti-HA antibody).

Firstly, the Rluc activity was measured by DLR assays on a little amount of cells from each samples. The remaining cells were lysed in RIPA buffer and then 60 µg of each lysate were used for WB analysis. In WB, immuno-decorated with an anti-HA tag antibody, we revealed the recombinant VDAC, also named VDAC-HA.

In WB (Fig. 46) it is visible that all the VDAC-HA constructs assayed are translated in SL2 cells. Moreover, the picture shows that 1B-VDAC-HA is unexpectedly translated. The mutant 1B(Δ16-31)-VDAC-HA is translated as well as the 1B-VDAC-HA, confirming that 16-31 region from 1B-5'UTR sequence is not involved in the mechanism of translation control.

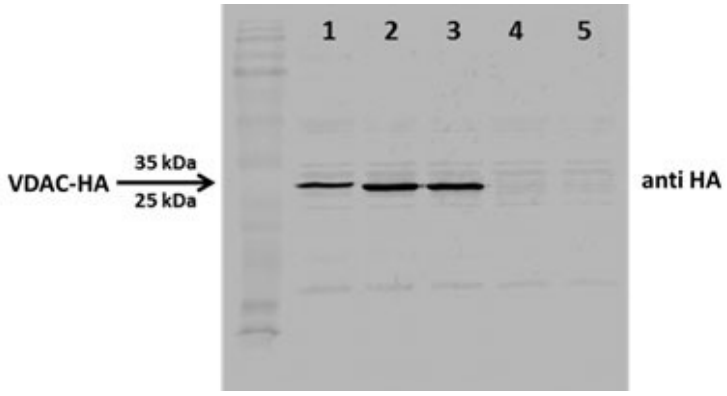

Figure 46: Western blotting with rabbit anti-HA-tag Ab (1:100) on total lysates of SL2cells transfected with 300 ng VDAC-HA constructs liked to wt or mutant 5'UTRs. Lane 1: 1A-VDAC-HA; lane 2: 1B(Δ16-31)-VDAC-HA; lane 3: 1B-VDAC-HA; lane 4: empty pAc vector; lane 5: untransfected SL2 cells. $3x10^6$ SL2 cells were seeded in $10cm^2$ plates (6well plates) in 10% FBS Schneider's Drosophila medium. After 24h cells were transfected by Lipofectamine 3000 with 20 ng of Renilla construct, and 300 ng of 1A, 1B- and 1B(Δ16-31)-VDAC-HA in pAc vector. 48h post-transfection the cells were collected and processed for protein and RNA extraction. 50 µg of total extract were separated by SDS page electrophoresis. Immunoblotting analysis was performed using a rabbit anti-HA-tag antibody (Santa-Cruz) (1:100).

Furthermore, we were interested to assess the expression of endogenous VDAC (eVDAC) after transfection of SL2 cells with the constructs carrying recombinant VDACs (rVDAC) tagged with HA sequence. Therefore, the expression of eVDAC was followed in the previous experiments on SL2 cells by using a polyclonal antibody (1:200 dilution) against the *D.m.* VDAC. This anti-*Dm*Porin1 is a home-made Ab, produced by rabbit immunization with purified recombinant *D.m.* VDAC protein.

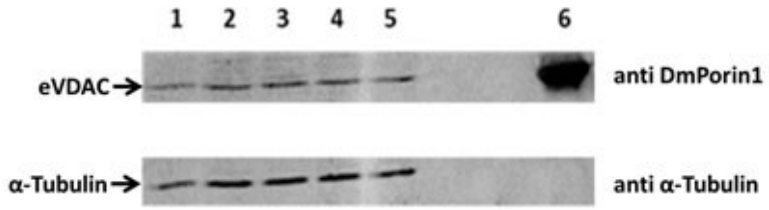

Figure 47: Western blotting with rabbit anti-*Dm*Porin1 Ab (1:200) on total lysates from SL2 transfected with 300 ng VDAC-HA constructs linked to wt or mutant 5'UTRs. Lane 1: 1A-VDAC-HA; lane 2: 1B-VDAC-HA; lane3: 1B(Δ16-31)-VDAC-HA; lane 4: empty pAc vector; lane 5: untransfected SL2 cells; lane 6: recombinant 7T21 VDAC protein. $3x10^6$ SL2 cells were seeded in $10cm^2$ plates (6well plates) in 10% FBS Schneider Drosophila medium. After 24h the cells were transfected by Lipofectamine 3000 with 20 ng of Renilla construct, and 300 ng of 1A, 1B- and 1B(Δ16-31)-VDAC-HA in pAc vector and empty pAc vector. 48h post-transfection the cells were collected and processed for protein and RNA extraction. 50 μg of total extract were separated by SDS page electrophoresis. Immunoblotting analysis was performed using rabbit anti Dm-porin antibody (1:200).

Results in Fig. 47 display that the expression in SL2 cells of eVDAC does not change after transfection with any tested HA-tagged rVDACs. VDAC was identified by its molecular size and also by comparison with the recombinant *D.m.* VDAC protein (purified from our 7T21 clone), loaded in the lane 6 of the gel. The same samples were also analyzed by anti α-Tubulin (Sigma) 1:500.

In order to visualize in the same blot both the HA-tagged rVDAC and the eVDAC (different in molecular size only for one kDa), total lysates from SL2 cells, transfected with 1A-VDAC-HA, 1B-VDAC-HA or 1B(Δ16-31)-VDAC-HA, were fractioned by electrophoresis in a gel containing a higher concentration of polyacrylamide (15%). The membrane from the corresponding WB, was first blotted with both rabbit anti HA-tag (1:100) and anti-*Dm*Porin1(1:200) antibodies and then with an 1:25.000 anti-rabbit antibody (Fig. 48).

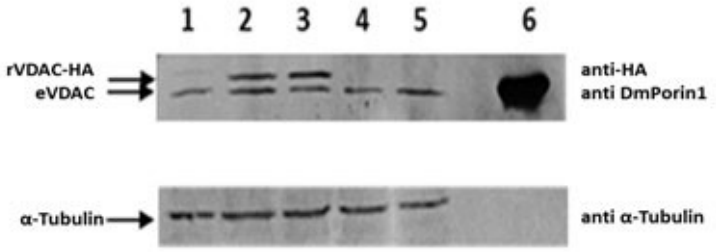

Figure 48: Western blotting on total lysates of SL2 transfected with 1A-, 1B- or 1B(Δ16-31)-VDAC-HA constructs and immuno-decorated with both anti-HA-tag (1:100) and anti-DmPorin1(1:200) antibodies. Lane 1: 1A-VDAC-HA; lane 2: 1B-VDAC-HA; lane 3: 1B(Δ16-31)-VDAC-HA; lane 4: empty pAc vector; lane 5: untransfected SL2 cells; lane 6 Recombinant 7T21 VDAC protein. $3x10^6$ SL2 cells were seeded in $10cm^2$ plates (6well plates) in 10% FBS Schneider Drosophila media. After 24h the cells were transfected by Lipofectamine 3000 with 20 ng of Renilla construct, and 300 ng of 1A, 1B- and 1B(Δ16-31)-VDAC-HA in pAc vector. 48h post-transfection the cells were collected and lysed with RIPA buffer.50 μg of total extract were separated by SDS page electrophoresis. Immunoblotting analysis was performed using rabbit anti-*Dm*porin1 (1:200), rabbit anti-HA-tag Santa-Cruz (1:100) and mouse anti-α-Tubulin Sigma (1:1000).

The Fig. 48 shows that it is possible to distinguish in WB the HA-tagged rVDAC from the eVDAC. In particular, we can see that the expression of eVDAC is the same in all assayed conditions and in comparison to the eVDAC in the not transfected sample. Interestingly, we can observe that the expression of 1A-VDAC-HA and 1B-VDAC-HA was very different after cell transfection of 300 ng of VDAC construct. In particular, we observed, with surprise, that 1A-VDAC-HA was expressed at very low concentration, while 1B-VDAC-HA was much more expressed.

4.6 Over-expression of 1A-VDAC enhances the transcription of 1B-VDAC mRNA in SL2 cells

Our data show that the splicing variants of the *D. melanogaster porin1* gene exert an influence on the gene expression efficiency. Therefore, it is possible that these alternatively spliced transcripts might work to finely tune the endogenous VDAC levels. To evaluate this hypothesis we determined whether the over-expression of 1A-VDAC cDNA in *D. melanogaster* embryonic cells leads to an alteration of endogenous levels of 1B-VDAC transcript. SL2 cells were transfected with increasing amounts of 1A-VDAC-HA construct (600/900/1500 ng) or with the empty vector as a control. After 48 hours the presence of both the recombinant and the endogenous VDAC proteins was detected by Western blot. In the same cells the production of the 1A-VDAC and 1B-VDAC mRNAs was analysed by qPCR. Figure 49A shows that 1A-VDAC transcription was, as expected, enhanced as well as the VDAC protein translated, that raised accordingly with the mRNA increase (Fig. 49B). Interestingly, upon over-expression of 1A-VDAC-HA also 1B-VDAC mRNA was highly enriched in cellular extracts (Fig. 49A). These data suggest that the intracellular levels of 1A-VDAC and 1B-VDAC mRNAs could be coordinated and did not affect the levels of endogenous VDAC protein.

The same experiment was performed transfecting SL2 cells with increasing amount of 1B-VDAC-HA construct (600/900/1500 ng) or with the empty vector as a control. After 48 hours the presence of both the recombinant and the endogenous VDAC proteins was detected by Western blot (Fig. 49C). In agreement with the WB in the Fig. 49C, the Fig. 49D shows that 1B-VDAC-HA mRNA raised, while 1A-VDAC mRNA on the contrary decreased, demonstrating, also in this case, that the intracellular levels of VDAC are established by the equilibrium of the two splicing variants, 1A- and 1B- VDAC.

Moreover, WBs in Fig. 49 A and 49 C show that the levels of endogenous VDAC do not change in all transfected cells including empty vector transfected cells.

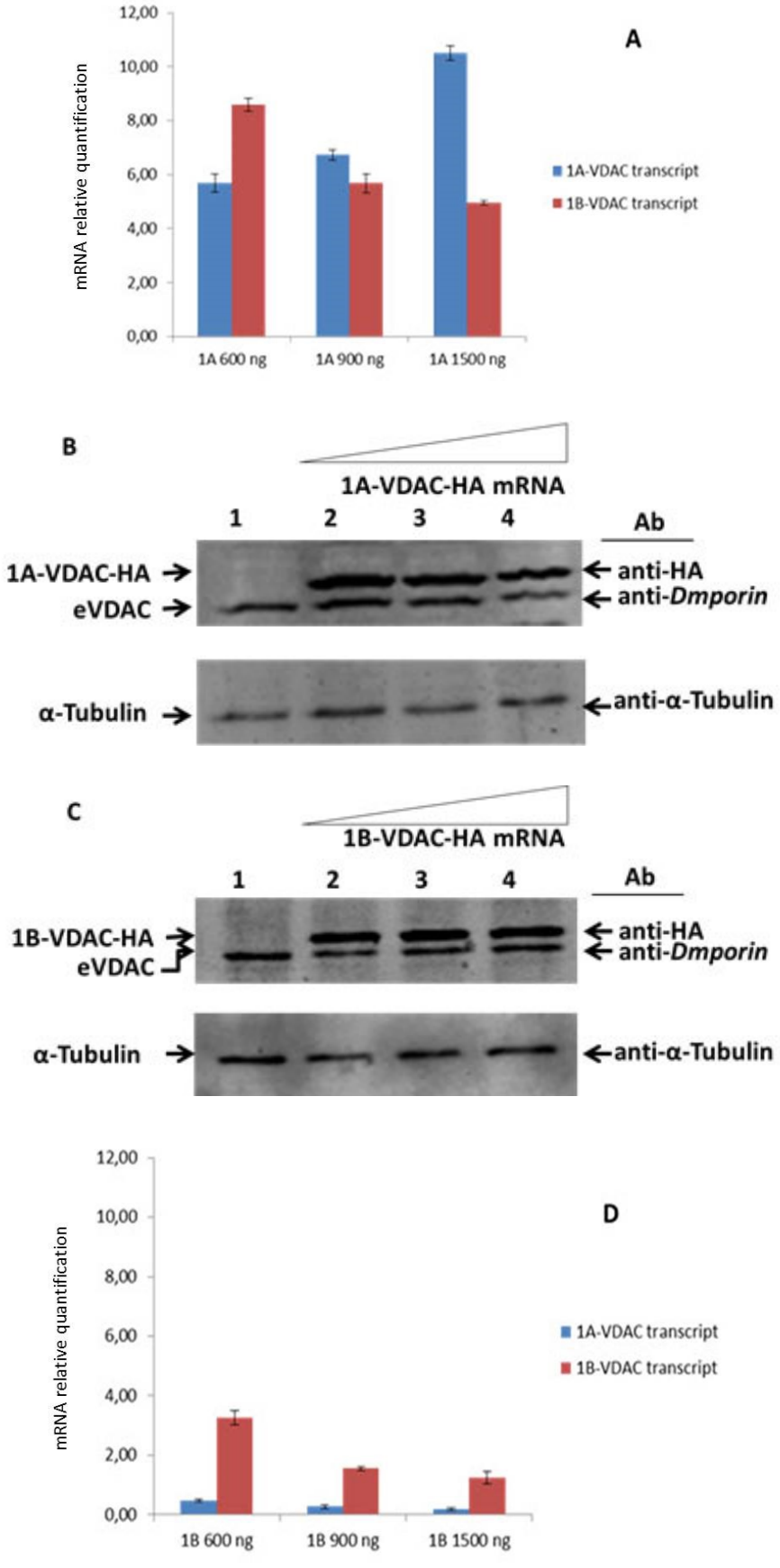

Figure 49: Over-expression of 1A-VDAC enhances the transcription of 1B-VDAC mRNA in *D. melanogaster* SL2 embryonic cells. A-B) $3x10^6$ SL2 cells were seeded in $10cm^2$ plates (6well plates) in 10% FBS Schneider Drosophila media. After 24h the cells were transfected by Lipofectamine 3000 with 20 ng of Renilla construct, and 600/900/1500 ng of 1A-VDAC-HA in pAc vector. 48h post-transfection the cells were collected and separated in two fractions: one fraction was lysed with RIPA buffer for protein extraction, while the second fraction was subjected to RNA extraction using ReliaPrep RNA Cell mini prep system (Promega). **A)** 2000 ng of each sample of RNA was reverse transcribed in cDNA using QuantiTect Reverse Transcription kit (Qiagen). 2 µl of cDNA were used as tamplete for qPCR, using primer amplifying specifically 1A-VDAC, 1B-VDAC and actin as control. **B)** Lane 1: empty pAc vector; Lane 2: 600 ng 1A-VDAC-HA; Lane 3: 900 ng 1A-VDAC-HA; Lane 4: 1500 ng 1A-VDAC-HA . 50 µg of total extract were separated by SDS page electrophoresis. Immunoblotting analysis was performed using rabbit anti-*Dm*porin1 (1:200), rabbit anti-HA-tag Santa-Cruz (1:100) and mouse anti-α-Tubulin Sigma (1:1000). **C-D)** $3x10^6$ SL2 cells were seeded in $10cm^2$ plates (6well plates) in 10% FBS Schneider Drosophila media. After 24h the cells were transfected by Lipofectamine 3000 with 20 ng of Renilla construct, and 600/900/1500 ng of 1B-VDAC-HA in pAc vector. 48h post-transfection the cells were collected and separated in two fractions: one fraction was lysed with RIPA buffer for protein extraction, while the second fraction was subjected to RNA extraction using ReliaPrep RNA Cell mini prep system (Promega). **C)** Lane1: empty pAc vector; Lane 2: 600 ng 1B-VDAC-HA; Lane 3: 900 ng 1B-VDAC-HA; Lane 4: 1500 ng 1B-VDAC-HA. 50 µg of total extract were separated by SDS page electrophoresis. Immunoblotting analysis was performed using rabbit anti-*Dm*porin1 (1:200), rabbit anti-HA-tag Santa-Cruz (1:100) and mouse anti-α-Tubulin Sigma (1:1000). **D)** 2000 ng of each sample of RNA was reverse transcribed in cDNA using QuantiTect Reverse Transcription kit (Qiagen). 2 µl of cDNA were used as tamplete for qPCR, using primer amplifying specifically 1A-VDAC, 1B-VDAC and actin as control.

4.7 1A- and 1B- 5'UTRs in species of *Drosophila* genus

In order to evaluate the importance of 1A-5'UTR and 1B-5'UTR in the translational control of the *porin1* transcript, a bioinformatics analysis was performed to investigate the evolutionary conservation of these sequences in the *Drosophila* genus. The BLAST software from FlyBase Database revealed that the 1A-5'UTR and 1B-5'UTR are present as whole sequences in any species of the *melanogaster* subgroup of *melanogaster* group of *Drosophila* genus. (Fig. 50-51) In particular, the 1A-5'UTR sequence is found in several species of the *melanogaster* group. Moreover, some species of the *melanogaster* group contain only the 1-37 stretch from 1B-5'UTR sequence. Most of these species have not yet their genome characterized, and therefore the 1B-5'UTR aligns with genomic sequences that are not defined as genic region.

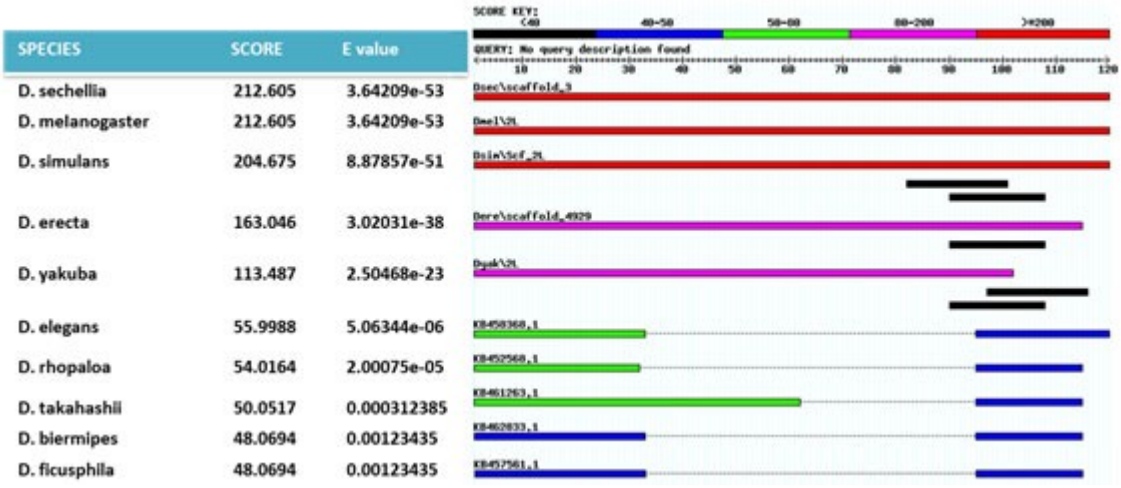

Figure 50: 1B-5'UTR in species of Drosophila genus

SPECIES	SCORE	E value
D. sechellia	145.205	3.86867e-33
D. melanogaster	145.202	3.86867e-33
D. simulans	137.275	9.43091e-31
D. erecta	131.328	5.81832e-29
D. rhopaloa	123.399	1.41837e-26
D. takahashii	123.399	1.41837e-26
D. yakuba	123.399	1.41837e-26
D. elegans	115.469	3.45766e-24
D. biarmipes	115.469	3.45766e-24
D. eugracilis	107.54	8.42896e-22
D. ficusphila	81.7694	4.82501e-14
D. kikkawai	71.8576	4.64771e-11
D. kikkawai	71.8576	4.64771e-11
D. Bipectinata	69.8753	1.83648e-10
D. ananassae	69.8753	1.83648e-10

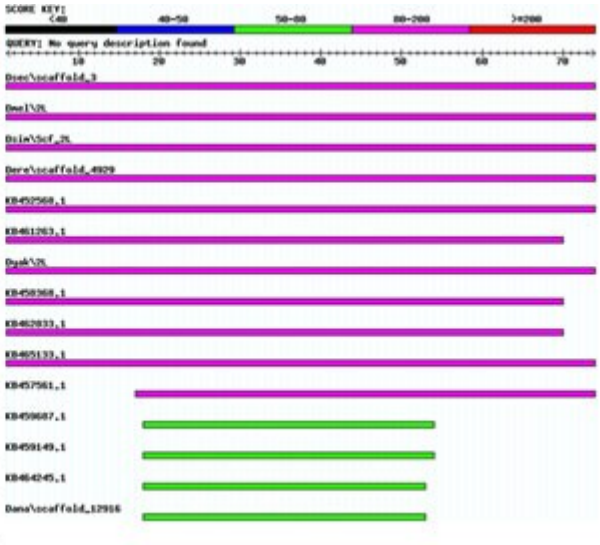

Figure 51: 1A-5'UTR in species of Drosophila genus

Overall, these evidences highlight that the 1A-5'UTR and 1B-5'UTR are sequences appeared about five millions years ago, thus relatively recently, suggesting that they must play an important function in the cell.

4.8 RNA-binding sites on1A- and 1B- 5'UTRs

Despite all results obtained by the several analysis performed on the 1A- and 1B-5'UTR sequences we wanted also to obtain data related to *Drosophila melanogaster* RNA-binding proteins (RBPs) that could control the VDAC translation. The online tool "RBPMap" was used for a bioinformatics analysis on the 1A- or 1B-5'UTR sequences. This analysis was useful to identify in 1A- and 1B-5'UTR sequences any putative motif that could be recognized by single *D.m.* RBPs. In particular, in the 1A-5'UTR we found relatively few proteins able to identify specific sequences on the mRNA (Table 12).

PROTEIN	MOTIF	POSITION	Z-SCORE	P VALUE	PROTEIN	MOTIF	POSITION	Z-SCORE	P VALUE
ARET	ukukugu	6	3.048	1.15e-03	PAPI	kgukugu	6	3.046	1.16e-03
		16	2.843	2.23e-03			16	2.954	1.57e-03
		20	2.831	2.32e-03			18	2.806	2.52e-03
		32	2.458	6.99e-03			20	2.816	2.43e-03
BRU-3	kugkugu	14	4.222	1.21e-05	SF1	acuaayv	49	3.351	4.08e-04
							53	2.919	1.76e-03
							58	3.568	1.80e-04
							64	3.338	4.22e-04
HOW	acuaacv	49	3.600	1.59e-04	SM	abacacv	45	1.772	3.82e-02
		58	3.550	1.98e-04			62	1.772	3.82e-02
ORB2	kuuuukkk	7	3.120	9.04e-04	SNRNP70	aucahg	67	2.352	9.34e-03

Table 12: RBPs-binding sites on the 1A-5'UTR sequence

Conversely, in the 1B-5'UTR sequence we found several RBPs-binding sites, specific for *Drosophila melanogaster* proteins (Table 13).

PROTEIN	MOTIF	POSITION	Z-SCORE	P VALUE	PROTEIN	MOTIF	POSITION	Z-SCORE	P VALUE
ARET	ukukugu	93 95 97 99 101	3.518 3.940 3.566 3.964 3.518	2.17e-04 4.07e-05 1.81e-04 3.69e-05 2.17e-04	RBP9	uuddguu	1 5 92 93 96 97	2.315 1.804 3.543 3.424 3.043 3.424	1.03e-02 3.56e-02 1.98e-04 3.09e-04 1.17e-03 3.09e-04
BRU-3	kugkugu	91 102 107	2.827 2.790 2.790	2.35e-03 2.64e-03 2.64e-03	ROX8	myauuuu	54 61	2.420 2.012	7.76e-03 2.21e-02
ELAV	uuudkuu	78 92 93 96 97	3.000 3.475 3.747 2.960 3.747	1.35e-03 2.55e-04 8.95e-05 1.54e-03 8.95e-05	SRP54	kkrgg	112	2.829	2.33e-03
FNE	uukdguu	1 5 92 93 96 97	2.011 1.954 3.448 3.161 3.161 3.161	2.22e-02 2.54e-02 2.82e-04 7.86e-04 7.86e-04 7.86e-04	SXL	uuuuuuu	78 79 91 92 93 94 96 97 98	2.600 2.573 2.600 2.927 2.927 2.555 2.600 2.927 2.555	4.66e-03 5.04e-03 4.66e-03 1.71e-03 1.71e-03 5.31e-03 4.66e-03 1.71e-03 5.31e-03
HRB87F	gguaggg	111	2.507	6.09e-03	U2AF50	uuuuuyy	79 81 92 93 94 97 98	2.390 2.390 2.560 2.500 2.370 2.500 2.370	8.42e-03 8.42e-03 5.23e-03 6.21e-03 8.89e-03 6.21e-03 8.89e-03
HRB98DE	gguaggg	111	2.534	5.64e-03	PAPI	kgukugu	93 95 97 99 101	3.437 3.943 3.483 3.954 3.425	2.94e-04 4.02e-05 2.48e-04 3.84e-05 3-07e-04
LARK	dcgcgcg	43	2.038	2.08e-02	PUF68	uawdrgr	109 111	2.000 2.111	2.27e-02 1.74e-02
ORB2	kuuukkk	91 92 96 100	3.193 3.398 3.398 3.602	7.04e-04 3.39e-04 3.39e-04 1.58e-04	RBP1-LIKE	aucadcr	30 72 85	2.910 2.896 2.343	1.81e-03 1.89e03 9.56e-03

Table 13: RBPs-binding sites on 1B-5'UTR sequence

Some of these proteins are not yet well characterized, while others are common RNA binding proteins. In particular, most of these RBPs recognize the same 91-107 region due to its enrichment of "U" nucleotides. Comparing RBPs in Table 12 and Table 13 we can see that each 5'UTR owned a specific set of RBPs able to recognize it.

This finding suggests that specific RBPs could differently regulate the expression of the two *porin*-alternative transcripts.

4.9 Bioinformatics analysis of *D. melanogaster* 1A- and 1B-VDAC mRNA

The sequences coding for 1A-VDAC (Genbank NM_057465) and 1B-VDAC (Genbank NM_134283) were submitted to the mfold web server (at http://www.bioinfo.rpi:edu/applications/mfold, Zuker, 2003) for nucleic acid folding analysis and RNA secondary structure prediction. Default conditions of analysis were used. The contribution of the alternative 5'UTRs to the mRNA folding was observed. Several secondary structures were calculated by the software. 1A-VDAC gave 29 individual structures with an initial ΔG between –518 and –506 kcal/mol. Comparable results were obtained for 1B-VDAC, that gave 32 individual structures with an initial ΔG between –520 and –509 kcal/mol. We focused our attention in the 5'UTR and in the next starting codon triplet. The alternative 5'UTRs were, indeed, joined with the AUG start codon, that is the beginning of the second exon. In 1A-VDAC the number of times in which the start codon (bases 116-118) and its surrounding bases are single stranded (i.e. the ss-count, defined as the propensity of a base to be single stranded) was very little but the sequence 100- 116 and 125-136 have a ss-count higher than 22 upon 29 structures. This indicates that the sequence encompassing the start codon has a very low probability to be in an ordered secondary structure. In turn this means that the AUG should be easily accessible to the translational machinery. On the opposite, the start codon of 1B-VDAC (bases 125-127) forms a loop in a stable hairpin, detected in as many as 30 upon 32 structures (sequence G119AGGAG AUGG CUCCUC134). In Fig. 52 are shown for comparison secondary structure predictions of the 1A-VDAC (Fig.52A and 52C) and of the 1B-VDAC (Fig.52B and 52D). These are only two representative structures, but the influence of the 5'UTRs on the secondary structural predictions is similar in the others. The exam of the translational start consensus shows that 1A-VDAC has an optimal consensus: CAAAA-AUG, while 1B-VDAC has a poor consensus sequence for the translational start: GAGGAGAUG. The optimal Drosophila-Kozak motif is predicted to be very rich in pyrimidine and in particular in A (CAAAACAUG) (Cavener, 1987). From these results it is likely that 1A-VDAC is more suitable for a productive translation than 1B-VDAC.

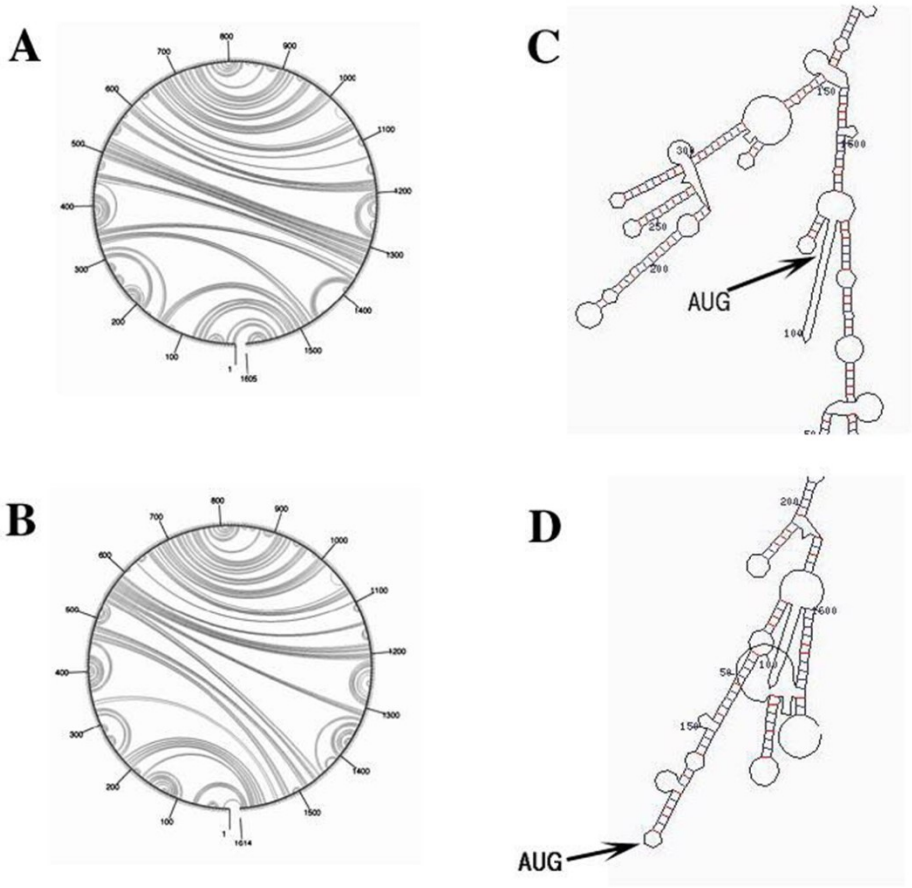

Figure 52: A and C) secondary structure predictions of the 1A-VDACmRNA; B and D) secondary structure predictions of the 1A-VDAC mRNA

5 DISCUSSION

The Voltage-Dependent Anion Channel (VDAC) lies in the OMM and forms a common pathway for the exchange of metabolites between the mitochondria and the cytosol, thus playing a crucial role in the regulation of metabolic and energetic functions of mitochondria. Porin/VDAC thus appears to be a convergence point for a variety of cell survival and cell death signals, mediated by its association with various ligands and proteins (Savabi, 1994; Linden et al., 1996; Kusano et al., 2000;Schwarzer et al., 2002; Drysdale et all., 2005; Sardiello et al., 2005; Roman et al., 2005; Shoshan-Barmatz et al., 2005; Elinder et al., 2005; Pastorino et al., 2005; Braat et al., 2004; Lai et al., 2004).

In a previous study, we observed that the *Drosophila melanogaster porin1* gene encodes two alternative transcripts named 1A-VDAC and 1B-VDAC comprising an identical coding sequence, but completely different 5'-UTRs [Oliva et al., 1998]. These two transcripts have been detected in embryos, larvae and adults of both sexes, where they are produced in different amounts: 1A-VDAC is very abundant, while 1B-VDAC is usually scarce [Oliva et al., 1998; Oliva et al., 2002].

The goal of this work of thesis was to gain new insights into the biological functions of these two alternative splicing forms of *D.m.* VDAC. Bearing this in mind, we have extensively studied the influence of the two alternative 5'UTRs on the expression of VDAC or two reporter genes, GFP and Luciferase, in yeast, *D. melanogaster* and in HeLa cells. GFP or VDAC, when their genes were fused to the 1A-5'UTR, were efficiently synthesised in yeast cell, while no induced protein was detected in yeast upon transformation with 1B-GFP or 1B-VDAC constructs, despite the high levels of their transcripts. These results are in agreement with the fact that only 1A-VDAC, and not 1B-VDAC, was able to complement the temperature-sensitive phenotype of the Δ*por1* yeast cells. Our data indicated that 1B-5'UTR impacts on the VDAC expression by inhibiting the protein translation, and such event is independent of the coding region cloned downstream of the UTR. Firstly, we verified in yeast that 1B-VDAC transcript was recognized by the ribosome as well as 1A-VDAC transcript. After this check, we focused on a detailed analysis of 5'UTR sequence. Therefore we focused to the little uORF localized into the 1B-5'UTR. We found that this uORF apparently does not influence the translation of 1B-VDAC transcript because, after mutagenesis of its AUG or UAA codon, no VDAC protein was expressed in Δ*por1* yeast. To understand whether the whole 1B-5'UTR sequence, or only a specific region of UTR, was essential to

inhibit the 1B-VDAC expression in yeast, we produced many mutants by deletion of consecutive 15 nt stretches. Interestingly, we found that removing the 16-31 nt region from 1B sequence, the 1B-VDAC translation was reactivated at the same level of 1A-VDAC.

Thanks to several experimental approaches we analysed, by bioinformatics tools, the presence of putative mechanisms embedded in the 1B(16-31) sequence and able to produce an inhibition on the protein synthesis. In particular, by RBP-RNA interactions analysis on 1B-5'UTR 10-37 sequence we identified some proteins acting as translational control factors.

Using specific software for prediction of RNA-RNA interactions we also discovered that 1B-5'UTR sequence complements with the 18S rRNA, in a long stretch of dsRNA with high hybridization energy, while 1A-5'UTR or 1B(Δ16-31)-5'UTR sequence are not able to do. Interestingly, the 18S rRNA sequences involved in the interaction with 1B sequence match with solvent-exposed regions or with the h34 helix, a region used by the ribosome to latch the mRNA in the mRNA-binding channel. Nevertheless, when we removed the 16-31 nt stretch from the 1B-5'UTR fused to reporter gene, again no protein was synthesized in yeast. The same data was also obtained in *D. melanogaster* and HeLa cells. These results thus proved that 1B-5'UTR is able to produce, in any cell system, an inhibitory effect on the translation of any coding sequence fused to it. Therefore, the 1B(16-31) region is certainly involved in the control of translation but its action on *D.m.* VDAC transcript is performed only in the presence of its 3'UTR region. When 1B(16-31) was indeed inserted into the 1A-5'UTR linked to GFP we obtained no increase of the corresponding protein, in *Dm* or HeLa cells. In conclusion, we hypothesize that in *D. melanogaster* the 1B-5'UTR controls translation of its VDAC mRNA probably by different mechanisms (involvement of specific RBPs or specific secondary structures in the 5'UTR and/or interaction with certain regions of 18S rRNA or other), some of which directly or indirectly affected by the 3'UTR from *D.m.* VDAC mRNA. Conversely, in yeast the translation of the same 1B-VDAC transcript is controlled only by the 16-31 region from 1B-5'UTR.

RNA electrophoresis mobility shift assay (REMSA) displayed that specific proteins are able to interact with the 10-37 region from 1B-5'UTR, which includes the 16-31 sequence. These proteins were purified by RNA pull down assay and then identified by mass spectrometry analysis. Interestingly, most of the identified proteins are usually involved in the transcription and translation regulation. Among the proteins interacting

with the assayed 1B(10-37) sequence (listed in Table 11, pag 58) we found highly interesting eIF4A and Asc1, proteins with a cell function directly linked to translation control. It is well known that binding of 43S pre-initiation complex to the capped-end of mRNA is facilitated by the cap-binding factor eIF4E and partners eIF4G and eIF4A in the eIF4F complex. EIF4A is the helicase subunit of eIF4F and promotes scanning of mRNAs containing secondary structure in their 5'-UTRs (Pestova et al., 2002). The weak helicase activity of eIF4A is enhanced upon binding to eIF4G. 4E-binding proteins (4E-BPs) compete with eIF4G for a common binding site on the companion eIF4F subunit, eIF4E (Raught et al., 1999), and are therefore inhibitory for translation. In addition, specific RNA-binding proteins on 5'UTRs or 3'UTRs interact through an intermediate protein with a cap-binding protein, forming an inhibitory loop that precludes access for eIF4F (Jackson et al., 2010). Therefore, the activity of eIF4A on the 1B-5'UTR could be stopped by different mechanisms producing the inhibition of 1B-VDAC mRNA translation.

Similarly to eIF4A, Asc1 is directly involved in the translation regulation. Asc1 in yeast (RACK1 in plants and animals) is a small ribosomal protein which binds the solvent-exposed face of the 40S subunit near the mRNA exit channel. In this region some proteins take contacts with the 5' end of mRNA during translation initiation, including eIF3 and eIF4G. The eIF3 interacts with mRNA and ASC1 promoting assembly of translation pre-initiation complexes. In particular, the C-terminal of eIF3 forms an important intermolecular bridge with the 40S head region by contacting ASC1 and most probably 18S rRNA (Kouba et al., 2012). eIF4G interacts also with Poly(A) binding protein (PABP), promoting a circular messenger ribonucleoprotein complex (closed loop) by linking the 5'-cap and the poly(A) tail. Some mRNAs are strongly associated closed loop factors (eIF4E, eIF4G, and PABP) and require Asc1 for efficient translation (Thompson et al., 2016). VDAC mRNA could have suitable features to be regulated from Asc1/RACK1. Moreover, our bioinformatics analysis revealed that 1B-5'UTR is able to interact with high energy to the solvent-exposed region of the yeast 18s rRNA, in particular with its h34 helix. This finding could mean that the transcript 1B-VDAC is recognized by ribosomes, but it is not translated because it could be blocked at the entry of ribosomal mRNA channel or by the action of specific RBPs.

Later, to study the effects of 1A- and 1B-UTRs on gene expression in a more physiological context, we used the *D. melanogaster* embryonic cells (SL2 cells) as a model system containing the two homologous alternative VDAC mRNA. The

expression of 1A-5'UTR fused to luciferase gene reporter showed an extraordinary increase in the protein activity, in comparison with the control (luciferase gene only). In contrast, the expression of 1B-5'UTR fused to the luciferase resulted in the absence of any protein activity. These results demonstrated that, also in *D. melanogaster* cells, 1B-5'UTR has an inhibitory effect on the translation of a protein fused downward. The same results were obtained transfecting HeLa cells with constructs carrying GFP fused to 1A- or 1B sequence. The GFP was highly expressed from 1A-GFP transcript. These finding means that 1A-5'UTR is able to increase the translation of the coding sequence fused to it, in any cell model.

The negative influence of 1B-5'UTR upon the translation of coding frames is outlined by the analysis of the secondary structure stability of mRNAs for VDAC differing only in the 5'UTR. 1B-VDAC shows predictions where the starting codon is constrained in a tight stem-loop structure. In 1A-VDAC the same analysis indicates that the starting codon is in an open context. Furthermore the Kozak-like sequence of 1B-VDAC is predicted to be less accessible than 1A-VDAC to the ribosome. Thus, experimental evidence and predictive analysis in silico both agree to define 1B-VDAC as a probably non-productive mRNA.

Surprisingly, SL2 cells transfected with 1B-VDAC-HA sequence produced the corresponding protein suggesting thus that the 3'UTR sequence is involved in the translation control of full-length 1B-VDAC transcript. In the 3'UTR of *D.m.* VDAC we detected, by bioinformatics analysis, several motifs for specific RNA binding proteins. These RBPs could be involved in the regulation of the VDAC mRNA translation.

One of the principal aims of this work was to answer to the question: "What is the biological significance of 1B-VDAC in fly cells?" Considering our results, it is now possible to say that the cell, modulating the expression of the two *porin* transcripts, can control the levels of the protein. Our data support this hypothesis. In fact, the over-expression of 1A-VDAC-HA in *D.m.* cells leads to the accumulation of the endogenous and inactive alternative mRNA 1B-VDAC ensuring a reduced amount of VDAC. On the other hand, the over expression of the 1B-VDAC mRNA produces reduced levels of the endogenous and active 1A-VDAC mRNA, avoiding the over production of VDAC protein.

The influence of 1B-VDAC in post-transcriptional regulatory events could be explained by the secondary structure of the two mRNAs. 1B-5'UTR might interact with the 1A-VDAC transcript or create interference with the translation machinery. Most likely this

effect is not due to the inhibition of the binding of the mRNA to the ribosomes, since both mRNAs bind to ribosomal fractions. The association of the not productive 1B-VDAC mRNA with polysomes is not surprising, since, for example, oskar mRNA is reported to associate, even though it is translationally repressed (Braat et al., 2004). Several sites of partial complementarity are specifically found between the 1B-5'UTR and the 3'UTR of the *porin1* mRNA (not shown). This could be the basis for a mechanism of post-transcriptional regulation reminding some characteristics of siRNA translation inhibition. Also miRNA are often involved in the translational regulation via an imprecise pairing with the 3'UTR of several mRNA (Lai et al., 2004; Wilhelm et al., 2005; Filipowicz et al., 2005) Interestingly, in the same *D.m*. VDAC locus nearby (about 1 Kb) the GC17140 gene there is a region encoding for the miR 4987-3p whose sequence is able to hybridize with a folding energy of -24 Kcal/mol to a sequence enclosed in the 3'UTR of VDAC transcript.

The meaningfulness of the alternative transcription at the 5'UTR of the *porin* gene is furthermore underscored by the conservation of the same 1B-5'UTR sequence in all *Drosophila* subgroup species and by the presence of similar alternative splicing events also in mammals VDAC genes. By cross-analysis between EST libraries and human genome we have found that at least three alternative transcripts encoding the same protein (i.e. the human VDAC1) may result from the splicing involving additional exons found in the genome. This suggests that the mechanism found in *Drosophila* might be adopted by other eukaryotes to control the VDAC protein levels in the cell. On the other side the last annotation of the *Drosophila melanogaster* genome revealed that in the fly about one third of the alternatively transcribed genes generate only one protein product and there are more examples of alternative 5'-UTRs (Misra et al., 2002). This may thus represent a general mechanism suggesting the use of alternative promoters and the possibility of a special regulation of the expression.

6 REFERENCES

Abu-Hamad S., Zaid H., Israelson A., Nahon E., and Shoshan-Barmatz V. **Hexokinase-I protection against apoptotic cell death is mediated via interaction with the voltage-dependent anion channel-1: mapping the site of binding.** J. Biol.Chem. 2008, 283, 13482–13490.

Adams J.M. and Cory S. **The Bcl-2 apoptotic switch in cancer development and therapy**. Oncogene 2007, 26, 1324–1337.

Adams M. D., Celniker S. E., Holt R. A., Evans C. A., Gocayne J. D., Amanatides P. G., Scherer S. E., Li P. W., Hoskins R. A., Galle R. F., et al. **The genome sequence of Drosophila melanogaster.** Science, 2000, 287, 2185-2195.

Adams V., Griffin L., Towbin J., Gelb B., Worley K., and McCabe E. R. **Porin interaction with hexokinase and glycerol kinase: metabolic microcompartmentation at the outer mitochondrial membrane.** Biochem. Med. Metab. Bio, 1991, 45, 271–291.

Aiello R., Messina A., Schiffler B., Benz R., Tasco G., Casadio R., De Pinto V. **Functional characterization of a second porin isoform in Drosophila melanogaster. DmPorin2 forms voltage-independent cation-selective pores.** The Journal of Biological Chemistry. 2004, 25364-25373.

Anantharaman, V., Koonin, E.V., and Aravind, L. (2002). **Comparative genomics and evolution of proteins involved in RNA metabolism.** Nucleic Acids Res. 30, 1427–1464.

Ashburner M. and Thompson J. N. **The laboratory culture of Drosophila. In The Genetics and Biology of Drosophila**, 1978, (ed. M. Ashburner and TRF. Wright), pp. 1-81. London and New York Academic Press Vol. 2A.

Ashburner M., Golic K.G. and Hawley R.S. **Drosophila: A Laboratory Handbook**. Cold Spring Harbor Laboratory press, 2001.

Azoulay-Zohar H., Israelson A., bu-Hamad S., Shoshan-Barmatz V. **In self-defence: hexokinase promotes voltage-dependent anion channel closure and prevents mitochondria-mediated apoptotic cell death.** Biochem.J., 2004, 377(Pt 2), 347–355.

Baker N.E., Li K., Quiquand M., Ruggiero R., and Wang L. **Eye development**. Methods 2014, 68, 252-259.

Bartel DP. **MicroRNAs: target recognition and regulatory functions.** Cell 2009, 136: 215–233.

Bayrhuber M., Meins T., Habeck M., Becker S., Giller K., Villinger S., Vonrhein C., Griesinger C., Zweckstetter M., Zeth K. **Structure of the human voltage-dependent anion channel.** Proc. Natl. Acad. Sci. U. S. A. 105 (2008) 15370–15375

Behr M. **Molecular aspects of respiratory and vascular tube development.** Respir. Physiol. Neurobiol. 2010, 173 Suppl., S33-S36.

Benz R. **Permeation of hydrophilic solutes through mitochondrial outer membranes: review on mitochondrial porins.** Biochim. Biophys. Acta, 1994, 1197(2): 167-196.

Bier E. **Drosophila, the golden bug, emerges as a tool for human genetics.** Nat. Rev. Genet. 2005, 6, 9-23.

Blachly-Dison E., Song J., Wolfgang W.J., Colombini M. and Forte M. **Multicopy Suppressors of Phenotypes Resulting from the Absence of Yeast VDAC Encode a VDAC-Like Protein.** Molecular and Cellular Biology, 1997, p5727-5738

Blachly-Dyson E., Forte M.. **VDAC channels**, IUBMB Life 52 (2001) 113–118

Blachly-Dyson E., Peng S., Colombini M. and Forte M. **Selectivity changes in site-directed mutants of the VDAC ion channel: structural implications.** Science, 1990, 247:1233–1236.

Blachly-Dyson E., Zambronicz E.B., Yu W.H., Adams V., McCabe E.R., Adelman J., Colombini M., Forte M. **Cloning and functional expression in yeast of two human isoforms of the outer mitochondrial membrane channel, the voltage-dependent anion channel.** J. Biol. Chem., 268, 1993, 1835– 1841.

Blanchette M., Green R.E., Brenner S.E. and Rio D.C. **Global analysis of positive and negative pre-mRNA splicing regulators in Drosophila.** Genes. Dev., 2005, 19, 1306–1314.

Borst A. and Helmstaedter M. **Common circuit design in fly and mammalian motion vision.** Nat. Neurosci. 2015, 18, 1067-1076.

Braat, A.K., Yan,, N., Arn, E., Harrison, D. and Macdonald, P.M. **Localization-dependent oskar protein accumulation; control after the initiation of translation.** Dev. Cell, 2004, 8, 1106-1116.

Buettner R., Papoutsoglou G., Scemes E., Spray D.C., Dermietzel R. **Evidence for secretory pathway localization of a voltage-dependent anion channel isoform.** Proc. Natl. Acad. Sci. U. S. A. 97 (2000) 3201–3206

Cavener, D.R. **Comparison of the consensus sequence flanking translational start sites in Drosophila and vertebrates.** Nucleic Acid Res., 1987, 15, 1353-1361.

Checchetto V., Reina S., Magri A., Szabo I., De Pinto V. **Recombinant human voltage dependent anion selective channel isoform 3 (hVDAC3) forms pores with a very small conductance.** Cell. Physiol. Biochem. 34 (2014) 842–853.

Chen E., Sharma M.R., Shi X., Agrawal R.K., Joseph S.. **Fragile X mental retardation protein regulates translation by binding directly to the ribosome.** Mol Cell 2014a, 54: 407–417.

Chien S., Reiter L.T., Bier E. and Gribskov M. **Homophila: human disease gene cognates in Drosophila.** Nucleic Acids Res. 2002, 30, 149-151.

Colombini M. **Voltage gating in the mitochondrial channel, VDAC.** J Membr Biol. 1989 Oct;111(2):103-11;

Davuluri R.V., Suzuki Y., Sugano S., Zhang MQ. **CART classification of human 5′ UTR sequences.** Genome Res 2000, 10: 1807–1816.

De Pinto V., Guarino F., Guarnera A., Messina A., Reina S., Tomasello FM., Palermo V., Mazzoni C. **Characterization of human VDAC isoforms: a peculiar function for VDAC3?** Biochim Biophys Acta. 2010 1797(6-7):1268-75

De Pinto V., Messina A., Lane D.J., Lawen A. **Voltage-dependent anion-selective channel (VDAC) in the plasma membrane.** FEBS Lett. 584 (2010) 1793–1799.

Djuranovic S., Nahvi A., Green R. **miRNA-mediated gene silencing by translational repression followed by mRNA deadenylation and decay.** Science 2012, 336: 237–240.

Draper D.E. **Protein–RNA recognition.** Annu Rev Biochem 1995, 64: 593–620.

Drysdale, R.A., Crosby, M.A. and The FlyBase Consortium **FlyBase: genes and gene models.** Nucleic Acids Res., 2005, 33, D390-D395.

Elinder, F., Akanda, N., Tofighi, R., Shimizu, S., Tsujimoto, Y., Orrenius, S. and Ceccatelli, S. **Opening of plasma membrane voltage-dependent anion channels (VDAC) precedes caspase activation in neuronal apoptosis induced by toxic stimuli.** Cell Death Differ., 2005, 12, 1134-1140.

Filipowicz, W., Jaskiewicz, L., Kolb, F.A. and Pillai, R.S. **Posttranscriptional gene silencing by siRNAs and miRNAs.** Curr. Opin. Struct. Biol.; 2005.

Forst D., Welte W., Wacker T., Diederichs K. **Structure of the sucrose-specific porin ScrY from Salmonella typhimurium and its complex with sucrose.** Nat. Struct. Biol., 1998, 5, 37-46.

Gabut M., Dejardin J., Tazi J. and Soret J. **The SR family proteins B52 and dASF/SF2 modulate development of the Drosophila visual system by regulating specific RNA targets.** Mol. Cell. Biol., 2007, 27, 3087–3097.

Galdiero S., Falanga A., Cantisani M., Tarallo R., Della Pepa ME, D'Oriano V. and Galdiero M. **Microbe-Host Interactions: Structure and Role of Gram-Negative Bacterial Porins.** Current Protein and Peptide Science, 2012, 13, 843-854

Galdiero S., Galdiero M., Pedone C. **beta-Barrel membrane bacterial proteins: structure, function, assembly and interaction with lipids.** Curr. Prot. Pept. Sci., 2007, 8, 63-82.

Gebauer F., Xu W., Cooper G.M., and Richter J.D. **Translational control by cytoplasmic polyadenylation of c-mos mRNA is necessary for oocyte maturation in the mouse.** EMBO J., 1994, 13, 5712-5720.

Glisovic T., Bachorik J.L., Yong J., Dreyfuss G. **RNA-binding proteins and post-transcriptional gene regulation.** FEBS Lett 2008, 582: 1977–1986.

Guardiani C., Leggio L., Scorciapino MA., De Pinto V., Ceccarelli M. **A computational study of ion current modulation in hVDAC3 induced by disulfide bonds.** Biochim Biophys Acta. 2016 Apr;1858(4):813-23

Hall MP., Nagel RJ., Fagg WS., Shiue L., Cline MS., Perriman RJ., Donohue JP., Ares M.JR. **Quaking and PTB control overlapping splicing regulatory networks during muscle cell differentiation.** RNA 2013, 19: 627–638.

Herskowitz I. **Life cycle of the budding yeast *Saccharomyces cerevisiae.*** Microbiological reviews 1988, p. 536-553.

Hiller S., Garces R.G., Malia T.J., Orekhov V.Y., Colombini M., Wagner G. **Solution structure of the integral human membrane protein VDAC-1 in detergent micelles.** Science 321 (2008) 1206–1210.

Ishizuka A., Siomi MC., Siomi H.. **A Drosophila fragile X protein interacts with components of RNAi and ribosomal proteins.** Genes Dev 2002, 16:2497–2508.

Jackson,R.J., Hellen,C.U. and Pestova,T.V. **The mechanism of eukaryotic translation initiation and principles of its regulation.** Nat. Rev. Mol. Cell Biol., 2010, 11, 113–127.

Jeibmann A. and Paulus W. **Drosophila melanogaster as a model organism of brain diseases.** Int. J. Mol. Sci. 2009, 10, 407-440.

Jin Y., Suzuki H., Maegawa S., Endo H., Sugano S., Hashimoto K., Yasuda K., Inoue K. **A vertebrate RNA-binding protein Fox-1 regulates tissue-specific splicing via the pentanucleotide GCAUG**. EMBO, 2003, J 22: 905–912.

Kahvejian A., Roy G., Sonenberg N. **The mRNA Closed-loop Model: The Function of PABP and PABP-interacting Proteins in mRNA Translation.** Cold Spring Harbor Symposia on Quantitative Biology 2001, 66:293–300.

Kielkopf CL., Lucke S., Green MR. **U2AF homology motifs: protein recognition in the RRM.** world. Genes Dev 2004, 18: 1513–1526.

Kouba T., Rutkai E., Kara´ skova ´ M., Vala´ sˇek L. **The eIF3c/NIP1 PCI domain interacts with RNA and RACK1/ASC1 and promotes assembly of translation preinitiation complexes.** Nucleic Acids Research2012, 40:2683–2699.

Kouba T., Rutkai E., Karaskova´ M. and Shivaya Valasek L. **The eIF3c/NIP1 PCI domain interacts with RNA and RACK1/ASC1 and promotes assembly of translation preinitiation complexes.** Nucleic Acids Research, 2012, Vol. 40, No. 6 2683–2699.

Kusano, H., Shimizu, S., Koya, R.C., Fujita, H., Kamada, S., Kuzumaki, N. and Tsujimoto, Y. **Human gelsolin prevents apoptosis by inhibiting apoptotic mitochondrial changes via closing VDAC.** Oncogene, 2000, 19, 4807–4814.

Lai, E.C., Wiel, C., and Rubin, G.M**. Complementary miRNA pairs suggest a regulatory role for miRNA:miRNA duplexes.** RNA , 2004, 10, 171-175. 15, 331-341.

Lander E. S., Linton L.M., Birren B., Nusbaum C., Zody MC., Baldwin J., Devon K., Ewar K., Doyle M., Fitz Hugh W., et al. **Initial sequencing and analysis of the human genome.** Nature 2001, 409, 860-921.

Le Mellay V., Troppmair J., Benz R., and Rapp U.R. **Negative regulation of mitochondrial VDAC channels by C-Raf kinase.** BMC Cell Biol. 3, 2002, 14.doi:10.1186/1471-2121- 3-14

Lee, I., and Hong, W. **RAP—a putative RNA-binding domain.** Trends Biochem. Sci., 2004, 29, 567–570.

Lesch B.J. and Page D.C.. **Genetics of germ cell development.** Nat. Rev. Genet. 2012, 13, 781-794.

Lewis HA., Musunuru K., Jensen KB., Edo C., Chen H., Darnell RB., Burley SK. **Sequence-specific RNA binding by a Nova KH domain: implications for paraneoplastic disease and the fragile X syndrome.** Cell, 2000, 100: 323–332.

Linden, M., and Karlsson, G. **Identification of porin as a binding site for MAP2.** Biochem Biophys Res Commun, 1996, 218, 833-836.

Llambi F. and Green D.R. **Apoptosis and oncogenesis: give and take in the BCL-2 family.** Curr.Opin. Genet.Dev. 2011, 21, 12–20.

Lunde, B.M., Moore, C., and Varani, G. (2007). **RNA-binding proteins: modular design for Efficient function.** Nat. Rev. Mol. Cell Biol. **8**, 479–490.

Magrì A., Belfiore R., Reina S., Tomasello MF., Di Rosa MC., Guarino F., Leggio L., De Pinto V. and Messina A. **Hexokinase I N-terminal based peptide prevents the VDAC1-SOD1 G93A interaction and re-establishes ALS cell viability**. Sci Rep. 2016 Oct 10;6:34802.

Manczak M., Reddy P.H. **Abnormal interaction of VDAC1 with amyloid beta and phosphorylated tau in Alzheimer's disease neurons cause mitochondrial dysfunction.** Hum. Mol. Genet. 2012, Dec 1;21(23):5131-46

Meijer H.A., Kong YW., Lu WT., Wilczynska A., Spriggs RV., Robinson SW., Godfrey JD., Willis AE., Bushell M. **Translational repression and eIF4A2 activity are critical for microRNA-mediated gene regulation.** Science 2013, 340: 82–85.

Messina A., Neri M., Perosa F., Caggese C., Marino M., Caizzi R. e De Pinto V.**. Cloning and chromosomal localization of a cDNA encoding a mitochondrial porin from Drosophila melanogaster**. FEBS Lett. 1996, 384, 9-13

Messina A., Reina S., Guarino F., De Pinto V. **VDAC isoforms in mammals**. Biochim. Biophys. Acta 1818 (2012) 1466–1476

Misra, S., Crosby, M.A., Mungall, C.J. et al. **Annotation of the Drosophila melanogaster euchromatic genome: a systematic review.** Genome Biol., 2002, **3**, 0083.1-0083.22

Morino S., Imataka H., Svitkin YV., Pestova TV., Sonenberg N. **Eukaryotic translation initiation factor 4E (eIF4E) binding site and the middle one-third of eIF4GI constitute the core domain for cap-dependent translation, and the C-terminal one-third functions as a modulatory region.** Mol Cell Biol. 2000, 20(2): 468-77

Niessing, D., Hu¨ ttelmaier, S., Zenklusen, D., Singer, R.H., and Burley, S.K. **She2p is a novel RNA binding protein with a basic helical hairpin motif.** Cell, 2004, 119, 491–502.

Nikaido H. **Porins and specific channels of bacterial outer Membranes.** Molecular Microbiology, 1992, 6(4), 435-442

Nilsson J., Sengupta J., Frank J., Nissen P. **Regulation of eukaryotic translation by the RACK1 protein: a platform for signalling molecules on the ribosome.** EMBO Reports 2004, 5:1137–1141.

Oliva M., De Pinto V., Barsanti P., Caggese C. **A genetic analysis of the porin gene encoding a voltage dependent anion channel protein in Drosophila melanogaster.** Mol Genet Genomics, 2002, 267: 746-756

Oliva M., Messina A., Ragone G., Caggese C. and De Pinto V. **Sequence and expression pattern of the Drosophila melanogaster mitochondrial porin: evidence of a conserved protein domain between fly and mouse.** FEBS Lett. 1998, 430, 327-332.

Pages J.M., James C.E., Winterhalter M. **The porin and the permeating antibiotic: a selective diffusion barrier in Gram negative bacteria.** Nat. Rev. Microbiol., 2008, 6, 893-903.

Pandey U.B. and Nichols C.D.. **Human disease models in Drosophila melanogaster and the role of the fly in therapeutic drug discovery.** Pharmacol. Rev. 2011, 63, 411-436.

Pastorino J.G., Hoek J.B. and Shulga N. **Activation of glycogen synthase kinase 3 beta disrupts the binding of hexokinase II to mitochondria by phosphorylating voltage-dependent anion channel and potentiates chemotherapy-induced cytotoxicity.** Cancer Res. 2005, 65, 10545–10554.

Paulk A., Millard S. and van Swinderen B. **Vision in Drosophila: seeing the world through a model's eyes.** Annu. Rev. Entomol. 2013, 58, 313-332.

Pestova,T.V. and Kolupaeva,V.G. **The roles of individual eukaryotic translation initiation factors in ribosomal scanning and initiation codon selection**. Genes Dev., 2002, 16, 2906–2922.

Pickering BM., Willis AE. **The implications of structured 5′ untranslated regions on translation and disease.** Semin Cell Dev Biol 2005, 16: 39–47.

Pisarev AV., Kolupaeva VG., Yusupov MM., Hellen CU., Pestova TV. **Ribosomal position and contacts of mRNA in eukaryotic translation initiation complexes.** The EMBO Journal 2008, 27:1609–1621

Rammelt, C., Bilen, B., Zavolan, M., and Keller, W. **PAPD5, a noncanonical poly(A) polymerase with an unusual RNA-binding motif.** RNA, 2011, 17, 1737–1746.

Raught,B. and Gingras,A.C. **eIF4E activity is regulated at multiple levels.** Int. J. Biochem. Cell Biol., 1999, 31, 43–57.

Reddy P.H. **Amyloid beta, mitochondrial structural and functional dynamics in Alzheimer's disease.** Exp. Neurol. 218 (2009) 286–292.

Reddy P.H. **Is the mitochondrial outer membrane protein VDAC1 therapeutic target for Alzheimer's disease?** Biochimica et Biophysica Acta 1832 (2013) 67–75

Reiter L.T., Potocki L., Chien S., Gribskov M. and Bier E. **A systematic analysis of human disease-associated gene sequences in Drosophila melanogaster.** Genome Res. 2001, 11, 1114-1125.

Roeder T., Isermann K., Kallsen K., Uliczka K. and Wagner C. **A Drosophila asthma model - what the fly tells us about inflammatory diseases of the lung.** Adv. Exp. Med. Biol. 2012, 710, 37-47.

Roman, I., Figys, J., Steurs, G. and Zizi, M. **In vitro interactions between the two mitochondrial membrane proteins VDAC and cytochrome c oxidase.** Biochemistry, 2005, 44, 13192-13201.

Rostovtseva T.K., Sheldon K.L., Hassanzadeh E., Monge C., Saks V., Bezrukov S.M., et al. **Tubulin binding blocks mitochondrial voltage-dependent anion channel and regulates respiration.** Proc. Natl. Acad. Sci. U.S.A. 2008b 105, 18746– 18751.

Rubin G. M., Yandell M. D., Wortman J. R., Gabor Miklos G. L., Nelson C. R., Hariharan I. K., Fortini M. E., Li P. W., Apweiler R., Fleischmann, W. et al. **Comparative genomics of the eukaryotes.** Science, 2000, 287, 2204-2215.

Sampson M.J., Lovell R.S., Craigen W.J. **The murine voltage-dependent anion channel gene family. Conserved structure and function.** J. Biol. Chem., 272, (1997), 18966– 18973.

Sardiello, M., Tripoli, G., Romito, A., Minervini, C., Viggiano, L., Caggese, C. and Pesole, G. **Energy biogenesis: one key for coordinating two genomes.** Trends Genet., 2005, 21, 12-16.

Savabi, F. **Interaction of creatine kinase and adenylate kinase systems in muscle cells.** Mol. Cell. Biochem., 1994, 133/134, 145-152.

Scherrer, T., Mittal, N., Janga, S.C., and Gerber, A.P. **A screen for RNA-binding proteins in yeast indicates dual functions for many enzymes.** PLoS One 5, 2010, e15499.

Schirmer, T.; Keller, T.A.; Wang, Y.F.;Rosenbusch, J.P. **Structural basis for sugar translocation through maltoporin channels at 3.1 A resolution.** Science, 1995, 267, 512-514.

Schlattner U., Dolder M., Wallimann T., and Tokarska-Schlattner, M. **Mitochondrial creatine kinase and mitochondrial outer membrane porin show a direct interaction that is modulated by calcium.** J. Biol.Chem., 2001, 276, 48027–48030.

Schredelseker J., Paz A., Lopez C.J., Altenbach C., Leung C.S., Drexler M.K., Chen J.N., Hubbell W.L., Abramson J. **High resolution structure and double electron-electron resonance of the zebrafish voltage-dependent anion channel 2 reveal an oligomeric population.** J. Biol. Chem. 289 (2014) 12566–12577

Schwarzer, C., Barnikol-Watanabe, S., Thinnes, F.P. and Hilschmann, N. **Voltage-dependent anion-selective channel (VDAC) interacts with the dynein light chain Tctex1 and the heat-shock protein PBP74**. Int J Biochem Cell Biol, 2002, 34, 1059–1070.

Sengupta J, Nilsson J, Gursky R, Spahn CM, Nissen P, Frank J. **Identification of the versatile scaffold protein RACK1 on the eukaryotic ribosome by cryo-EM.** Nature Structural & Molecular Biology 2008, 11:957–962.

Shoshan-Barmatz V., De Pinto V., Zweckstetter M., Raviv Z., Keinan N., Arbel N. **VDAC, a multi-functional mitochondrial protein regulating cell life and death.** Mol. Asp. Med. 31 (2010) 227–285.

Shoshan-Barmatz V., Hadad N., Feng W., Shafir I., Orr I., Varsanyi M., Heilmeyer L.M., **VDAC/porin is present in sarcoplasmic reticulum from skeletal muscle.** FEBS Lett. 386 (1996) 205–210

Shoshan-Barmatz V., Israelson A., Brdiczka D., and Sheu S.S. **The voltage-dependent anion channel (VDAC): function in intracellular signalling, cell life and cell death.** Curr.Pharm.Des. 2006, 12, 2249–2270.

Shoshan-Barmatz, V. and Israelson, A. **The voltage-dependent anion channel in endoplasmic/sarcoplasmic reticulum: characterization, modulation and possible function.** J. Membr. Biol., 2005, 204, 57-66.

Simpson J. H. **Mapping and manipulating neural circuits in the fly brain.** Adv. Genet. 2009, 65, 79-143.

Stoiber M.H., Olson S., May G.E., Duff M.O., Manent J., Obar R., Guruharsha K.G., Bickel P.J., Artavanis-Tsakonas S., Brown J.B., and Celniker S.E. **Extensive cross-regulation of post-transcriptional regulatory networks in Drosophila.** Genome research 2015, 25:1692–1702

Suzuki C., Garces R.G., Edmonds A.E., Hiller S., Hyberts S.G., Marintchev A., and Wagner G. **PDCD4 inhibits translation initiation to eIF4A using both its MA3 domains.** Proc. Natl. Acad. Sci. U. S. A., 2008, 105(9): 3274-3279

Thompson M.K., Rojas-Duran M.F., Gangaramani P., Gilbert W.V. **The ribosomal protein Asc1/RACK1 is required for efficient translation of short mRNAs.** eLife 2016;5:e11154.

Tsvetanova, N.G., Klass, D.M., Salzman, J., and Brown, P.O. **Proteome-wide search reveals unexpected RNA-binding proteins in Saccharomyces cerevisiae.** PLoS One **5**, 2010. e12671.

Ugur B., Chen K. and Bellen H. J. **Drosophila tools and assays for the study of human diseases.** Dis. Model. Mech. 2016, 9, 235-244.

Ujwal R., Cascio D., Colletier J.P., Faham S., Zhang J., Toro L., Ping P., Abramson J. **The crystal structure of mouse VDAC1 at 2.3 A resolution reveals mechanistic insights into metabolite gating.** Proc. Natl. Acad. Sci. U. S. A. 105 (2008) 17742–17747

Venter J. C., Adams M. D., Myers E. W., Li P. W., Mural R. J., Sutton G. G., Smith H. O., Yandell M., Evans C. A., Holt R. A. et al. **The sequence of the human genome.** Science 2001, 291, 1304-1351.

Vyssokikh M.Y., and Brdiczka D. **The function of complexes between the outer mitochondrial membrane pore (VDAC) and the adenine nucleotide translocase in regulation of energy metabolism and apoptosis.** ActaBiochim.Pol. 2003, 50, 389–404.

Wanjun GU, Yuming Xu, Xueying Xie, Ting Wang, Jae-Hong Ko, and Tong Zhou. **The role of RNA structure at 5′ untranslated region in microRNA-mediated gene regulation.** RNA journal, 2015, 044792.114

Wernet M. F., Huberman A. D., and Desplan C. **So many pieces, one puzzle: cell type specification and visual circuitry in flies and mice.** Genes Dev. 2014, 28, 2565-2584.

Wilhelm, J.E. and Smibert, C.A. **Mechanisms of translational regulation in Drosophila**. Biol. Cell, 2005, 97, 235-252.

Wolf M. J., and Rockman H. A. **Drosophila melanogaster as a model system for the genetics of postnatal cardiac function.** Drug Discov. Today Dis. Models 2008, 5, 117-123.

Zalfa, F., Adinolfi, S., Napoli, I., Ku¨ hn-Ho¨ lsken, E., Urlaub, H., Achsel, T., Pastore, A., and Bagni, C. **Fragile X mental retardation protein (FMRP) binds specifically to the brain cytoplasmic RNAs BC1/BC200 via a novel RNA-binding motif.** J. Biol. Chem., 2005, 280, 33403–33410.

Zuker, M. **Mfold web server for nucleic acid folding and hybridization prediction.** Nucleic Acids Res. ,2003, 31, 3406-15.